



מכון ויצמן למדע
WEIZMANN INSTITUTE OF SCIENCE

Thesis for the degree
Doctor of Philosophy

Submitted to the Scientific Council of the
Weizmann Institute of Science

By
Yochai Wolf

חקר מקרופאגים ממוצא עוברי ומקרופאגים המתמיינים ממונוציטים
בחיה
Studying embryonic and monocyte-derived tissue macrophages *in vivo*

Advisor:
Prof. Steffen Jung

May 2015

עבודת גמר (תזה) לתואר
דוקטור לפילוסופיה

מוגשת למועצה המדעית של
מכון ויצמן למדע
רחובות, ישראל

מאת
יוחאי וולף

מנחה:
פרופ' שטפן יונג

סיוון התשע"ה

Contents

List of abbreviations	4
Abstract	6
1. Introduction.....	7
1.1 Tissue macrophages vs. monocyte-derived macrophages: a shifting paradigm	7
1.2. Brown adipose tissue macrophages, obesity and MeCP2	10
1.3. Microglia vs. monocyte-derived macrophages in neuropathologies.....	13
1.4. Cardiac macrophages	19
1.5. Aims.....	20
2. Methods	20
2.1. Mice.....	20
2.2. Reagent administration.....	21
2.3. EAE assessment	22
2.4. Glucose tolerance and insulin tolerance test (GTT, ITT)	22
2.5. Metabolic studies	22
2.6. Cold challenge	22
2.7. Isolation of tissue samples.	23
2.8. Ex vivo stimulation	23
2.9. Flow cytometry.....	24
2.10. Histology.....	25
2.11. Genomic DNA extraction.....	25
2.12. RNA Isolation, Library Construction, and Analysis	26
2.13. ELISAs.....	26
2.14. Quantitative real time PCR.....	26
2.15. Western blot.....	27
2.16. Statistical analysis.....	27
3. Results - Part I: Brown adipose tissue macrophages control energy expenditure	27
3.1. The CX3CR1 ^{Cre} and CX3CR1 ^{CreER} mouse models allow the study of tissue macrophages.....	27
3.2. MeCP2 deletion in brown adipose tissue macrophages results in spontaneous obesity	32
4. Results - Part II: The contribution of microglia and monocytes to CNS autoimmunity	48
4.1 . Microglial antigen presentation is not required for the induction of EAE	48
4.2. Monocyte-derived, cell intrinsic TNF is pivotal for EAE induction	52
5. Results - Part III: Ontogeny of cardiac macrophages in adulthood	60

6. Discussion.....	63
6.1. Brown adipose tissue macrophages have a homeostatic role in energy balance	63
6.2. Microglia, monocytes, and monocyte-derived macrophages in neuroinflammation: roles of MHCII and TNF.....	66
6.3. Cardiac macrophages undergo progressive replacement by monocyte-derived cells in adulthood	70
6.4. Concluding remarks.....	71
References.....	74
Appendix- Progressive replacement of embryo-derived cardiac macrophages with age, by Molawi, Wolf <i>et al.</i>	93
Statement of the supervisor.....	102
Acknowledgements.....	103

List of abbreviations

ATM - adipose tissue macrophages

BAM- brown adipose tissue macrophages

BAT - Brown adipose tissue

BBB - blood brain barrier

BM - bone marrow

cMOP - common monocyte precursor

CM ϕ - cardiac macrophages

DC - dendritic cells

EAE - experimental autoimmune encephalomyelitis

EMP - erythro-myeloid progenitors

GTT - glucose tolerance test

H & E - hematoxylin and eosin

HSL - hormone sensitive lipase

ITT - insulin tolerance test

MDP - monocyte/macrophage-dendritic cell precursor

MeCP2 - methyl CpG binding protein 2

MFI - mean fluorescence intensities

MHCII - Major Histocompatibility Complex 2

MS - Multiple sclerosis

PGC1 α - Peroxisome proliferator-activated receptor gamma coactivator 1-alpha

PRDM16- PR domain containing 16

RTT - Rett's syndrome

scWAT - subcutaneous white adipose tissue

TACE, - TNF-alpha converting enzyme, also ADAM17

TAK1- transforming growth factor β activating kinase 1

TAM - tamoxifen

TH - Tyrosine hydroxylase

Th₁, Th₁₇- T helper 1 cell, T helper 17 cell

TNF- α - tumor necrosis factor alpha

UCP1 - uncoupling protein 1

vWAT - visceral white adipose tissue

WAM - white adipose tissue macrophages

Abstract

Macrophages are members of the mononuclear phagocyte system, alongside monocytes and dendritic cells (DC). In recent years it is becoming increasingly clear that tissue resident macrophages, other than monocyte-derived macrophages, are important not only for immune responses, but also for maintaining the homeostasis and integrity of the tissue. Data accumulated in the past decade describe pronounced complexity and heterogeneity of the tissue macrophage compartment, both in terms of ontogeny, gene expression and functionality. Collectively, this renders these cells highly challenging to study. Specifically, their unique features require robust and specific experimental systems to study the cells in high resolution in tissue context. Cre transgenic mouse models allow in combination with conditional reporter genes to differentially label embryo-derived and adult monocyte-derived tissue macrophages to refine their characterization and ontogeny. Moreover, this approach enables the genetic manipulation of specific cells *in vivo*.

In this PhD study I investigated developmental and functional aspects of three different types of tissue macrophages, residing in adipose tissue, brain and heart, respectively. I generated mice, which lack the transcription regulator methyl-CpG binding protein 2 (MeCP2), known to be involved in Rett's syndrome (RTT), a neurodevelopmental disease. Mice with total MeCP2 deletion in mononuclear phagocytes did not develop symptoms of RTT, and MeCP2-null microglia did not show any overt inflammatory phenotype. However, we unexpectedly found that deletion of the MeCP2 mutant mice displayed spontaneous obesity, most likely due to absence of the gene from brown adipose tissue macrophages (BAM). The spontaneous obesity was phenocopied in mice with the further-restricted, tamoxifen (TAM) -induced MeCP2 deletion. Metabolic profiling established that defect was due to reduced energy expenditure, and the MeCP2 deletion was associated with an altered BAM transcriptome, suggesting a role of these macrophages in tissue homeostasis. In my studies on brain macrophages, i.e. microglia, I found using the experimental autoimmune encephalomyelitis (EAE) model, that activated microglia and monocyte-derived macrophages express distinct cell surface markers. To probe for antigen presenting function of microglia we deleted the *i-a^b* gene, encoding a component of the Major Histocompatibility Complex 2 (MHC-II), critical for cognate cross-talk with CD4⁺ T cells. Surprisingly, we found that microglial MHCII was dispensable for the onset of EAE. To probe for the role of tumor necrosis factor alpha (TNF- α) in microglia and monocytes, we generated mice harboring a TNF- α mutation in both cell types or restricted to microglia. The former

delayed the onset of EAE, in a T cell independent manner, without effecting the demyelination *per se*, but by reducing infiltration of monocytes into the spinal cord. Our data suggest that the TNF deletion in monocytes caused a cell intrinsic survival defect, ultimately leading to delayed EAE onset. Microglial TNF on the other hand was found not to be required for the onset of EAE. Finally, we used the different CX3CR1-Cre approaches to fate map and characterize a recently described population of cardiac macrophages. We could segregate the cells into four subpopulations based of their MHCII and CX3CR1 expression, and established, that they are embryo-derived cells that are with time progressively replaced by monocyte-derived macrophages.

1. Introduction

1.1 Tissue macrophages vs. monocyte-derived macrophages: a shifting paradigm

The mononuclear phagocyte system is composed of tissue macrophages, DC, and blood-circulating monocytes, capable of differentiate to either macrophage- or DC- like cells¹. Macrophages are specialized in ingesting cellular debris and pathogens and contribute to the inflammatory response. In recent years it was shown that macrophages also have steady state roles as non-inflammatory cells, contributing to development, tissue homeostasis and regeneration². Examples include Kupffer cells of the liver; the red pulp macrophages, important for phagocytosis of aged erythrocytes and iron recycling^{3,4}; osteoclasts, which are key players in bone resorption⁵ and microglia, which were shown to mediate synaptic pruning, eliminate synaptic material, and even to promote spine growth⁶⁻⁸ (**Figure 1**). As the study of macrophages has traditionally focused on settings of pathology, these homeostatic functions have been notoriously underappreciated. Indeed, only more recent notions hold that these cells also contribute critical to the integrity, maintenance and repair of the tissue, rather than acting only in response to pathogens in the inflammatory context. In the past, it was assumed that all macrophages derive from monocytes, i.e. circulating cells, which are bone-marrow (BM)-derived⁹; however, recent studies have now firmly established that a substantial part of resident tissue macrophages is derived from embryonic precursors and that these cells are disconnected from adult BM precursors and ongoing hematopoiesis. In such a scenario, monocyte-derived macrophages may act as an “emergency squad” recruited to sites of inflammation¹⁰, where they are instrumental for the inflammatory response; in certain cases, such as the CNS, monocyte-derived macrophages do not persist after the inflammation is resolved¹¹. In other cases, such as

peritonitis, they can at least partially integrate into the local macrophage pool¹² or even replace the embryonic-derived macrophages (**Figure 2**)¹²⁻¹⁷.

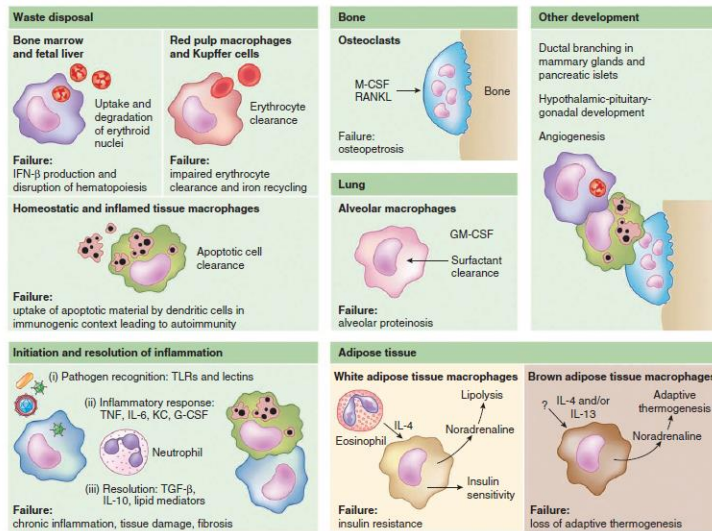


Figure 1. Homeostatic functions of tissue macrophages, (adopted from reference²)

Recent works suggest that certain tissue macrophage compartments might even be independent of hematopoietic stem cells (HSC)¹⁸, although this point remains under debate. Kupffer cells, microglia, lung macrophages, Langerhans cells and most other macrophage are established early during embryogenesis. Microglia are derived from yolk sac precursors, which are independent of the transcription factor Myb, which is essential for HSC development^{14,17}. These precursors are Tie2+ erythro-myeloid progenitors (EMP), which develop as early as E8.5, and colonize the fetal liver before E10.5, before the colonization by the “definitive” precursors¹⁹. Some macrophages might also arise from early definitive hematopoiesis occurring in the fetal liver. We and others have previously shown that under steady state conditions, the majority of tissue-resident macrophages are not replaced by monocytes^{12,16,19}, with the exception of gut macrophages, which are in adulthood entirely monocyte-derived^{20,21}; their different origin might suggest that embryo-derived macrophages perform functions within the tissue, which are different than that of the inflammation-associated, monocyte-derived macrophages. However, such distinct functions remain to be defined.

Monocytes are per definition circulating mononuclear phagocytes. The rodent immune system comprises two monocyte subsets, which can be defined in this species as CCR2⁺ CX₃CR1^{int}Ly6C^{hi} and CCR2⁺ CX₃CR1^{hi}Ly6C^{lo} cells. These cells are the equivalent of CD16⁺CD14⁻ and CD16⁻CD14⁺ human monocytes and display different roles²²⁻²⁵. Monocytes develop in the BM from common monocyte precursors (cMOP), derived from the monocyte/macrophage-DC

precursors (MDP)²⁶⁻²⁸. Ly6C^{hi} monocytes are plastic and can depending on the tissue environment and the conditions that the cells encounter upon extravasation acquire either DC and macrophage features²⁹.

Whenever studied, monocyte-derived macrophages that are recruited under inflammation to tissues display gene expression profiles distinct from the resident macrophages, which suggest distinct functionality. This has for instance been demonstrated for CNS and liver inflammation^{30,31}. Moreover, also steady state tissue macrophages show significant heterogeneity from one another, both in terms of gene expression³² and epigenetic signatures³³; thus, various tissue macrophages seem to adopt in response to local cues distinct identities according to the needs of the microenvironment, in which they reside. To conclude, recent data demonstrate that macrophage biology is extraordinary complex and dynamic. Moreover the characterization of macrophage function within a given tissue in a given immune context is highly challenging. The study of the ontogeny and role of several tissue macrophages in the brain, brown adipose tissue, and heart, in comparison to pathogenic monocyte-derived macrophages was the main topic of this PhD thesis. The work benefited from recently generated novel mouse models, i.e. the CX3CR1^{Cre} and CX3CR1^{CreER} mice, developed by Drs. Simon Yona and Ki-Wook Kim in the Jung laboratory

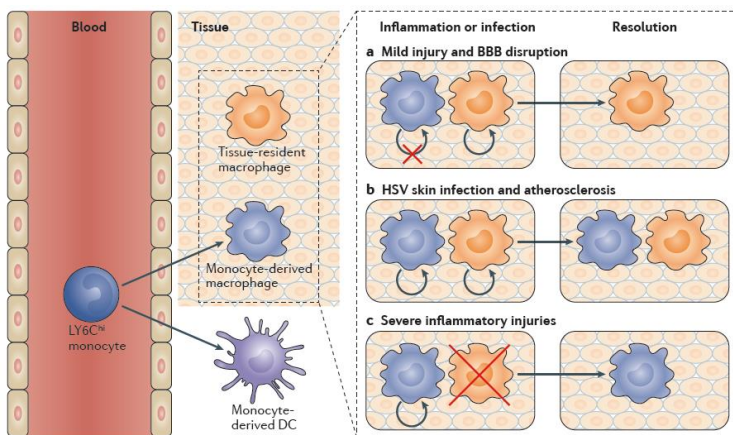


Figure 2. Interactions between tissue resident and monocyte-derived macrophages in health and disease. Embryonic tissue resident macrophages populate most tissue throughout the organism. Some tissues host an additional macrophage population, derived from circulating Ly6C⁺ blood monocytes. Upon disruption of tissue homeostasis, such as injury or immune challenge, monocytes infiltrate the tissue, and depending on the pathologic context

are upon resolution either removed, integrate into the resident macrophage population, or replace the embryonic macrophages. Adopted from reference¹⁰.

1.2. Brown adipose tissue macrophages, obesity and MeCP2

In the last decade it is becoming more and more evident that hematopoietic cells participate in metabolism control, both in the homeostatic steady state and in obesity. A current paradigm holds that metabolic homeostasis has to be maintained by the immune system³⁴, and that obesity is a condition of low-grade inflammation³⁵. As such, obesity itself recruits monocytes into “inflamed” adipose tissue^{36,37} and induces both myelopoiesis³⁸ and local proliferation within the tissue³⁹. In addition, leukocytes themselves can alter the metabolic state of the fat tissue, as well as the organism. In obesity, macrophages can modulate the signaling of the insulin receptor on adipocytes and muscle cells, a process known as insulin resistance⁴⁰. Adipocytes also can interact with CD4+ T cells in order to polarize adipose tissue macrophages, a process which enhances obesity⁴¹. Interestingly, adipose tissue macrophages are activated not only in the obese state, but also under fasting and lean conditions⁴². In addition, adipose tissue macrophages also participate in cold challenge, in which the organism has to adapt rapidly to abrupt changes in the environment⁴³⁻⁴⁵. However, these immune-metabolic interactions have mainly been attributed to the altered metabolism, with little understanding as to how the immune system maintain metabolic homeostasis. Recently, it was shown that specific immune cells, i.e. type-2 innate lymphoid cells (ILC2), contribute to the homeostatic metabolism of the fat tissue. Thus, in ILC2 absence the balance between food consumption and energy expenditure was disrupted, which in turn lead to obesity⁴⁶. Thus, immune cells are not only involved in the obese state of the fat tissue, but also in maintaining its normal functioning. Contributions of adipose tissue macrophages to metabolic homeostasis have however not been described

The brown adipose tissue (BAT) is a specialized type of fat tissue, whose purpose is contributing to non-shivering thermoregulation in mammals⁴⁷. BAT is composed of specialized adipocytes, which express and utilize the mitochondria protein Uncoupling Protein 1 (UCP1, also called Thermogenin) in order to burn lipid droplets to generate heat instead of ATP⁴⁸. Brown adipocyte develop from the myoblast lineage, and their identity is dictated by the action of the master regulator transcription factor PR domain containing 16 (PRDM16)^{49,50}. PRDM16 activates the transcription co-activator Peroxisome proliferator-activated receptor gamma coactivator 1-alpha (PGC1 α)^{49,51}, which is upstream of UCP1 transcription (**Figure 3**). Activation of BAT adipocytes depends on noradrenergic stimulation by the sympathetic nervous system which innervates the tissue⁵². BAT adipocytes sense norepinephrine via the β 3 adrenergic receptor, whose stimulation results in increase of PGC1 α levels and thereby UCP1 induction

expression and the switch of mitochondrial functions^{47,48,51}. This thermogenic machinery is known to act in cold-challenged rodents, and recent PET-scan studies have described an equivalent tissue in humans^{53,54}. BAT was proposed to contribute to thermogenesis not only under cold stress, but also under steady state, as an energy expenditure mechanism, known as the “diet-induced thermogenesis”. Indeed, under thermo-neutral conditions, UCP1-null mice do become spontaneously obese⁵⁵.

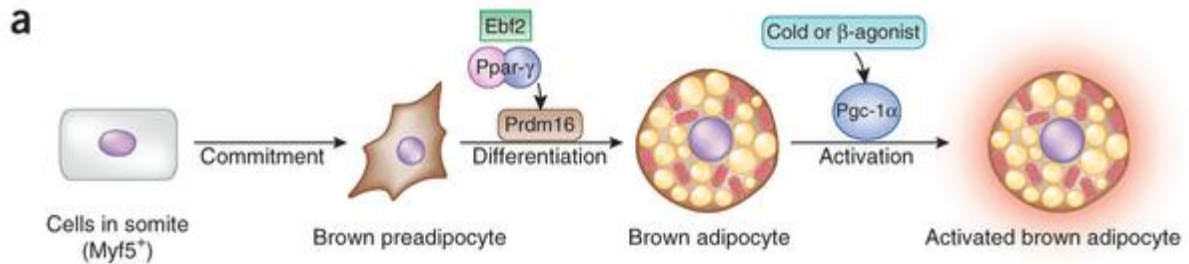


Figure 3. Development of brown adipocytes. Adapted from ref⁵¹

Importantly, a certain subset of white adipocytes located in the subcutaneous white adipose tissue (scWAT) can under conditions of adrenergic signaling also express UCP1 and thus participate in thermogenesis, a process known as “browning” of WAT or “beiging”⁵¹; thus, the two tissues share certain similarities, although their precise contribution in diet-induced thermogenesis is at the moment unclear. Beige adipocytes differ from brown adipocytes according to origin and steady state UCP1 expression. BAT functions, as well the beiging of WAT, have been reported to involve immune cells, and also macrophages^{44,45}; however contributions of the latter are at the moment poorly characterized.

The vast majority of research of macrophages residing in adipose tissue has so far concentrated on macrophages of the WAT, or (thereafter termed WAM). Recently, it was shown that BAT hosts F4/80⁺ macrophages (thereafter termed brown adipose tissue macrophages or BAM). These cells are known to respond to cold challenge, in which case the cells were proposed to proliferate⁴³, apparently in association with macrophage polarization towards an anti-inflammatory, so called 'M2', signature⁴⁴. However, to date the BAM remain uncharacterized, and their function within the tissue, specifically in the context of energy expenditure under thermo-neutral conditions, is not clearly defined. Also, it is not clear whether these are cells derived from the BM, similar to gut macrophages²⁰, or are embryo-derived similar to many other

tissue macrophages^{12,17}; with the identification of functional BAT in humans⁵⁶, understanding the function and origin of the BAM has become of clinical importance.

The X chromosome-linked nuclear transcription factor methyl-CpG binding protein 2 (MeCP2) is strongly linked to many neuro-developmental diseases, specifically with Rett's syndrome (RTT). RTT is a postnatal progressive neuro-developmental disorder, which predominately occurs in females during early childhood. RTT patients develop normally up to 6-18 months, before the onset of neuro-developmental symptoms, which include growth arrest, autistic behavior, movement disorders, mental retardation culminating in respiratory deficits, lack of speech and anxiety⁵⁷. MeCP2-deficient mice or animals, which carry specific inactivating MeCP2 mutations, phenocopy the human disease⁵⁸⁻⁶¹. MeCP2 transgenic mice that exhibit MeCP2 overexpression also show developmental symptoms, which are very similar to those resulting from a MeCP2 deficiency^{62,63}. This suggests that the actual function of MeCP2 is more complex, and that the protein can modulate gene expression in via distinct mechanisms, which might differ between tissues and cell types⁶⁴. Classically considered a transcriptional repressor, MeCP2 acts through chromatin condensation and transcriptional repression; alternatively, MeCP2 might also directly block transcription⁶⁵. However, by forming a complex with CREB1⁶⁶, MeCP2 can also act as a transcriptional activator. Other mechanisms of action were attributed to MeCP2 in terms of gene expression regulation, such as altering alternative splicing, controlling miRNA function and the direct modification of histone structure⁶⁴ (**Figure 4**); In addition, MeCP2 itself undergo many post-translational modifications, such as phosphorylation and acetylation in multiple sites⁶⁷; thus MeCP2's net influence on gene expression is elusive, and may account for the puzzling phenotypic similarities between gain-of-function and loss-of-function mutations⁵⁷. In macrophages, a recent work from the lab of Jonathan Kipnis described MeCP2 as a survival factor and modifier of inflammatory output⁶⁸. However, since MeCP2 can act differently in distinct cell types, it might also have different functions in specific macrophage types, depending on tissue and immune context.

RTT-related MeCP2 functions were originally believed to be cell-autonomous and restricted to post-mitotic neurons⁶⁰. However, MeCP2 is also expressed in other cell types, which may contribute to RTT, such as microglia⁶⁹. Interestingly, while most MeCP2-null males are small, some do become obese⁵⁸, corresponding to sporadic obesity reported for RTT patients⁷⁰. More specifically, Sim1^{Cre}:MeCP2^{f/y} mice, in which MeCP2 is specifically deleted in

hypothalamic neurons, do not develop RTT symptoms, but become obese due to increased food consumption⁷¹; a similar phenotype occurs also in specific deletion of MeCP2 in neurons producing the negative feeding regulator POMC⁷². Thus, the mechanism for the obesity phenotype in these mice is central, and involves broad hypothalamic dysfunction, as *Sim1^{Cre}:MeCP2^{f/y}* males also exhibit heightened aggressiveness. In addition, functions of the sympathetic nervous system, such as respiratory regulation⁷³ and thermo-regulation^{74,75} are altered in MeCP null males and MeCP2 heterozygote females.

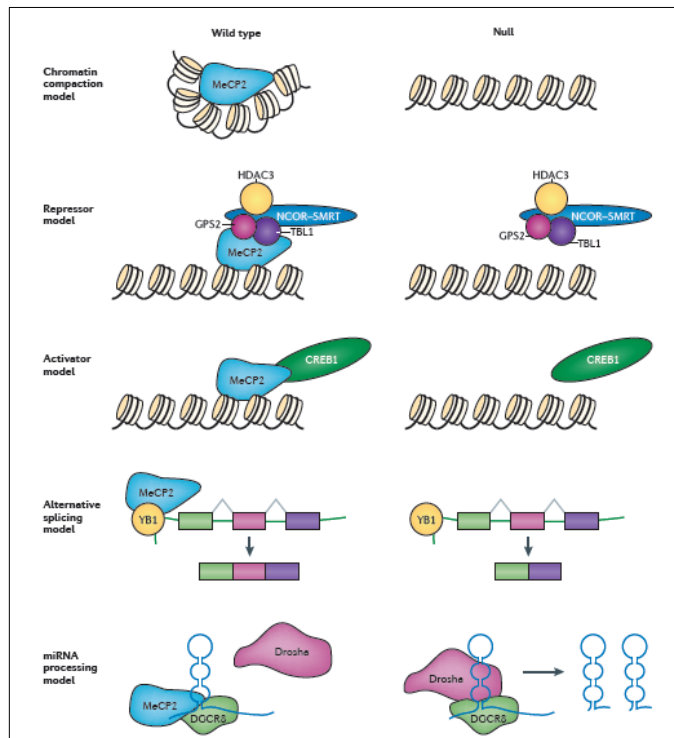


Figure 4. Proposed molecular mechanisms for gene regulation by MeCP2. adapted from ref⁶⁴.

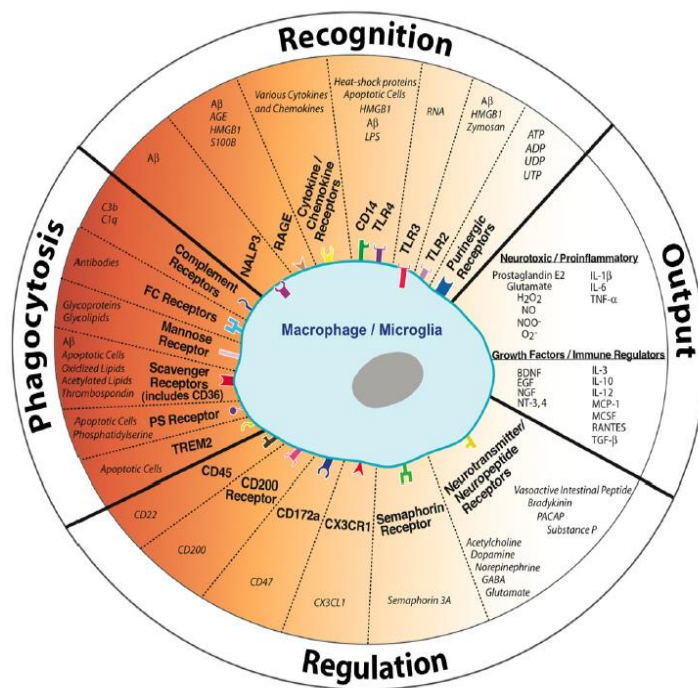
In this thesis we investigated the role of BAT macrophages in general, and the role of MeCP2 in these macrophages- in particular, in the maintenance of energy expenditure and metabolism. The work was performed with the assistance of Dr. Sigalit Boura-Halfon.

1.3. Microglia vs. monocyte-derived macrophages in neuropathologies

Microglia are hematopoietic cells that develop independent of neuroectoderm-derived neurons, astrocytes and oligodendrocytes⁷⁶. Sequestered behind the blood brain barrier (BBB) in the unique neuronal/ microglial context, microglia display a gene expression profile and enhancer landscape that significantly differ from other tissue macrophages^{32,33}. Moreover, highlighting its independence, the microglia compartment is established well before birth from an early “primitive”

hematopoietic wave originating in the yolk sac. More specifically, microglia originate from the EMP and thus are independent of hematopoietic stem cells⁷⁷. Microglia subsequently maintain themselves throughout adulthood by virtue of longevity and limited self-renewal¹⁴. Microglia share the prenatal establishment with most other tissue macrophage populations¹⁷. Steady state microglia are distributed throughout the CNS, including brain and spinal cord, and are sensors of injury and pathologic conditions. More recent studies have furthermore revealed that microglia critically contribute to CNS development and brain homeostasis⁷⁸. Microglia furthermore are believed to be key players in neuro-inflammation and neurodegeneration^{79,80} (**Figure 5**). Of note, while microglia are the prime macrophages of the CNS parenchyma, non-parenchymal regions of the brain, such as the meninges, the perivascular niches and the choroid plexus, are populated by a smaller macrophage population distinct from microglia⁸¹.

Figure 5. Microglia function and its molecular mediators in the healthy and inflamed CNS parenchyma. Adapted from ref⁸⁰



Prenatally established, the hard-wired resident microglia compartment can be complemented on demand by macrophages that arise from monocytes recruited from the blood circulation during injury or challenge⁸². The latter cells are purged from the CNS after resolution of the inflammation¹¹. Monocytic infiltrates are particularly evident in neuro-inflammatory disorders, such as the multiple sclerosis (MS) model of experimental autoimmune encephalomyelitis (EAE) that involves a BBB breakage⁸². Emerging evidence from mixed BM chimeras and parabiotic mice indicates that functional contributions of monocyte-derived cells differ from that of the microglia

¹¹. However, definitive evidence for distinct functions of microglia vs. monocyte-derived macrophages calls for experimental systems that allow the exclusive manipulation of microglia in non-irradiated mice, and, unlike *in vitro* studies, in their unique physiological CNS environment.

MS is the most common non-traumatic disabling neurological disease of adults in the northern hemisphere⁸³. Pathological features of MS are the infiltration of autoreactive T cells and myeloid cells into the CNS leading to demyelination and axonal degeneration⁸⁴. This condition is represented in the well-established animal model for brain inflammation and MS, known as EAE⁸⁵. In the classical murine EAE protocol, peripheral injection of the myelin peptide MOG₃₅₋₅₅ leads in conjunction with adjuvant and pertussis toxin, to priming of autoreactive T cells in the lymph nodes and their differentiation into Th1 and Th17 effector cells. MOG-specific CD4⁺ T cells then enter the CNS, where they are thought to require reactivation by CNS-resident antigen presenting cells (APCs) to exert their damaging role (**Figure 6**). The critical role of the T cells was established by the demonstration that *ex vivo* stimulated MOG-specific CD4⁺ T cells can upon their adoptive transfer induce EAE independently of an immunization (passive EAE)⁸⁶.

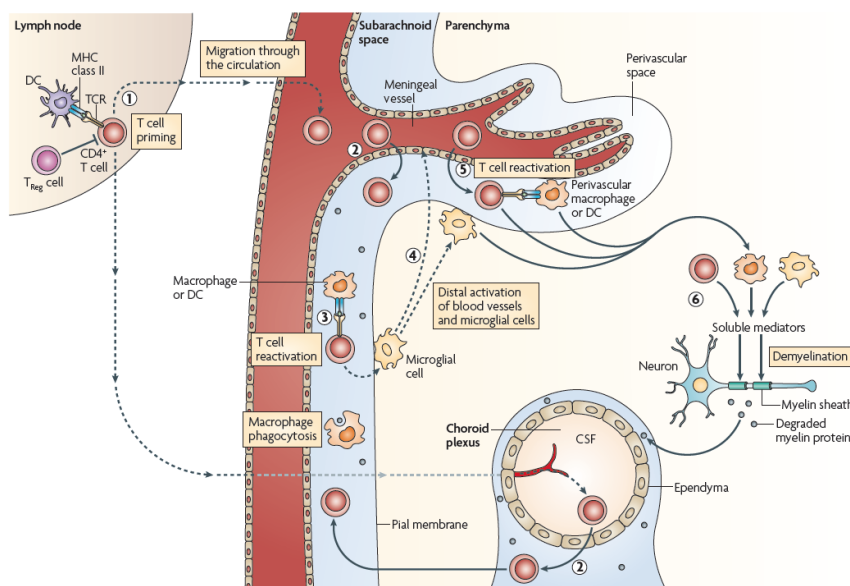


Figure 6. Scheme summarizing the current view of the CD4⁺ T cell contribution to in MS and EAE. adapted from⁸⁷.

It is often assumed that microglia are crucial for the development of EAE⁸⁸, and that they may have either a direct detrimental effect or indirectly contribute by interacting with other cells. Interestingly, Ajami and colleagues reported that microglia enter the cell cycle and proliferate during the early stages of the EAE, even prior to monocyte infiltration, and in correlation with disease severity¹¹. Blocking microglia proliferation using the CD11b-TK system⁸⁸, or

preventing microglial pro-inflammatory gene expression by deleting the transforming growth factor β activating kinase 1 (TAK1)⁸⁹, was found to reduce the severity of the disease.

Challenging the notion of a disease promoting activity of microglia, using CCR2^{flp}:CX3CR1^{gfp} double reporter mice it was reported that monocyte-derived macrophages are primarily responsible for the stripping of neurons from their myelin, while microglia adopted an “inert” phenotype by silencing their gene expression, and merely cleared debris as bystander cells³⁰; thus, the role of microglia as disease-mediating cells in CNS autoimmunity is still under debate.

One of the crucial steps in the progression of EAE is believed to be the re-stimulation of infiltrating, primed myelin-specific T cells by CNS-resident APCs; thus, one key question in describing the role of microglia in CNS autoimmunity is, whether or not microglia can present myelin antigen and prime T cells. Antigen presentation within the CNS has been speculated to be performed by CNS DC⁹⁰, recruited monocyte-derived macrophages⁹¹ and the resident microglia⁸⁸. Of these, DC contributions were shown to be critical for EAE^{90,92} and recently a novel subset of Flt3-dependent DC, which reside in the CSF-producing choroid plexus and the meninges, with ability to prime T cells in the presence of MOG *in vitro*, was described⁹³. However, DC are not sufficient in inducing EAE, when mice are immunized with recombinant MOG protein⁹⁴. This suggests that antigen presentation by DC does not account for the entire phenotype of the disease, and that other CNS APC also have a substantial contribution⁹⁴. In line with this observation, it was recently shown that counter intuitively the ablation of DC worsened EAE symptoms, again suggesting that other cells compensate for the lack of DC-mediated antigen presentation⁹⁵.

In steady state, microglia express very low amounts of MHC II and co-stimulatory molecules, that are required for the interaction with and activation of T cells⁹⁶. However, following an *in vitro* challenge, such as exposure to TLR ligands, or *in vivo*, following EAE induction, the cells can upregulate MHC II^{97,98}, readying them for potential T cell stimulation. Supporting this notion, MHC II induction on microglia is at day 10 post immunizations and corresponding to the onset of disease, accompanied by an upregulation of costimulatory molecules⁹¹. Following immunization with MOG₃₅₋₅₅ peptide, spinal cord microglia alter their phenotype from a quiescent CD45^{int} MHC II⁻ mode to an active CD45^{hi} MHC II⁺ state⁹¹. Interestingly, it was reported that suppression of this activation by systemic delivery of miR-124 can prevent the onset of EAE⁹⁹. The up-regulation of MHC II seen in microglia in EAE may be related to GM-CSF-

secreting Th₁₇ cells, an inflammatory CD4⁺ T cell subset now recognized to be crucial for EAE¹⁰⁰. Some *in vitro* data show a very low capacity for T cell stimulation by microglia^{92,93}, as compared for instance to DC; however these reports involved cells obtained from steady state, which were MHCII negative. Microglia are in fact capable of uptake of myelin antigen, in both steady state and during the initial phase of EAE; particularly at this early time, before the infiltration of monocyte-derived cells¹⁰¹, microglia might be the sole myeloid cells ingesting myelin antigens. A recent study found that a subpopulation of activated CD11c⁺ MHCII⁺ microglia isolated from sick animals could indeed prime T cells to some extent *in vitro* with the MOG₃₅₋₅₅ peptide¹⁰²; it was also shown that microglia could induce in the presence of MOG₃₅₋₅₅ and low dose IFN γ , T_{reg} cells *in vitro*, which were active in suppressing EAE *in vivo*¹⁰³. However, at the moment no *in vivo* evidence for such T cell priming by microglia exists. Nevertheless, recent state-of-the-art imaging data did describe contact between parenchymal microglia and infiltrating T cells in EAE; thus T cell priming by microglia remains still a possibility¹⁰⁴.

Up-regulation of microglial MHC II is not limited to EAE and MS, but also associated with other neuro-inflammatory conditions, such as CNS injury¹⁰⁵. Another prominent example of microglial MHC II induction occurs in the cuprizone model that leads to a specific demyelination/remyelination reaction restricted to the corpus callosum¹⁰⁶. Cuprizone is a copper chelating reagent, which can be given to mice by diet; following a period of 4-6 weeks it induces oligodendrocyte death and reversible demyelination¹⁰². In microglia research, cuprizone challenge is a powerful model, since it minimizes the involvement of myeloid cells other than microglia. In the process of demyelination, microglia undergo activation and proliferation, especially during the late stage of demyelination, characterized by expression pro-inflammatory cytokines and activation-associated cell surface marker, as well as increased phagocytic capacity¹⁰⁶⁻¹⁰⁸; for instance, CX3CR1-null microglia display impaired debris clearance, which interferes with the remyelination stage¹⁰⁹, and mice deficient for TREM2 undergo an altered remyelination phase, due to impaired activation and phagocytosis¹¹⁰. Interestingly, it was suggested that microglia also participate in the repair process, by secreting oligodendrocyte-related factors, such as IGF-1, which promote the maturation of oligodendrocyte precursors, thus supporting remyelination. In this process, a subset of microglia also upregulated MHCII¹⁰⁷. Importantly, the cuprizone model of demyelination does not depend on T and B cells, in contrast to EAE or human MS. The function of the newly-expressed MHCII in the cuprizone model is ill-defined; MHCII-null mice

have diminished demyelination^{111,112}, but also delayed and reduced remyelination. Moreover, the diminished demyelination seems to be dependent specifically on the intact cytoplasmic tail of MHCII, which is involved in the proliferation and the active phenotype of the microglia¹¹¹.

MHC II induction has also been reported for the facial nerve axotomy model, in which microglia accumulate specifically in the axotomized facial nerve nuclei¹¹³. These reports are intriguing, as again they do not involve T cells, autoimmune reactions or a pathogenic agent. Of note however, it has been suggested that MHC II molecules might have functions independent of T cells and antigen presentation^{106,111}, potentially involving intracellular signaling enhancing TLR signaling¹¹⁴. This would be consistent with the fact that microglia-associated MHC II is essentially sequestered in their endosomal compartment, rather than exposed on their surface, unlike in DC, which even before maturation express readily detectable levels of surface MHCII⁸¹. Combined, these reports hint strongly at alternative functions for microglial MHCII, other than its involvement in T cell priming.

A key element in the neuropathology of MS is the release of pro-inflammatory cytokines, such as IL-1, IL-6 and tumor necrosis factor alpha (TNF α) to the inflamed CNS¹¹⁵. Of these cytokines, TNF α , which is highly abundant in MS lesions and produced by many cells in the inflamed CNS^{116,117}, is of particular importance, due to its pleotropic actions and its association with many autoimmune conditions, such as rheumatoid arthritis and Crohn's disease¹¹⁸. TNF α is first produced as a membrane-bound precursor, which is subsequently cleaved by the metalloprotease TNF- α converting enzyme (TACE, also known as ADAM17)¹¹⁹. Both the transmembrane and the secreted form of TNF are active. In addition, TNF has two distinct receptors, TNFR1 (p55) which preferably binds to the soluble TNF and contain the so-called "death domain", a cytoplasmic protein interaction region which can induce apoptosis as well as NF κ B activation, and TNFR2 (p75), which binds preferably to the transmembrane form, and seem to promote survival. Since both membrane-bound TNF α and its cleaved product are functional, and interact with different receptors, TNF α may act in diverse and even adverse functions¹²⁰. Although TNF α was initially considered detrimental in MS, and anti-TNF α drugs are used clinically to treat other autoimmune diseases, such as rheumatoid arthritis, TNF α antagonists actually worsen MS symptoms¹²¹, suggesting that TNF α may ameliorate the disease. TNF α ^{-/-} mice indeed develop slightly delayed and reduced symptoms of EAE, but eventually the disease is much more severe than that observed in TNF α sufficient mice, and no remission of the

symptoms is seen^{122,123}. It was suggested that TNFR1 signaling triggered by the soluble TNF form is detrimental for neurons¹²⁴. Conversely, signaling of TNFR2 in oligodendrocytes that is preferentially triggered by transmembranal TNF is considered beneficial¹²⁵. Indeed, TNFR2^{-/-} mice develop EAE symptoms very similarly to control mice, but fail to remyelinate¹²⁶. These observations support the idea that TNF has a pleiotropic action in EAE, and suggest that TNF is detrimental in the initiation phase of the disease but might be beneficial for the re-myelination phase via different signaling cascades. Microglia produce TNF α in an apparently T cell-dependent manner^{115,121} and upregulate TNF α expression during cuprizone-induced de- and remyelination¹⁰⁸. Microglia-derived TNF α , either secreted or membrane bound, might hence be involved in EAE and MS development, alongside TNF that is secreted by monocyte-derived macrophages.

Using mice harboring conditional mutant “floxed” TNF α alleles in combination with cell specific Cre recombinase expression, it was shown that the TNF α produced by Lysozyme M⁺ myeloid cells mediates LPS-induced septic shock and protection from intracellular pathogens, with little or no contribution of TNF α produced by lymphoid cells¹²⁷. Prior data concerning TNF expression in myeloid cells in the context of EAE, which involved the use of LysM-Cre:TNF^{ff} mice, showed slight delay in disease onset and decreased myeloid and T cell infiltration at day 14, with no effect on the later, chronic stage, thus suggest that myeloid TNF has a specific role in the onset of the disease¹²⁸. However, LysM-Cre expression has low penetrance in the microglia compartment⁸⁹. Thus, the exact role of TNF in microglia and monocyte-derived macrophages, as well as the puzzling nature of TNF in in CNS autoimmunity, is still unclear.

In this thesis, we investigated the function of microglial MHCII, as well as microglial and monocyte-derived macrophage TNF in both autoimmune and sterile demyelination. The work regarding microglial MHCII was performed in collaboration with Anat Shemer.

1.4. Cardiac macrophages

Cardiac macrophages (CM ϕ) are critical for early postnatal heart regeneration and fibrotic repair in the adult heart, but their origins and cellular dynamics during postnatal development have not been well characterized. Studies of cardiac repair after myocardial infarction in the adult have highlighted the critical role of infiltrating monocytes and monocyte-derived macrophages for the

healing process^{129,130}. However, these studies focused on the pathological “emergency” state, rather than the steady-state or development; tissue resident CM ϕ have largely escaped attention. Only recently it was shown that tissue-resident CX3CR1⁺ CM ϕ can be found throughout the myocardium¹³¹. The cells were reported to exhibit the canonical macrophage markers such as F4/80 and CD14, and molecules matching a 'M2 signature', such as IL-10 and CD163. A recent study identified several CM ϕ populations, including short-lived monocyte-derived cells that resemble monocyte-derived DC, as well as tissue-resident CM ϕ , which were suggested to be of pure embryonic origin and to self-maintain under homeostatic conditions¹³². In this thesis, we will present data supporting the notion of a progressive, age-dependent replacement of embryonic CM ϕ by monocyte-derived macrophages, which integrate into the resident pool and have a tendency to express high levels of MHCII. These data were generated in collaboration with group of Michael Sieweke, Centre d'Immunologie de Marseille-Luminy (CIML), France, and were recently published¹³³ and the manuscript is attached as an appendix.

1.5. Aims

The current thesis aims to study tissue and monocyte-derived macrophages in variety of settings, using novel, state-of-the-art experimental tools. We focused on macrophages within three distinct tissues- the brown adipose tissue, the CNS, and the heart, all populated by CX3CR1⁺ macrophages. We aimed to fate-map the macrophages and thus understand their ontogeny and kinetics, and also to knock-down specific genes of interest in order to uncover specific functions. We hypothesized that 1) the transcription regulator MeCP2 have a role in maintaining macrophage function; 2) myeloid-derived TNF has an important role in EAE ; 3) Microglial MHCII have functional significance; 4) cardiac macrophage have distinct ontogeny and kinetics.

2. Methods

2.1. Mice

Mice were maintained in a special pathogen-free (SPF), temperature-controlled (22°C \pm 1°C) mouse facility on a reverse 12-hour light, 12-hour dark cycle at the Weizmann Institute of Science. Food and water were given ad libitum. Mice were fed regular chow diet (Harlan Biotech Israel Ltd, Rehovot, Israel). CD45.2 C57BL/6 and CD45.1 (B6/SJL) mice were purchased from Harlan, Israel and bred in house, respectively. The following mouse strains were developed in house: *Cx3cr1*^{gfp/+} mice¹³⁴, *Cx3cr1*^{Cre} and *Cx3cr1*^{CreER} mice¹². To analyze recombinase activity in

Cx3cr1^{cre} or *Cx3cr1^{creER}* mice, these animals were crossed to *Rosa-26-yfp* (JAX stock 006148 B6.129X1-Gt(ROSA)26Sor<tm1(EYFP)Cos>/J)¹³⁵, *Rosa-26-rfp* (JAX stock 006067 129-Gt(ROSA)26Sor<tm2(CAG-Dsred2/EGFP)Luo>/J)¹³⁶ or *dTomato* reporter mice (007908 B6;129S6-Gt(ROSA)26Sor<tm14(CAG-tdTomato)Hze>/J)¹³⁷. In order to generate conditional MHC II mutant mice, Cre recombinase-transgenic animals were crossed with *I-Ab^{-/-}* (JAX stock 003584 B6.129S2-H2<dIAb1-Ea>/J)¹³⁸ and *I-Ab^{ff}* mice (JAX stock 013181 B6.129X1-H2-Ab1<tm1Koni>/J)¹³⁹. In order to generate conditional TNF mutant mice, Cre recombinase-transgenic animals were crossed to the *TNF^{ff}* strain, a gift of Sergei Nadospasov¹²⁷. In order to generate conditional MeCP2 mutants, Cre recombinase-transgenic mice were crossed with *MeCP2^{ff}* mice (JAX stock 007177 B6.129P2-Mecp2<tm1Bird>/J)⁶⁰. For the mixed BM chimeras with CCR2 deficiencies, the *CCR2^{-/-}* mice were used (JAX stock 004999 B6.129S4-Ccr2<tm1Ifc>/J)¹⁴⁰. For BM chimeras, 7–10-wk-old recipient animals were lethally irradiated (950 rad) and reconstituted with donor BM by i.v. injection of a minimum 10⁶ BM cells. Donor BM was isolated from femur and tibiae of donor mice, filtered through a 70µm mesh and resuspended in PBS for i.v. injection. All mice studied were on C57BL/6 background and handled under protocols approved by the Weizmann Institute Animal Care Committee (IACUC) in accordance with international guidelines.

2.2. Reagent administration

Tamoxifen (TAM; Sigma-Aldrich) was dissolved in 100% ethanol to a 1 g/ml solution and was 10-fold diluted in corn oil (Sigma-Aldrich) to a 100 mg/ml final solution for oral or i.p. administration. To induce Cre-mediated gene recombination in 5- to 7-wk-old *CX3CRI^{creER}* mice, 5 mg TAM was administered orally for 5 consecutive days (25 mg total) by gavage or subcutaneous injections. For active EAE induction, mice were injected into each flank with 50 µl emulsion containing 1mg/ml MOG₃₅₋₅₅ peptide (GeneScript, USA), 1:4 PBS and 1:2 Freund's incomplete adjuvant (Sigma) enriched with killed *M. tuberculosis* (BD), supplemented with 250ng pertussis toxin (Sigma) administered *i.p.* on day 0 and 2. For monocyte ablation, the anti-CCR2 antibody MC21¹⁴¹ was manufactured in-house by the Weizmann antibody unit, and 200ul of MC21 containing medium was administered *ip.* To induce a fever response, mice were administered 2mg/kg of LPS (Sigma) *i.p.*¹⁴².

2.3. EAE assessment

EAE was assessed according to accepted assessment index¹⁴³. The mice were monitored daily by being held at the base of the tail. The index is as follows: 0 - no symptoms; 0.5 - partial tail limp; 1 - complete tail limp; 1.5 - impaired gait; 2 - lose of pinch reflex in hind-limbs; 2.5 - one hind limb paralysis; 3 -complete hind limb paralysis; 3.5 - one forelimb paralysis; 4 - complete fore limb paralysis; 5 - death.

2.4. Glucose tolerance and insulin tolerance test (GTT, ITT)

Single-caged mice were put on starvation for 4 hours prior to test. For GTT, mice were weighed and injected with 2g /kg D-Glucose (Sigma). For ITT, mice were weighed and injected with 0.75 units/kg of human recombinant insulin (Beit Ha'emek, Israel). For both tests, blood glucose levels were measured using the Accu-check performa glucometer (Rosch Diagnostics) by tail bleeding 0, 15, 30, 60, 90 and 120 minutes after glucose or insulin injection.

2.5. Metabolic studies

Indirect calorimetry and food and water intake, as well as locomotor activity were measured using the Labmaster system (TSE-Systems, Bad Homburg, Germany). The LabMaster instrument consists of a combination of feeding and drinking sensors for automated online measurement. The calorimetry system is an open-circuit system that determines O₂ consumption, CO₂ production, and respiratory exchange ratio. A photobeam-based activity monitoring system detects and records ambulatory movements, including rearing in every cage. All the parameters are measured continuously and simultaneously. Data were collected after 48 hours of adaptation in acclimated singly housed mice. Cumulative food intake data was recorded every 30 seconds and was further used for meal microstructure analysis. Body composition was assessed using Echo-MRI (Echo Medical Systems, Houston, Texas).

2.6. Cold challenge

7 days before challenge, mice were anesthetized with ketamine/xylazine solution, and an implantable programmable temperature transporter 300 (iPTT 300; Bio medic data system, USA) was transplanted subcutaneously. At the day of the cold challenge, the mice were single-caged and transferred to a 4°C room in the animal facility. The mice were then monitored every 30 minutes for their body temperature changes using the SP-6005 data acquisition probe (Bio

medic data system, USA) over a period of 8 hours. After the cold challenge the mice were sacrificed and tissues were collected.

2.7. Isolation of tissue samples.

For peripheral analysis peripheral blood was collected by tail bleeds; mononuclear cells were enriched by Ficoll density gradient centrifugation (1000 x g. 15 min at 20°C with low acceleration and no brake). For spleen and lymph node analysis, tissues were collected and digested for 1 hour with 1 mg/ml collagenase D (Roche) in PBS containing magnesium and calcium (PBS +/-; Beit Ha'emek, Isarel), then macerated mechanically and filtered through a 70 µm mesh. For CNS analysis mice were perfused with 10 ml PBS via the left ventricle. Brain and spinal cord samples were harvested from individual mice and tissues were homogenized and incubated with a HBSS solution containing 2% BSA (Sigma-Aldrich), 1 mg/ml collagenase D (Roche), and 0.15 mg/ml DNase1, filtered through a 70 µm mesh. Homogenized sections were filtered through 80 µm wire mesh and resuspended in 40% Percoll, prior to density centrifugation (1000 x g. 15 min at 20°C with low acceleration and no brake). For spinal cord endothelium extraction, spinal cord were removed as above and digested with 0.1 mg/ml Collagenase 11, 2mg/ml Collagenase 2, 0.2 mg/ml Dnase1 and 0.1mg/ml Hylurodinase 1 (Sigma-Aldrich). For heart macrophage analysis, the heart was macerated and incubated with 1 mg/ml collagenase-2 (Sigma) and 0.15 mg/ml DNase1 (Sigma-Aldrich) at 37°C for 30 min during constant agitation. The resulting cell suspension was filtered through a 70 µm mesh and erythrocytes were removed by ACK lysis. For adipose tissues (BAT, vWAT and scWAT) the tissues were collected, shredded roughly by scissors and then incubated for 30 minutes with DMEM medium (Beit Ha'emek, Israel) containing 1 mg/ml collagenase-2 (Sigma-Aldrich), 2% BSA (Sigma-Aldrich) and 30Mm HEPES buffer (Beit-Ha'emek, Israel). The resulting cell suspension was filtered through a 70 µm mesh and erythrocytes were removed by ACK lysis.

2.8. Ex vivo stimulation

For Th1/17 stimulation, spinal cord or lymph nodes samples were prepared as above, and were incubated for 3 hours in RPMI medium containing 10% fetal calf serum, 1:100 pen strep antibiotic, 1:100 l-glutamine, 1:100 MEM and 1:100 sodium pyruvate (Beit Ha'emek, Israel) supplemented with either 20ug/ml MOG₃₅₋₅₅ peptide (GeneScript, USA) or ionomycin and PMA (Sigma). The cell suspensions were then further incubated with the same solution as above,

supplemented with 1ug/ml Brefeldin A (Sigma-Aldrich) for 3 additional hours, prior to antibody staining. For recall assay, CX3CR1^{Cre}:TNF^{f/f} mice were subjected to the EAE protocol as above, and at day 6 inguinal and popliteal lymph nodes were removed, digested, and incubated with the above RPMI medium containing MOG₃₅₋₅₅ peptide for 72 hours, prior to antibody staining. For ex vivo LPS stimulation, brain cell suspensions were incubated with the above RPMI medium supplemented with 10 ug/ml LPS for 2 hours, followed by incubation in the presence of Brefeldin A for additional 2 hours.

2.9. Flow cytometry

Following cell suspension, cells were incubated in FACS buffer (PBS with 1% BSA, 2mM EDTA and 0.05% sodium azide) in the presence of staining antibody. For intracellular staining, the CytoFix/Cytoperm Kit (BD) was used according to the instruction of the manufacturer. Cells were acquired on FACSCanto, LSRII, and LSRFortessa systems (BD) and analyzed with FlowJo software (Tree Star). For cell sorting, the FacsAria (BD) was used. Antibodies used throughout the research are depicted in Table 1. For the CX₃CL1-Fc stain, cell suspensions were blocked with goat IgG for 10 mins, incubated with the CX₃CL1 -Fc fusion protein¹³⁴ for 20 mins followed by staining with a cy5-goat anti human IgG was added, for additional 20 minutes.

Table 1. Antibodies used in this research.

Antibody name	Clone/ cat no.	manufacturer
CD11b	M1/70	Biolegend
CD11c	N418	Biolegend
CD14	Sa2-8	Biolegend
F4/80	BM8	Serotech
MHCII	M5/114.15.2	Biolegend
CD45.1	A20	Biolegend
CD45.2	104	Biolegend
B220	RA3-6B2	Biolegend
CD115	AFS98	Biolegend
Gr1	RB6-8C5	Biolegend
Ly6C	AL21	Biolegend
Ly6G	1A8	Biolegend
CD4	H129.19	Biolegend
CD8	53-6.7	Biolegend
MerTK	BAF591	R & D systems
CD135/Flt3	A2F10	Biolegend
CD45	30F11	Biolegend
CD62L	MEL14	Biolegend
CD64	90322	Biolegend
CD86	GL-1	Biolegend
CD80	16-10A1	Biolegend
CD40	3/23	Biolegend

MAC3	M3/84	Biologend
IL-17A	TC11-18H10.1	Biologend
IFN-gamma	XMG1.2	Biologend
TNF	MP6-XT22	Biologend
CD44	IM7	Biologend
CD31	390	Biologend
PDL1	10F.9G2	Biologend
CD206	C068C2	Biologend
CD301	LOM-14	Biologend
MeCP2		Millipore
TH		Abcam
GFP		Abcam
Iba1		WAKO
Anti-rabbit Alexa 488		Jackson
Anti-goat Alexa 488		Jackson
Anti-chicken Alexa 488		Jackson
Anti-rat cy3		Jackson
Cy5 Goat anti human IgG		Jackson

2.10. Histology

For hematoxylin and eosin (H & E) or luxol fast blue (LFB) staining, tissues were embedded in paraffin and serially sectioned. For immunofluorescence, tissues fixed in 4% paraformaldehyde overnight at 4°C, incubated with 30% sucrose overnight and flash-frozen with isopentane before sectioning by cryostat. Samples were blocked with 0.3% triton and 1:20 normal horse serum before incubation with primary antibodies overnight in 4°C, following an incubation with secondary antibody in PBS at RT for 2 hours. For immunohistochemistry of UCP1, immunohistochemistry was carried out on paraffin sections with the avidin-biotin-peroxidase (avidin biotin complex method; Vector Laboratories, Burlingame, California) using rabbit anti-Ucp1 Ab (Abcam).

2.11. Genomic DNA extraction

Sorted cells were lysed and digested in TES buffer (10mM Tris buffer, pH=8, 5mM EDTA, 0.1 M NaCl, 0.5% SDS and 100 ug PK) overnight in 56°C. DNA was precipitated in 70% ethanol for 30 mins in RT, centrifuged twice at top speed and the tubes were left to dry. The pellet was reconstituted with TE buffer for subsequent PCR. Genomic PCR for TNF was performed with the following primer: TACACAGAAGTCCCAAATG, GAAATCTTACCTACGACGTG, CTCTTAAGACCCACTTGCTC. Genomic PCR for MeCP2 was performed using the following primers: TGGTAAAGA CCCATGTGACCCAAG, GGCTTGCCACATGACAAGAC, TCCACCTAG CCTGCCTGTACTTTG.

2.12. RNA Isolation, Library Construction, and Analysis

RNA-seq was performed as described earlier¹⁴⁴. Briefly, 10^4 – 10^5 cells from each population were sorted into 100–200 μ l of lysis/binding buffer (Life Technologies). mRNA was captured with 12 μ l of Dynabeads oligo(dT) (Life Technologies), washed, and eluted at 70°C with 10 μ l of 10 mM Tris-Cl (pH 7.5). We sequenced an average of 4 million reads per library and aligned them to the mouse reference genome (NCBI 37, mm9) using TopHat v2.0.10 with default parameters. Expression levels were calculated and normalized using ESAT software (<http://garberlab.umassmed.edu/software/esat>). RNA-seq analysis focused on genes in 25th percentile of expression with a 2-fold differential between at least two populations.

2.13. ELISAs

IL-1b was measured using the DueSet kit (R & D). Leptin was measured using the Quantikine kit (R & D). Insulin was measured using the mouse/rat Insulin kit (Millipore). ELISA were performed according to the manufacturer's instructions.

2.14. Quantitative real time PCR

Total RNA was extracted with RNeasy Mini Kit (QIAGEN). RNA was reverse transcribed with a mixture of random primers and oligo-dT with a High-Capacity cDNA Reverse Transcription Kit (Applied Biosystems). PCRs were performed with SYBR Green PCR Master Mix kit (Applied Biosystems). Real-time PCRs were carried out on a 7500 real-time PCR system using fluorescent SYBR Green technology (Applied Biosystems). Quantification of the PCR signals of each sample was performed by comparing the cycle threshold values (Ct), in duplicate, of the gene of interest with the Ct values of the GAPDH housekeeping gene. DNA primers used in the research are detailed in Table 2.

Table 2. list of DNA primers used for real time PCR in the research.

<i>Gene</i>	<i>Forward primer</i>	<i>Reverse primer</i>	<i>Accession number</i>
<i>Adrb3</i>	GGCAACCTGCTGGTAATCAT	GCATTACGAGGAGTCCCAC	NM_013462.3
<i>AgRP</i>	AAGCTTTGGCGGAGGTGCTAGAT	AAGCAGGACTCGTGCAGCCTTACA	NM_007427.2
<i>Dio2</i>	TCCTCCTAGATGCCTACAAACAGG	ATTCAGGATTGGAGACGTGCAC	NM_010050.2
<i>lpr</i>	ACACTGAAGGGAAGACACT	GGGTTCTTAGGTAATGGCTCC	NM_146146

<i>Mc3r</i>	CTGTAGCAACGGGTGTCGG	ATCAGCCTGCCTCATCCC	NM_008561.3
<i>Mc4r</i>	CAAGAACCTGCACTCACCCA	GACCCATTGAAACGCTCAC	NM_016977.3
<i>npy</i>	TCAGACCTCTTAATGAAGGAAAGCA	ATGAGGGTGGAAACTTGAAAAG	NM_023456
<i>Ucp1</i>	GGCATTGAGAGGCAAATCAGCT	CAATGAACACTGCCACACCTC	NM_009463
<i>th</i>	CCAAGGTTTCATTGGACGGC	CTCTCCTCGAATACCACAGC	NM_009377
<i>Pgcal</i>	AGCCGTGACCACTGACAACGAG	GCTGCATGGTTCTGAGTGCTAAG	NM_008904
<i>tnf</i>	CTGAACTTCGGGGTGATCGG	GGCTTGTCACCTCGAATTTTGAGA	NM_001278601
<i>inos</i>	CTGCAGCACTTGGATCAGGAACCTG	GGGAGTAGCCTGTGTGCACCTGGA	NM_010927
<i>Mecp2</i>	GCTTTCTGATGTTTCTGCTTTGC	ACCTTAGCCCACCATTCTG	NM_001081979
<i>Gapdh</i>	CAAGGTCATCCATGACAACCTG	GGCCATCCACAGTTCTGG	NM_001289726

2.15. Western blot

Adipose tissues were harvested in buffer A (25 mmol/l Tris-HCl [pH 7.4], 10 mmol/l sodium orthovanadate, 10 mmol/l sodium pyrophosphate, 100 mmol/l sodium fluoride, 10 mmol/l EDTA, 10 mmol/l EGTA, and 1 mmol/l phenylmethylsulfonyl fluoride). Supernatants (12,000 g) of cell extracts (50–150 μ g CHO-T cells; 15–30 μ g murine islets) were resolved by SDS-PAGE and Western blotted with the indicated antibodies.

2.16. Statistical analysis

Results are expressed as means \pm SEM. Statistical analysis was performed using Student's T test, Mann-Whitney's U test, ANOVA or repeated-measurements 2-way ANOVA with post hoc Student's *t* tests or paired Student's *t* tests, as appropriate using the GraphPad Prism (San Diego, CA). PCA analysis was performed using the MATLAB interface. GO analysis was performed using the DAVID bioinformatics resources¹⁴⁵.

3. Results - Part I: Brown adipose tissue macrophages control energy expenditure

3.1. The CX₃CR1^{Cre} and CX₃CR1^{CreER} mouse models allow the study of tissue macrophages

We recently generated CX₃CR1^{Cre} and CX₃CR1^{CreER} animals¹² by targeted insertion of the respective Cre recombinase genes into CX₃CR1 loci, mimicking the CX₃CR1^{gfp} locus, previously shown to tightly reflect endogenous CX₃CR1 expression¹³⁴ (**Figure 7**). CX₃CR1^{Cre} mice express

constitutively active Cre recombinase resulting in the spontaneous irreversible rearrangement of loxP site-flanked ('floxed') alleles in CX₃CR1 expressing cells. In contrast, the CX₃CR1^{CreER} system comprises a conditional active Cre recombinase that is fused to a mutated ligand-binding domain of the human estrogen receptor (ER)¹⁴⁶. Two point mutations in the ER-LBD prevent constitutive activation of the CreER protein by endogenous estradiol, still allowing binding of the synthetic estrogen antagonist tamoxifen (TAM)¹⁴⁶. In the unbound form, the CreER fusion protein resides in the cytoplasm in an inactive complex with heat shock proteins. TAM administration frees the CreER protein to translocate to the nucleus and mediate the site-specific recombination.

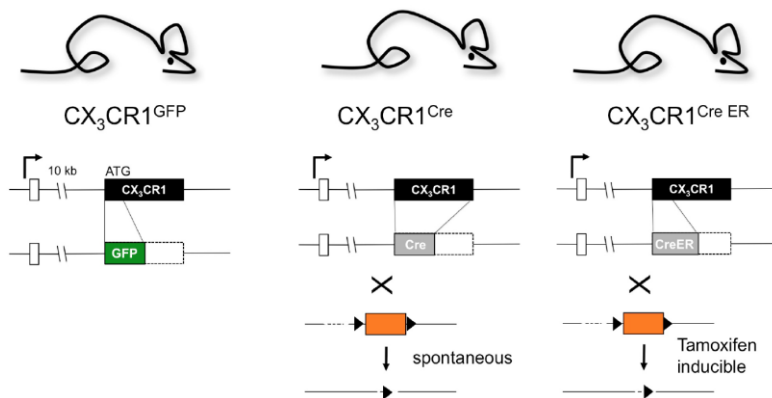


Figure 7. Scheme of CX₃CR1^{Cre} and CX₃CR1^{CreER} systems¹².

Importantly, CX₃CR1^{Cre} and CX₃CR1^{CreER} animals differ considerably with respect to the cells they target. CX₃CR1^{Cre} animals target CX₃CR1⁺ expressing cells and cells derived from CX₃CR1⁺ cells that subsequently silenced CX₃CR1 expression. CX₃CR1^{Cre} animals can therefore report on the history of cells and be used for fate mapping, as well as gene manipulation¹². After crossing the CX₃CR1^{Cre} mice with Rosa26:YFP reporter animals¹³⁵, virtually all tissue macrophages were found labeled, because all these cells pass a CX₃CR1⁺ stage during their development (**Figure 8A**); in addition, also blood monocytes of CX₃CR1^{Cre}:YFP animals are found efficiently labeled (**Figure 8B**). Thus, the CX₃CR1^{Cre} system targets the mononuclear phagocyte system broadly, including all tissue resident macrophages, monocytes and their progeny and also partially DC¹⁴⁷. In contrast, the CX₃CR1^{CreER} system depends on cells actively transcribing from the CX₃CR1 promoter at the time of TAM exposure. Accordingly, microglia and gut macrophages, which are CX₃CR1⁺ cells at the adult steady state, are efficiently labelled

in TAM-treated CX3CR1^{CreER}:R26-YFP mice; however, most other tissue macrophages, which silenced their CX3CR1 promoter remain unlabeled, even following extended TAM exposure¹². Importantly, the latter finding excludes ongoing contributions of CX3CR1⁺ monocytes to these resident macrophage compartments (**Figure 8A**). Another prominent feature of the CX3CR1^{CreER} system are its kinetics; CX3CR1⁺ macrophages with long half-lives, such as the self-renewing microglia, will permanently retain TAM-induced genetic modifications after the induction. In contrast, CX3CR1⁺ monocytes and CX3CR1⁺ gut macrophages have, with 20 hrs and 3 weeks¹², a much shorter half-life and are after TAM-treatment replaced by new BM-derived cells with genomic WT configuration. When combined CX3CR1^{Cre} and CX3CR1^{CreER} mice thus allow studying the relationship of monocyte-derived macrophages and resident tissue macrophages.

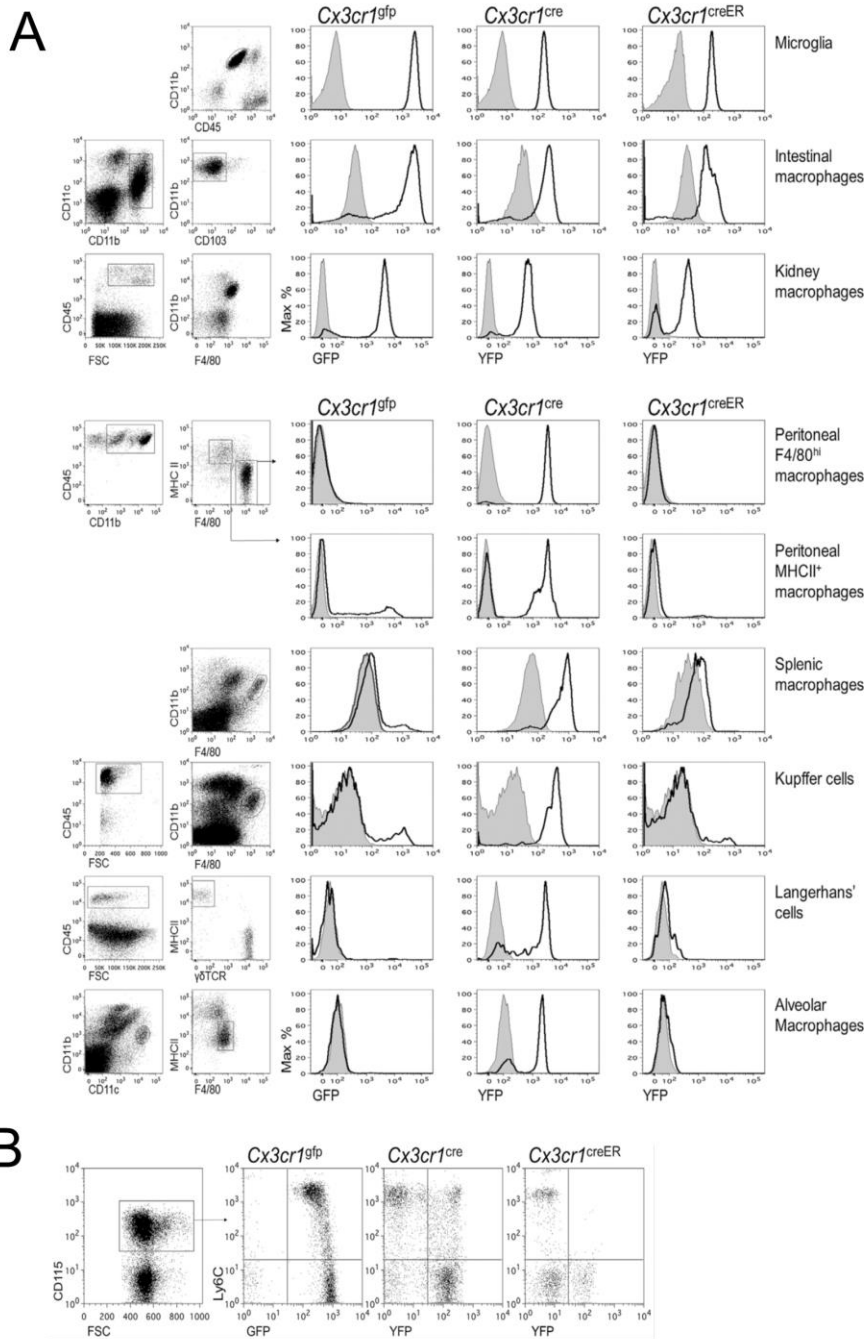


Figure 8. Tissue macrophage and monocyte targeting by the CX3CR1 Cre and CreER systems. A. Flow cytometry (FACS) analysis of mononuclear phagocyte populations of $CX3CR1^{gfp}$, $CX3CR1^{Cre}$:R26-YFP, and $CX3CR1^{CreER}$:R26-YFP mice. $CX3CR1^{CreER}$:R26-YFP mice were treated for 4 weeks with TAM prior to analysis. Results are representative of six mice per group. (B) FACS analysis of blood monocytes of $CX3CR1^{gfp}$, $CX3CR1^{Cre}$:R26-YFP, and $CX3CR1^{CreER}$:R26-YFP mice. $CX3CR1^{CreER}$:R26-YFP mice were treated for 4 weeks with TAM prior to analysis. Results are representative of four to six mice per group. published in reference¹².

Like CX3CR1^{gfp} mice¹³⁴, also the CX3CR1^{CreER} system emerged as a powerful tool for microglia research, due to the high activity of the promoter in these cells¹⁴⁸ and microglial self-renewal capacity. To establish the robustness of the CX3CR1^{CreER} system for the use in microglia research, we generated CX3CR1^{CreER}:R26:YFP/R26:RFP double reporter mice, in which the alleles of the Rosa26 locus carry insertions of lox-stop-lox flanked YFP or RFP reporter genes^{135,149}, respectively. These double reporter mice were given TAM either via oral administration (gavage), or by subcutaneous injection. 30 mg of orally administered TAM, and 40 mg of subcutaneously administered TAM were sufficient to induce either YFP or RFP expression in >95% of microglia, and >80% of microglia co-expressed both reporter genes (**Figure 9A**). Thus, the CX3CR1^{CreER} model is sufficiently robust to drive the excision of two ‘floxed’ alleles in a majority of cells. Of note, certain lymphocyte subsets and myeloid cells, other than microglia express CX₃CR1¹³⁴. TAM treatment of CX₃CR1^{CreER} mice results accordingly also in gene rearrangement in these cells¹² (**Figure 9B**), including monocytes, some DC and peripheral macrophages. Importantly, these are exactly the cells that have confounded the functional analysis of the microglia compartment in the previous studies. However, most peripheral myeloid cells that underwent Cre activation and rearrangements have a limited half-life and are continuously replaced by BM-derived cells. Genetic modifications, such as the activation of the YFP reporter gene or the deletion of “floxed” alleles are thus progressively lost with time in these populations. In contrast, the resident microglia pool, which self-renews without further input from the BM³, retains once introduced gene modifications throughout the life of the organism (**Figure 9B**). This feature thus allows generation of animals that harbor specific genetic manipulations restricted to microglia and other defined CX3CR1 expressing tissue macrophages, such as BAT macrophages (see below). Of note, there are also other tissue macrophage populations, such as Kupffer cells and peritoneal macrophages that are established before birth and then self-renew^{12,17}. However, as most of these cells lack CX₃CR1 expression, they are not targeted by the CX₃CR1^{CreER} system in adulthood¹². Classical DC that derive from CX₃CR1⁺ precursors or themselves express the receptor¹⁵⁰ on the other hand lose their gene modifications, as they are short lived and hence progressively replaced by BM-derived cells (**Figure 9B**). Taken together, the combination of CX₃CR1^{Cre} and CX₃CR1^{CreER} animals provides a novel and unique tool to probe for the involvement of microglia in CNS development, CNS maintenance and CNS responses to pathological challenges, which does not involve artifacts such as the ones

introduced by BM transplantations. At the same time the system can be used to study defined tissue macrophage populations, such as the ones residing in BAT.

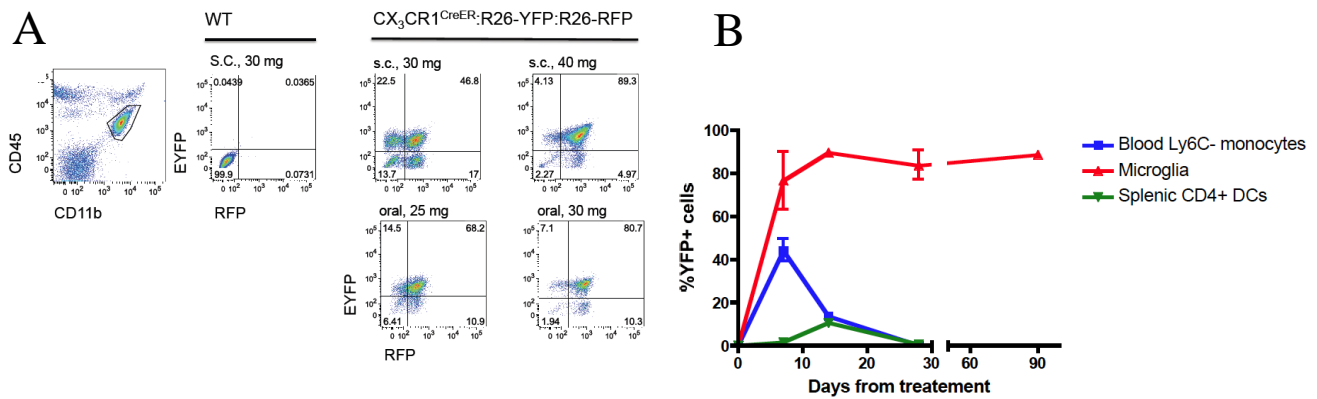


Figure 9. The $CX3CR1^{CreER}$ system is robust and can be used to exclusively target microglia in the brain. A. $CX3CR1^{CreER}:R26-YFP/R26-RFP$ double reporter mice were treated with TAM either by subcutaneous injections (10 mg for 3 or 4 consecutive days) or oral administration (5 mg for 5 or 6 consecutive days). B. $CX3CR1^{CreER}:R26-YFP$ mice were treated with 30 mg TAM orally, and then the YFP+ fractions of cells were assessed 7, 14, 28 and 90 days after administration in the blood, spleen and brain.

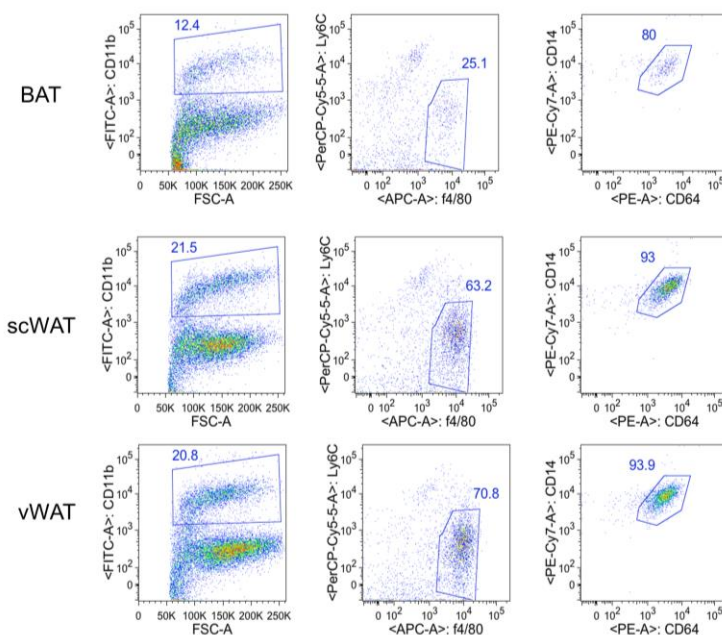
3.2. MeCP2 deletion in brown adipose tissue macrophages results in spontaneous obesity

Tissue resident macrophages display distinct transcriptomes and enhancer landscapes^{32,33} that are prominently imprinted by the specific environment they reside in³³. The study of tissue macrophages and their contribution to tissue functions hence requires the analysis of *ex vivo* isolates, rather than cultured cells. Macrophages in adipose tissue including BAT, vWAT or scWAT all display a canonic ‘macrophage signature’ of cell surface markers³² and can be characterized as CD11b⁺ F4/80⁺ CD14⁺ CD64⁺ cells, similar to other macrophages, including cardiac macrophages¹³³ (**Figure 10**). To further define these macrophage populations in adipose tissue, as well as their specific contributions to maintenance and function of the distinct fat tissues, we profiled their transcriptomes by RNA-seq. PCA analysis of the transcriptomes of adipose tissue macrophage (ATM) revealed, that they clustered together and remote from other tissue resident macrophages, most notably those of inner organs, such as intestinal, Kupffer cells and peritoneal macrophages (**Figure 11A**). Thus, ATM are a distinct compartment within the tissue resident macrophages. We are currently in the process of defining distinctive features of brown and white fat macrophages. Preliminary clustering of the cells show, surprisingly, that the

ATM of the subcutaneous white fat are distant from either macrophages residing in the brown adipose tissue or the visceral adipose tissue.

Flow cytometry analysis of ATM revealed that BAM, but not WAM comprise a distinct and prominent populations of CX3CR1^{hi} cells, as revealed in CX3CR1^{gfp} mice, and by direct staining for CX3CR1 using a CX3CL1-Fc fusion protein¹³⁴ (**Figure 11B-D**). In contrast, BAM and WAM obtained from CX3CR1^{Cre}:R26-RFP mice were both >90% labelled, establishing that the CX3CR1^{Cre} systems broadly targets all ATM (**Figure 11E**). Importantly, TAM-induced fate mapping of the macrophages of the various fat tissues using CX3CR1^{CreER}:TdTomato mice revealed that BAM are long lived cells compared to the macrophages of the vWAT and scWAT. In TAM-treated CX3CR1^{CreER}:TdTomato over 50% of the BAM were found stably labeled (**Figure 11F**) even after prolonged time; thus the majority of the BAM has self-renewal capacity with limited input from the BM. Unlike WAM, BAM can hence be efficiently targeted by the CX3CR1^{CreER} system. Finally, we tested the radiosensitivity of the cells by lethally irradiating CD45.1 recipient mice and transplanting BM from CD45.2: CX3CR1^{gfp} donors. The majority of the BAM were found replaced by the transplant-derived cells, although to some less extent than cardiac and WAT macrophages; thus, the cells are radiation-sensitive, unlike microglia (**Figure 11G**).

Figure 10. Gating and sorting strategy for the various ATM throughout the research.



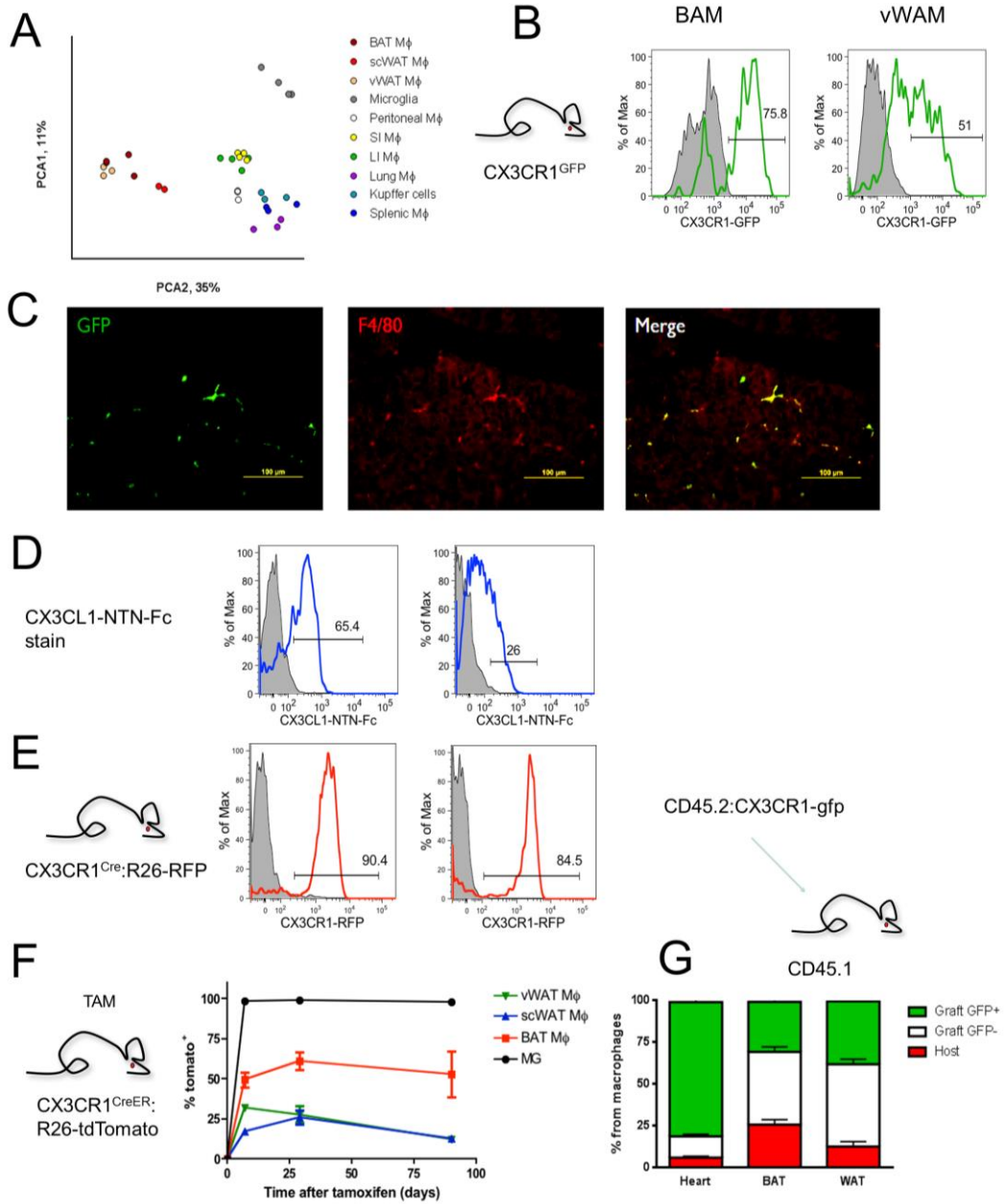


Figure 11. Brown adipose tissue macrophage (BAM) characterization. A. FACS analysis of BAM isolated from WT mice. B. GFP fluorescence in BAM and white adipose tissue macrophages (WAM) isolated from CX3CR1^{gfp} mouse. C. Histological analysis of GFP expression (green) and F4/80 (red) in BAT of CX3CR1^{gfp} mouse. D. CX3CL1-Fc stain of BAM and WAM isolated from the same WT mouse. E. RFP fluorescence in BAM and WAM obtained from CX3CR1^{Cre}:R26-RFP mouse. F. Fate mapping of the various ATM in TAM- treated CX3CR1^{CreER}:tdTomato mice. N=3. G. FACS analysis of chimersim of cardiac macrophages, BAM and vWAM in lethally irradiated CD45.1 mice reconstituted with 2×10^6 CD45.2: CX3CR1^{gfp} BM cells. N=4.

Mutations in the Methyl DNA-binding protein MecP2 have emerged as critical drivers of the RETT syndrome. Recent evidence show that MeCP2 is expressed in many tissue macrophages, and contributes to the fine-tuning of their survival and output⁶⁸. To investigate potential contributions of MecP2-deficient macrophages to RETT disease development, we crossed CX3CR1^{Cre} animals with mice that harbor a conditionally mutant, 'floxed' MeCP2 gene⁵⁸. The *MeCP2* locus is on the X chromosome and we hence worked exclusively with male mice, in order to avoid female mosaicism due to X chromosome inactivation⁵⁷. Cre recombinase-mediated rearrangement of the 'floxed' *mecp2* allele results in a deletion between exon 3 and 4, resulting in a truncated transcript⁶⁰. RNA-seq analysis and the respective Integrative Genomics Viewer (IGV) tracks revealed that in microglia isolated from CX3CR1^{Cre}:MeCP2^{fl/y} mice, exon 4 is indeed truncated, while the neighboring gene IRAK1 was found intact (**Figure 12A**). In order to confirm the genomic deletion of the *MeCP2* gene, MeCP2^{fl/Y} and CX3CR1^{Cre}:MeCP2^{fl/Y} microglia were sorted from the respective mice, and primers which amplify the deleted allele (400 bp), as well as the intact floxed allele (500 bp) were used for the diagnostic PCR. The deleted allele was only detected in samples containing CX3CR1^{Cre}:MeCP2^{fl/Y} DNA (**Figure 12B**). In addition, MeCP2 protein levels were reduced in microglia isolated from CX3CR1^{Cre}:MeCP2^{fl/Y} mice, as indicated by flow cytometry following intracellular staining for the nuclear protein (**Figure 12C**).

Unlike MeCP2^{-/-} mice¹⁵¹, or MeCP2^{fl} animals crossed with general Cre deleter mice⁶⁰, CX3CR1^{Cre}:MeCP2^{fl/y} mice were viable and did not exhibit any RTT-like symptoms, such as reduced weight, abnormal hind limb clasping, anxiety, breathing abnormalities or premature death (**Figure 13A-B**). In fact, CX3CR1^{Cre}:MeCP2^{fl/y} mice were indistinguishable from their CX3CR1^{Cre} littermates until the age of 3-4 months. However then, CX3CR1^{Cre}:MeCP2^{fl/y} mice started to increasingly gain weight and from 15 weeks of age on, the mice were significantly heavier than their CX3CR1^{Cre} littermates. By the age of 6 months, CX3CR1^{Cre}:MeCP2^{fl/y} mice were severely obese, weighing ~30% more than controls (**Figure 13C-D**). CX3CR1^{Cre}:MeCP2^{fl/y} mice exhibited 2 - 3 fold enlarged and fatty livers, and larger visceral adipose tissue; spleens were however normal with no signs of splenomegaly (**Figure 14A-B**). Histology revealed enlarged adipocytes and the formation of characteristic 'crown-like structure', as well as fat-loaded

hepatocytes (**Figure 14C**). In addition to total body weight gain, the percentage of fat tissue, measured by ECHO-MRI was found significantly increased in $CX3CR1^{Cre}:MeCP2^{fl/y}$ mice (**Figure 14D**).

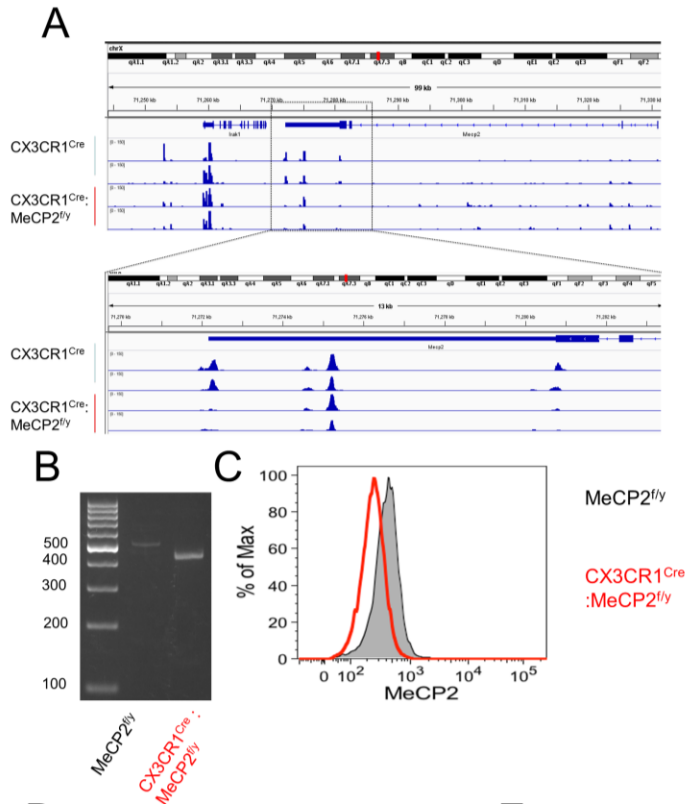


Figure 12. Efficient MeCP2 deletion in $CX3CR1^{Cre}:MeCP2^{fl/y}$ mice. A.

Integrative Genomics Viewer (IGV) tracks of the MeCP2 transcript in sorted MeCP2^{fl/y} and $CX3CR1^{Cre}:MeCP2^{fl/y}$ microglia. B. PCR of the unrearranged (~500 bp) and excised MeCP2^{fl} alleles (~400 bp) on genomic DNA of sorted microglia from MeCP2^{fl/y} and $CX3CR1^{Cre}:MeCP2^{fl/y}$ mice. C. FACS analysis of MeCP2 expression by WT and mutant microglia by intracellular stain.

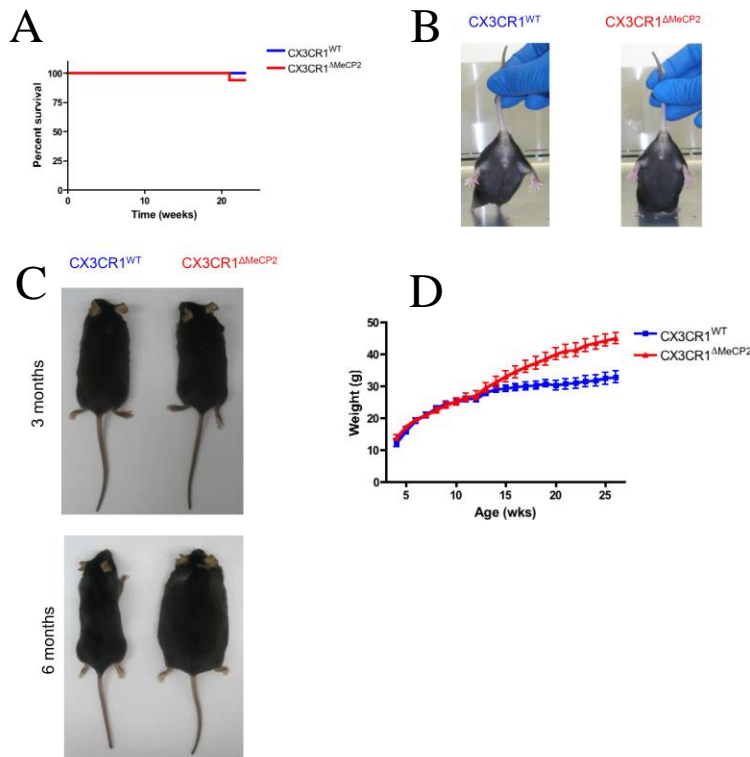


Figure 13. A. Myeloid MeCP2 deletion does not cause a RTT symptom, but spontaneous obesity.

(A) Survival curve of $CX3CR1^{Cre}$ ($n=8$) and $CX3CR1^{Cre}:MeCP2^{fl/y}$ ($n=14$) mice over 6 months. B. $CX3CR1^{Cre}$ and $CX3CR1^{Cre}:MeCP2^{fl/y}$ littermates at the age of 3 months exhibit intact hind limb clasping. C. $CX3CR1^{Cre}$ and $CX3CR1^{Cre}:MeCP2^{fl/y}$ littermates at the ages of 3 months (top panel) and 6 months (bottom panel). D. Weight of $CX3CR1^{Cre}$ ($n=9$) and $CX3CR1^{Cre}:MeCP2^{fl/y}$ mice ($n=14$) over 6 months. *** $p < 0.001$, two-way Anova, interaction eff

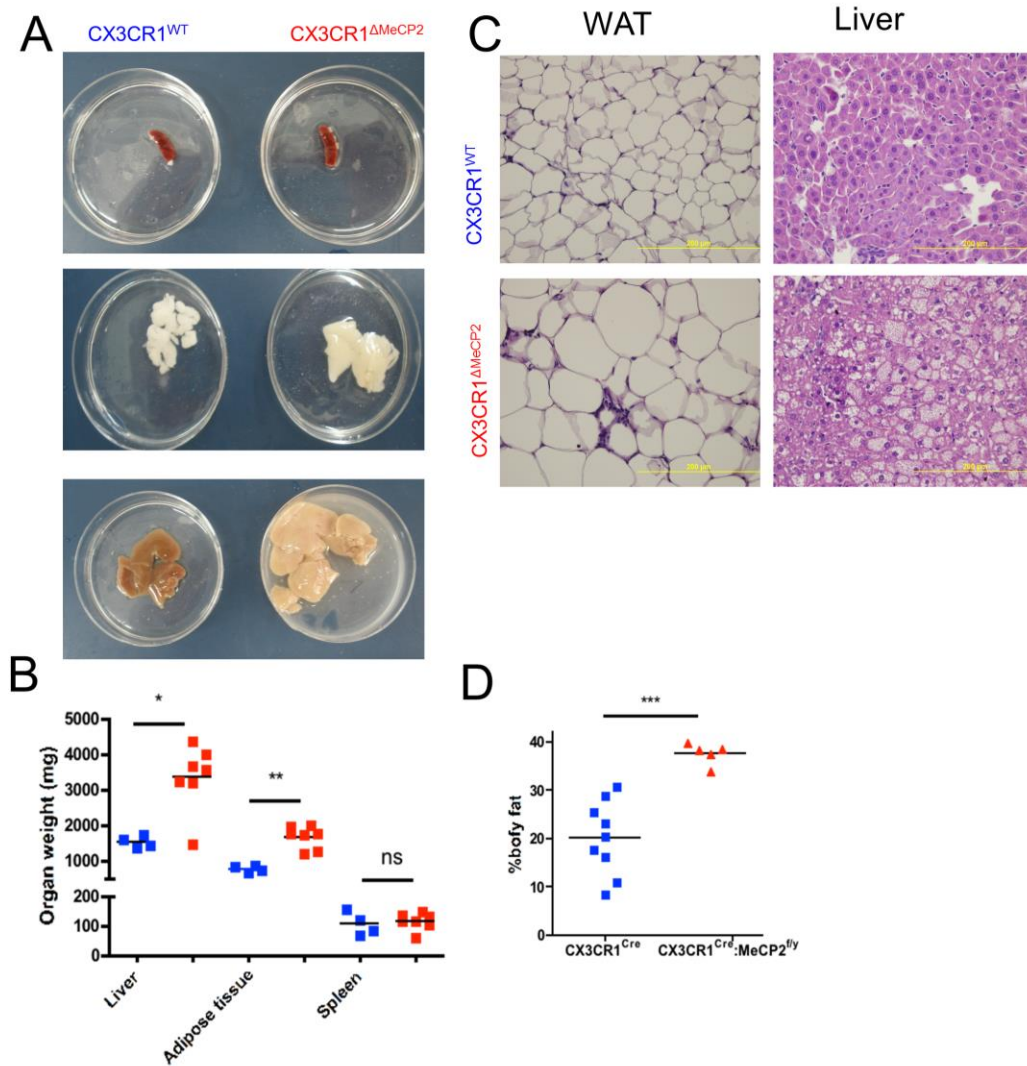


Figure 14. Increased livers and adipose tissues, but not spleens, in $CX3CR1^{Cre}:MeCP2^{fl/y}$ mice. A. Spleen, liver and adipose tissue of littermate $CX3CR1^{Cre}:MeCP2^{fl/y}$ and $CX3CR1^{Cre}$ mice at 6 months. B. Organ weight at 6 months. $N=4-7$, * $p<0.05$, ** $p<0.01$, Mann-Whitney's *u*-test. C. H & E stain of white adipose tissue (left) and liver (right) of $CX3CR1^{Cre}$ and $CX3CR1^{Cre}:MeCP2^{fl/y}$ littermates at the age of 6 months. D. % body fat out of whole body composition of $CX3CR1^{Cre}$ and $CX3CR1^{Cre}:MeCP2^{fl/y}$ littermates at the age of 6 months. $N=5-9$, *** $p<0.001$, Student's *t*-test.

To further restrict the MeCP2 myeloid deficiency, we crossed the MeCP2^{fl} mice to the TAM-inducible CX3CR1^{CreER} mice. Upon TAM administration, MeCP2 was efficiently deleted in microglia, as documented both on the genomic level and by flow cytometry (**Figure 15A-B**). CX3CR1^{CreER}:MeCP2^{fl/y} mice and control littermates were administered TAM at 6 weeks of age. Both groups of mice initially responded to the TAM administration with a loss of body weight,

but soon caught up. Interestingly, TAM-treated $CX3CR1^{CreER};MeCP2^{fl/y}$ mice but not control littermates exhibit a significant weight gain by 6 months post TAM, similar to the $CX3CR1^{Cre};MeCP2^{fl/y}$ mice (**Figure 15C-D**). In concordance with the $CX3CR1^{Cre};MeCP2^{fl/y}$ mice, these animals also displayed increased liver, adipose tissue and percentage of body fat (**Figure 15E**). Three months after TAM administration $CX3CR1^{CreER};MeCP2^{fl/y}$ mice exhibited an intact glucose metabolism, as their glucose removal rate in a glucose tolerance test was indistinguishable from that of littermate controls (**Figure 16A**). An insulin tolerance test revealed similar rates of glucose removal, thus the mice also do not develop hidden insulin resistance at this stage (**Figure 16B**). By 6 months after TAM however, hallmarks of obesity and impaired glucose metabolism, such as leptin, fed insulin and fed glucose levels were elevated in sera of the mice (**Figure 16C-E**). Thus the mice become diabetic not as a direct effect of the TAM treatment, but as a secondary event due to the excessive weight.

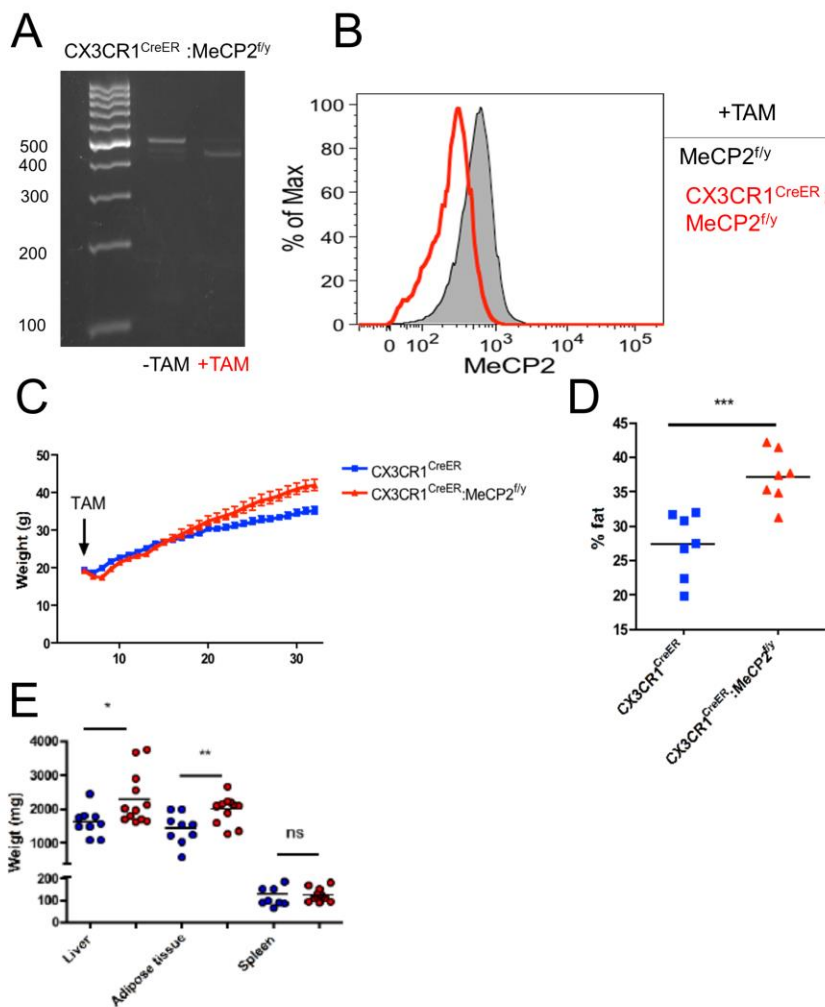


Figure 15. Conditional MeCP2-deficiency results in spontaneous obesity of $CX3CR1^{CreER};MeCP2^{fl/y}$ mice. A. PCR for the intact and the excised $MeCP2^{fl/y}$ allele (~400 bp) on DNA of sorted microglia from $CX3CR1^{CreER};MeCP2^{fl/y}$ mice, either non-treated or treated with TAM in vivo. B. intracellular FACS analysis for MeCP2 on microglia from the same mice. D. Weight of $CX3CR1^{CreER}$ ($n=13$) and $CX3CR1^{CreER};MeCP2^{fl/y}$ ($n=14$) mice over 6 months, all administered with TAM at the age of 6 weeks. *** $p<0.001$, interaction effect following two way annova. B. % body fat out of whole body composition of $CX3CR1^{CreER}$ and $CX3CR1^{CreER};MeCP2^{fl/y}$ littermates at the age of 6 months, all treated with

tamoxifen at the age of 6 weeks. $N=7$, *** $p<0.001$, Student's t-test. C. Organ weights at 6 months. $N=9-11$, * $p<0.05$, ** $p<0.01$, Student's t-test.

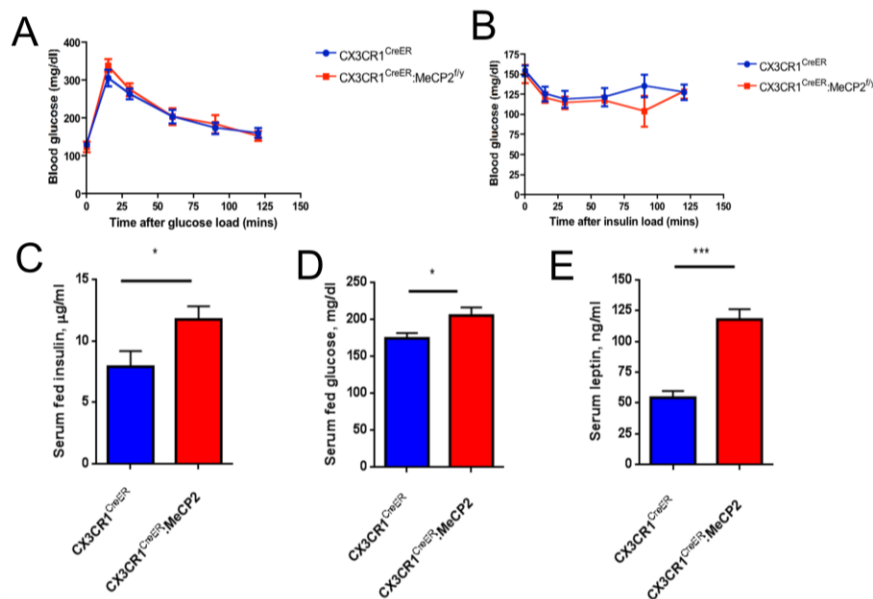


Figure 16. Metabolic parameters of $CX3CR1^{CreER};MeCP2$ mice at 3 months and 6 months of age. A. Glucose tolerance test (GTT, A) and insulin tolerance test (ITT, B) performed in pre-obese starved mice 3 months after TAM administration. $N=7$. C-E. Serum insulin (C), glucose (D) and leptin levels (E) in $CX3CR1^{CreER}$ and $CX3CR1^{CreER};MeCP2^{fl/y}$ mice 6 months after TAM administration. $N=13$, * $p<0.05$, *** $p<0.001$

We next performed a series of metabolic measurement to unravel the mechanism behind the obesity phenotype in the absence of myeloid MeCP2. We chose to focus on the $CX3CR1^{CreER};MeCP2^{fl/y}$ mice, since these mice have a restricted and limited MeCP2 deletion and thus are less prone to confounds and artifacts. $CX3CR1^{CreER};MeCP2^{fl/y}$ mice were given TAM and evaluated for food consumption and energy expenditure 3 and 4 months after. Of note, by this time, the mice were not yet obese. Effects seen in the metabolic evaluation are hence unlikely to be secondary effect of the obesity phenotype itself. $CX3CR1^{CreER};MeCP2^{fl/y}$ mice presented normal circadian oscillations in food consumption (**Figure 17A**) and did not consume more food compared to their littermate controls (**Figure 17B**). However, $CX3CR1^{CreER};MeCP2^{fl/y}$ mice displayed significantly less energy expenditure, as calculated by indirect measurement¹⁵² at both time points (**Figure 17C-D**). The mice expand less energy specifically during the dark phase, which is the active phase in which both food consumption, locomotion and energy expenditure are elevated. Interestingly, 3 months after TAM, $CX3CR1^{CreER};MeCP2^{fl/y}$ mice partially compensated for the attenuated energy expenditure by elevating their locomotion, thereby likely delaying the weight gain (**Figure 17E-F**). However, at 4 months the locomotion patterns were not significantly different between the groups, suggesting that the heightened locomotion of $CX3CR1^{CreER};MeCP2^{fl/y}$ mice was a transient, adaptive mechanism to sustain body weight, which is progressively lost.

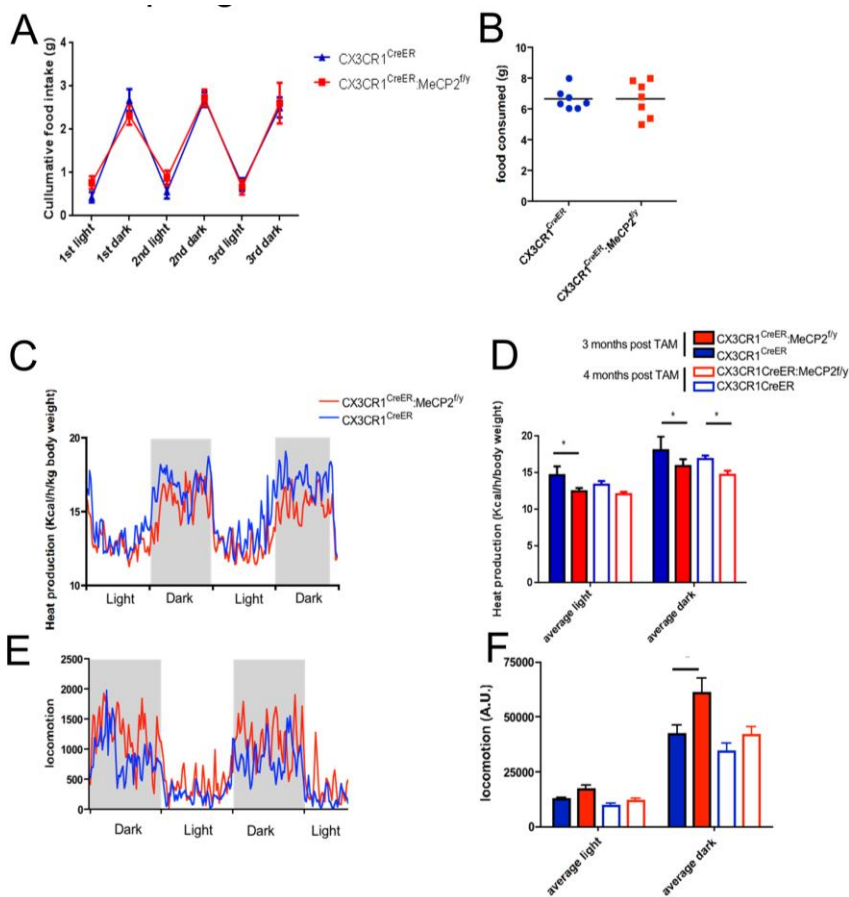
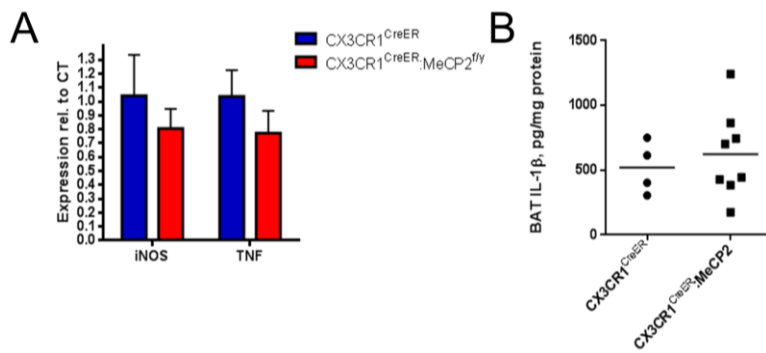


Figure 17. Metabolic assessment of $CX3CR1^{CreER}:MeCP2$. A. 4 day food consumption of TAM-treated $CX3CR1^{CreER}$ and $CX3CR1^{CreER}:MeCP2^{f/y}$ mice. A. food uptake cycles at 3 months after TAM treatment. B. accumulated food intake of 48 hours of A. C-D. Energy expenditure, calculated by indirect calorimetry, at 3 and 4 months after TAM. $N=6-8$, $*p<0.05$, student's t -test. E-F. Locomotion at 3 months) and 4 month) after TAM. $N=6-8$, $*p<0.05$, student's t -test.

To investigate, whether the reduced energy expenditure results from a peripheral or central alteration, we isolated BAT and hypothalami of $CX3CR1^{CreER}:MeCP2^{f/y}$ mice and littermate control. Importantly, mRNA levels of iNOS and TNF, as well as IL-1b levels as measured by ELISA, were not significantly altered in the BAT, indicating that the tissue is not inflamed (**Figure 18**). Levels of PRDM16 were unchanged following the MeCP2 deletion, indicating that the identity of the brown adipocytes is maintained (**Figure 19A**). Importantly though, levels of UCP1, whose expression is restricted to brown adipocytes, were reduced by 40%. This may indicate a reduced nor-adrenergic tone¹⁵². Expression of the thyroid signaling-associated, thermogenic gene $Dio2$ ¹⁵³ was also strongly reduced, while expression of the critical thermogenic transcriptional co-activator $PGC\alpha1$ ¹⁵⁴ was unaltered. Expression of the noradrenergic $\beta3$ receptor was reduced, without reaching significance. Histological analysis of BAT and WAT in young pre-obese $CX3CR1^{CreER}:MeCP2^{f/y}$ mice at the age 10 weeks revealed altered BAT morphology, while WAT was intact (**Figure 19C**). In the BAT of the animals,

UCP1 levels were reduced, alongside decreased phosphorylation of the hormone sensitive lipase (HSL), which is phosphorylated upon activation of the $\beta 3$ adrenergic receptor and release of fatty acids from triglyceride stores (**Figure 19B**). Interestingly, HSL was found also to be hypophosphorylated in the vWAT of $CX3CR1^{Cre};MeCP2^{fl/y}$ animals. Histochemical UCP1 staining further confirmed the reduction of the protein in the BAT of $CX3CR1^{Cre};MeCP2^{fl/y}$ animals (**Figure 19D**). Intriguingly, tyrosine hydroxylase (TH) was also strongly reduced in the whole tissue extract, which could again suggest a reduced norepinephrine tone (**Figure 19A**). The latter



could be triggered either by the nerves of the sympathetic nervous system, or from cells secreting norepinephrine within the tissue.

Figure 18. No BAT inflammation in

$CX3CR1^{CreER};MeCP2^{fl/y}$ mice. A. mRNA levels of iNOS and TNF as measured by qRT-PCR in total BAT obtained $CX3CR1^{CreER};MeCP2^{fl/y}$ mice, 4 months after TAM induction. B. BAT IL-1 β levels in same BAT samples as in A.

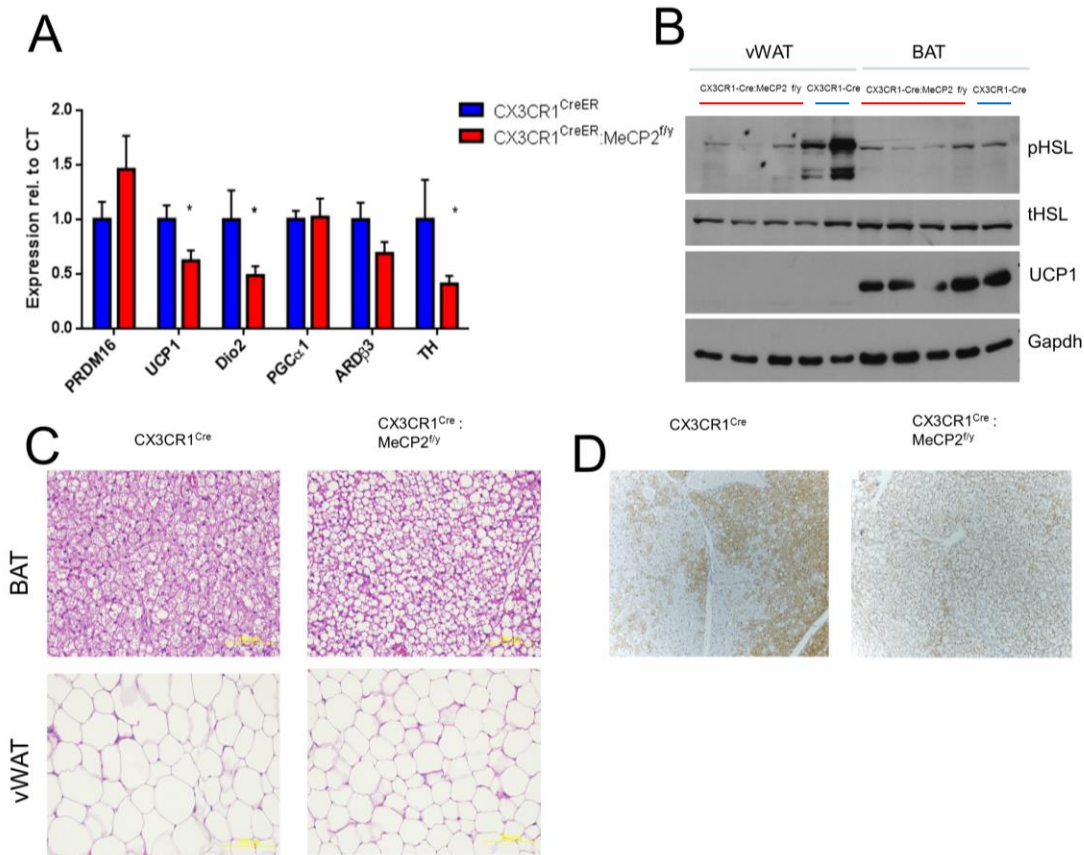


Figure 19. altered BAT morphology and gene expression if the absence of macrophage MeCP2. A. qRT-PCR analysis of BAT obtained from obtained CX3CR1^{CreER}:MeCP2^{f/y} mice, 4 months after TAM induction. B. Western blot analysis of tissues obtained from 10 week old pre-obese CX3CR1^{Cre}:MeCP2^{f/y} mice and littermates C. H+E stain of tissues, as in B. D. histochemical UCP1 staining for tissue as in B.

BAT activity is related to cold-induced thermogenesis⁴⁸. To test, if this acute response is impaired in the mice which harbor MecP2-deficient BAM, we subjected both pre-obese CX3CR1^{Cre}:MeCP2^{f/y} and TAM-treated CX3CR1^{CreER}:MeCP2^{f/y} mice to a standard cold shock treatment (4⁰C for a period of 8 hours). Surprisingly, both mouse strains were able to maintain their body temperature comparable to control littermates (**Figure 20A-B**). Gene expression analysis of the BAT of the cold-challenged TAM-treated CX3CR1^{CreER}:MeCP2^{f/y} mice revealed only minor differences as compared to controls.. Thus, UCP1, PGC α -1, Dio2 and ADRB3 levels were not different between WT and mutants (**Figure 20C**). Additionally, histological assessment revealed a similar depletion of fat stores in BAT (**Figure 20D**). However, in the scWAT of the TAM-treated CX3CR1^{CreER}:MeCP2^{f/y} animals, UCP1 and PGC α -1 mRNAs were found 7-fold increased, accompanied by excessive phosphorylation of HSL and an increase of UCP1⁺ positive cells (**Figure 20E-G**). In addition, excessive HSL phosphorylation was evident in the vWAT of the cold-challenged CX3CR1^{Cre}:MeCP2 mice (**Figure 20H**). Thus, although CX3CR1^{CreER}:MeCP2^{f/y} mice display at 22⁰C reduced UCP1 levels and lower lipid combustion, they are able to cope with the cold stress by (1) restoring the reduced UCP1 levels in the BAT, and (2) excessive beiging of their scWAT. Collectively, these data might suggest a hypersensitization of the β 3 adrenergic receptor signaling cascade, potentially due to a reduced norepinephrine tone.

Feeding behavior is centrally regulated in the hypothalamus, where interactions between hypothalamic nuclei maintain energy homeostasis through regulation of food intake and energy expenditure¹⁵⁵. Key components of this hypothalamic circuit controlling hyperphagy are Sim1 neurons¹⁵⁶ and neurons expressing melanocortin receptors 3, 4, which negatively regulate food consumption^{152,157,158}, in the paraventricular nuclei. Moreover, also POMC neurons and the positive regulator AgRP/NPY^{159,160} neurons of the arcuate nucleus, which are themselves

regulated by the peripheral hormone leptin through its activation of the melanocortin system, control food consumption. Interestingly, also microglia were reported to respond to leptin^{161,162}.

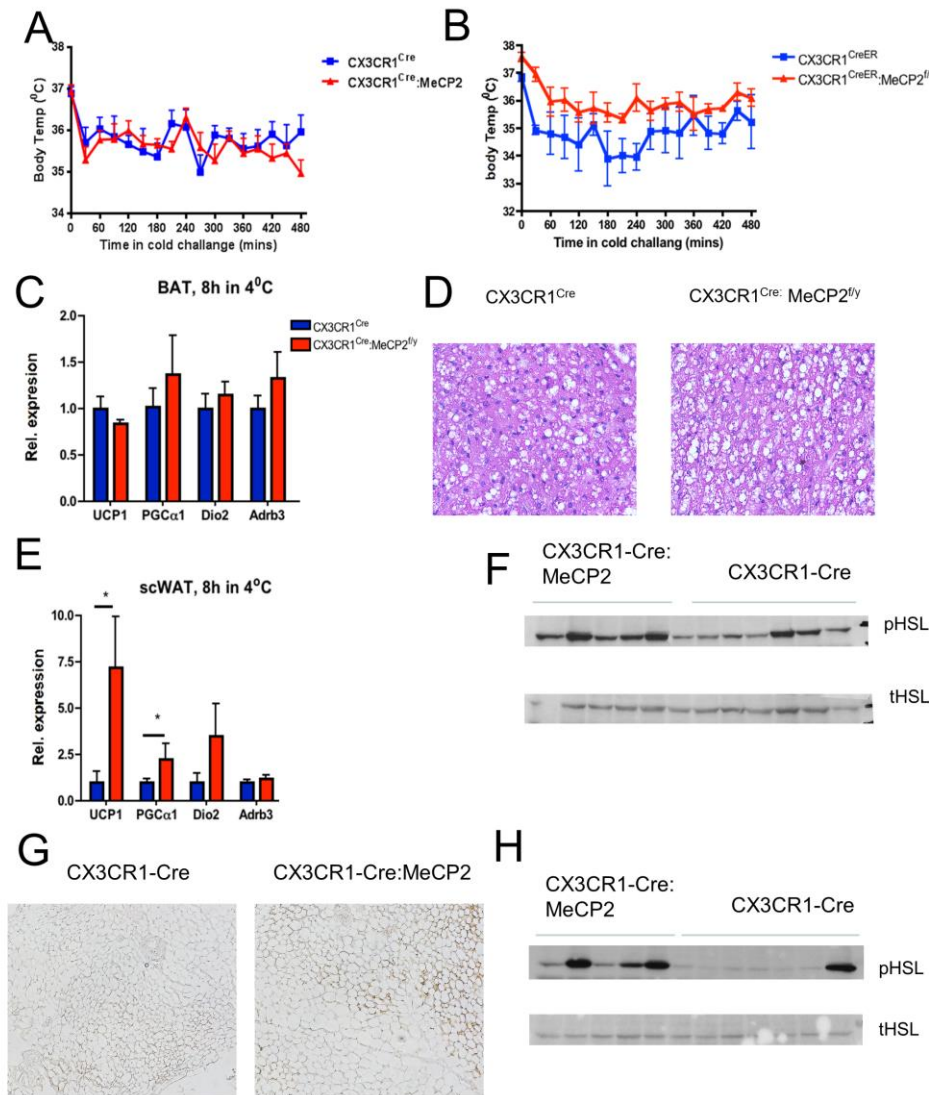


Figure 20 . Unimpaired cold-induced thermogenesis in the absence of macrophage MeCP2.
 A-B. Body temperature of pre-obese CX3CR1^{Cre}:MeCP2 (A) and TAM-treated CX3CR1^{CreER}:MeCP2^{f/y} mice (B) and their respective littermates exposed to 4°C for a period of 8 hours. n=7-4. C. qRT-PCR of BAT taken from the mice in A. *p<0.05. D. H&E stain of the BAT of mice in A. E qRT-PCR of scWAT taken from the mice in A. *p<0.05. F. Western blot analysis of scWAT taken from the mice in A. G. UCP1 histochemical stain in scWAT obtained from mice in A. H. Western blot analysis of vWAT obtained from mice in A.

However, it is unclear whether and how microglia can have an impact on the neuronal circuits controlling feeding behavior. Although feeding behavior of the mutant mice was not changed, we decided to test the activation status of microglia in the hypothalami of CX3CR1^{CreER}:MeCP2^{f/y} mice; since the mice do not suffer from RTT symptoms, they are a unique tool to study cell-

intrinsic microglial defects in the absence of MeCP2, without confounding secondary effects potentially resulting from altered parenchyma. Hypothalamic MeCP2-null microglia did not differ from control microglia in terms of numbers and morphology (**Figure 21A-C**), as well as a panel of microglial activation markers (CD45, CD11b, MHCII, CD86, CD68 and CD11c) (**Figure 21D**). In addition, RNA-seq analysis of hypothalamic microglia did not reveal major changes in the gene expression profile in the absence of MeCP2 (**Figure 21E-F**). In addition, we analyzed mRNA expression of specific genes in the hypothalamic tissue. mRNA levels of *mcr3*, *mcr4*, *pomc* and *agrp* were found unchanged in the mutants, whereas *npy* and the leptin receptor expression were down- and upregulated, respectively, probably in response to elevated serum leptin levels (**Figure 21G**). Finally, we analyzed, if hypothalamic functions that are not related to feeding are compromised in the absence of microglial MeCP2. To this end, we injected the animals with LPS to test their fever response, which is known to be controlled by the hypothalamus¹⁴². Measurement of body temperature revealed that both control and CX3CR1^{CreER}:MeCP2^{f/y} mice displayed a similar response pattern of rapid hyperthermia followed by a prolonged hypothermia (**Figure 21H**). To conclude, no overt microglial or hypothalamic phenotype was observed in the absence of microglial MeCP2 under steady state conditions, and the overall the combination of the metabolic and molecular assessment does not suggest impaired central feeding regulation.

The energy expenditure reduction alongside the altered BAT gene expression strongly suggest a MeCP2-related BAM dysfunction. Specifically, our data suggest a role of BAM in general, and MeCP2 expression in BAM in particular, in diet-induced homeostatic thermogenesis. We thus investigated the possible molecular mechanism, which dictates BAT contributions to energy balance. Similar to the microglia, BAM isolated from CX3CR1^{Cre}:MeCP2^{f/y} mice also harbor truncated *mecp2* transcripts confirming efficient Cre recombination in this population (**Figure 22A**). Flow cytometry analysis revealed that MeCP2 protein levels of BAM of CX3CR1^{CreER}:MeCP2^{f/y} mice were reduced, even after 6 months post TAM administration (**Figure 22B**). This establishes that MecP2-deficient macrophages are not generally impaired and can efficiently compete with presumably residual WT BAM that are spared from the TAM-induced recombination. Given the CX3CR1 expression of BAM, and the fact that BAT in CX3CR1^{CreER}:MeCP2^{f/y} mice are functionally impaired, we decided to determine the specific impact of the MeCP2 deletion on BAM.

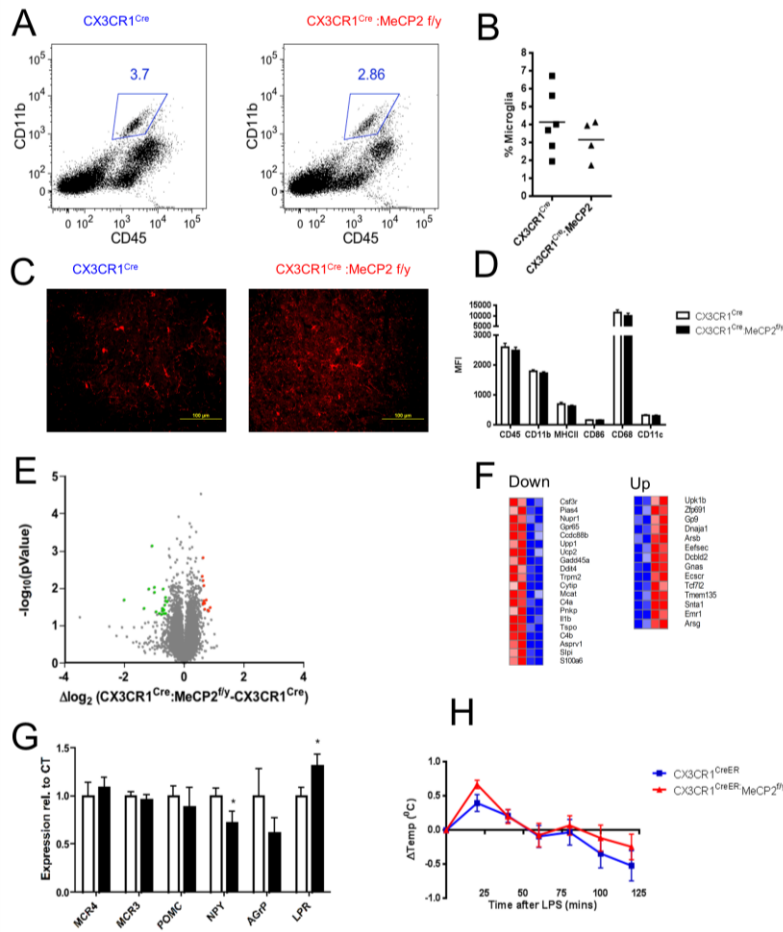


Figure 21. Normal microglia phenotype and hypothalamic function in the absence of microglial MeCP2. A-B. FACS analysis (A) and quantification (B) of hypothalamic microglia in $CX3CR1^{Cre}:MeCP2^{f/y}$ and control $CX3CR1^{Cre}$ mice. $N=4-6$. C. Iba1 staining of cortex sections of $CX3CR1^{Cre}$ and $CX3CR1^{Cre}:MeCP2^{f/y}$ mice. D. Summary of FACS analysis of microglia of mice in A. E-F. volcano plot of gene expression in hypothalamic microglia obtained from $CX3CR1^{Cre}:MeCP2^{f/y}$ Vs. $CX3CR1^{Cre}$ mice. G. qRT-PCR of hypothalami of mice in figure 18A. H. Body temperature differences (Body temperature_(t)-body temperature₍₀₎) of TAM-treated $CX3CR1^{CreER}$ and $CX3CR1^{CreER}:MeCP2^{f/y}$ mice after LPS treatment. $N=8-10$.

Recently, the group of Jonathan Kipnis, University of Virginia, reported that MeCP2 can in macrophages act as a survival factor⁶⁸. However, BAM numbers were unaltered in the absence of MeCP2 (**Figure 22A**). Moreover, as outlined above mutant BAM competed with WT BAM. It has been reported that upon cold-challenge BAM change their phenotype towards an M2-like pattern, a process, which also was reported to dictate TH expression and to be dependent on IL-4/13 signaling⁴⁴. However, in our analysis we found no alterations of the reported M1 (CD11c, CD274) or M2 (CD206, CD301) markers in MeCP2-deficient BAM, in accordance with the lack of inflammation in the tissue (**Figure 22B**). Thus, MeCP2 deletion in BAM does not affect their survival or inflammatory state. To investigate the effect of the MeCP2 absence on their gene expression profile, we sorted BAM from $CX3CR1^{Cre}$ and $CX3CR1^{Cre}:MeCP2^{f/y}$ mice and performed RNA-seq analysis. In light of the reported subtle, modulatory effect of MeCP2 on gene expression^{164,165}, we focused on genes, which are at least 1.5 fold changed between the two groups and the changes that reached statistical significance (p value = 0.05). This filter yielded

146 genes, which were upregulated (**Figure 22C**). In line with the notion that MeCP2 is a transcriptional repressor only 16 genes were downregulated. In the brain it was recently shown that MeCP2 represses preferentially long genes, which span more than 100kbp^{163,164}. In the BAM, however, no such preference was seen and the length of the upregulated genes in the absence of MeCP2 was not statistically different from that of the average gene length throughout the genome (**Figure 22D**). Gene ontology analysis using the DAVID resources revealed that many of the upregulated genes are involved in mRNA processing, as well as other biological processes including axonal guidance, corroborating the notion that MeCP2 acts broadly but with subtle 'fold change impact'^{165,166} (**Figure 22E**). The full list of genes altered in MeCP2-null BAM shown in **Figure 23**.

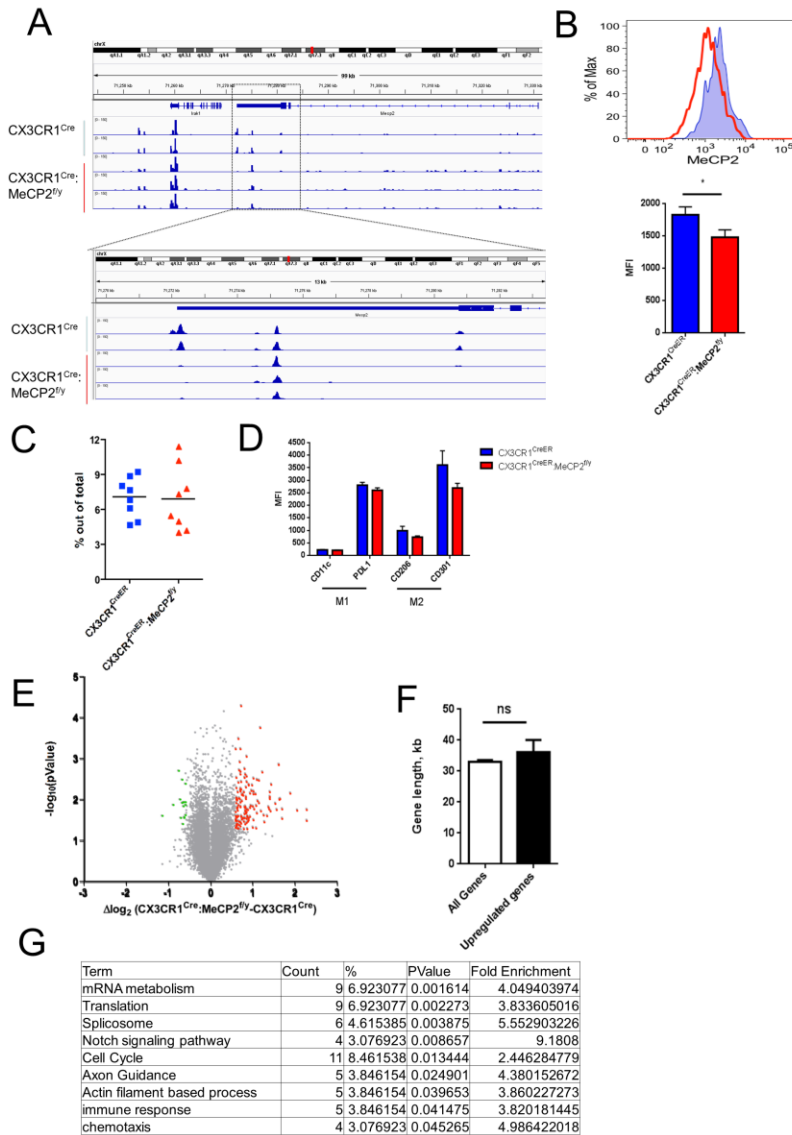


Figure 22. Consequences of the MecP2 Deletion in BAM. **A.** IGV of MeCP2 transcript in isolated CX3CR1^{Cre} and CX3CR1^{Cre};MeCP2^{f/y} BAMs. **B.** Intracellular FACS analysis of MeCP2 in TAM-treated CX3CR1^{CreER} and CX3CR1^{CreER};MeCP2^{f/y} mice 6 months after TAM treatment. N=5, * p<0.05, Mann-Whitney's u-test. **C.** FACS analysis of BAM cell numbers in TAM-treated CX3CR1^{CreER};MeCP2^{f/y} mice and littermates. **D.** FACS analysis of M1/M2 surface markers. **E.** volcano plot of transcriptomes of BAMS obtained from CX3CR1^{Cre};MeCP2^{f/y} vs. CX3CR1^{Cre} mice. Genes significantly upregulated are depicted in red, and genes significantly downregulated are depicted in green. **F.** average gene length of the entire mouse genome (N=24022) vs. genes upregulated in the absence of MeCP2 in BAMS (N=146). **G.**

Gene ontology analysis for genes upregulated in absence of BAM MeCP2.

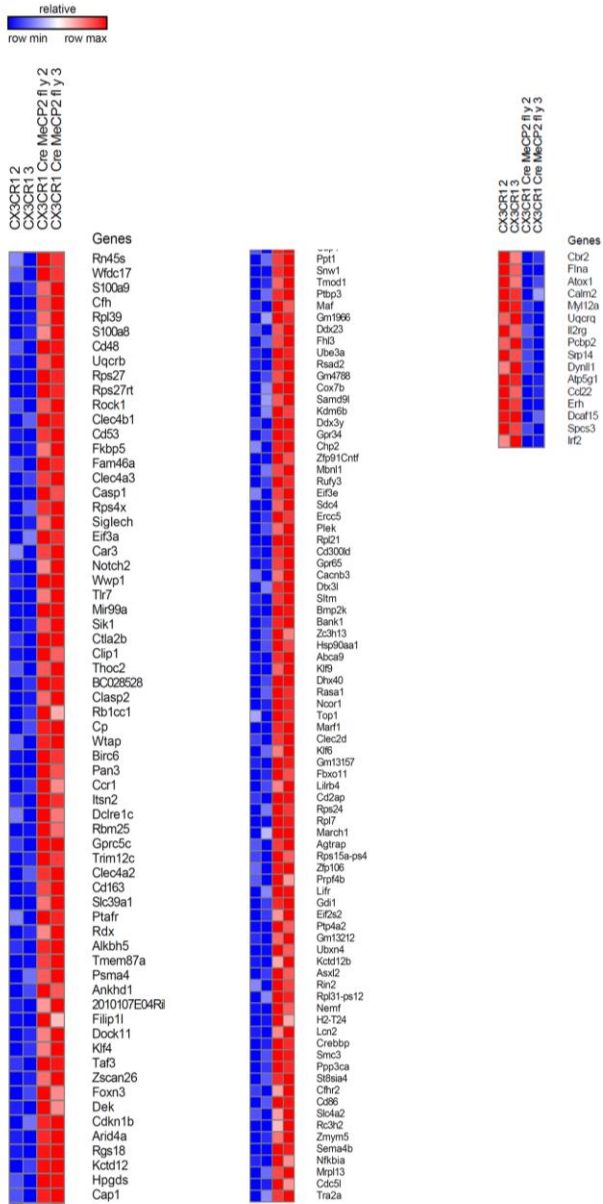


Figure 23. List of all genes altered in MeCP2-null BAM versus control cells (fold difference >0.5 or <-0.5, p>0.05)

4. Results - Part II: The contribution of microglia and monocytes to CNS autoimmunity

4.1 . Microglial antigen presentation is not required for the induction of EAE

A major challenge for the study of microglia is their distinction from BM-derived phagocytes⁹⁸. In order to discriminate resident CNS microglia from BM-derived macrophages in a pathological autoimmune setting, we treated CX3CR1^{CreER}:R26-YFP mice with TAM, and then immunized the animals with MOG₃₅₋₅₅ peptide for the induction of EAE. Mice were analyzed at day 0 or day 20 following MOG immunization, at which time most animals develop severe ascending paralysis. In the flow cytometry analysis microglia were gated as CD11b⁺ YFP⁺ cells, while BM-derived cells were defined as the CD11b⁺ YFP⁻ population. When CD11b⁺ YFP⁺ microglia and CD11b⁺ YFP⁻ fractions were compared based on their Ly6C and CD45 expression, microglia and BM-derived phagocytes remained distinct entities, with the former being CD45^{int} Ly6C^{lo}, and the latter either CD45^{hi} Ly6C^{hi} (from here on referred to as “effector monocytes”) or CD45^{hi} Ly6C^{lo} (**Figure 24A**). These two populations increased dramatically over the course of EAE. This held in particular for the CD45^{hi} Ly6C^{lo} population, which was almost absent in the beginning of EAE (**Figure 24B**). In line with published data concerning infiltrating monocytes²⁵, the CD45^{hi} Ly6C^{hi} population thus likely corresponds to recently infiltrating monocytes, while CD45^{hi} Ly6C^{lo} are likely represent differentiated monocyte-derived inflammatory macrophages.

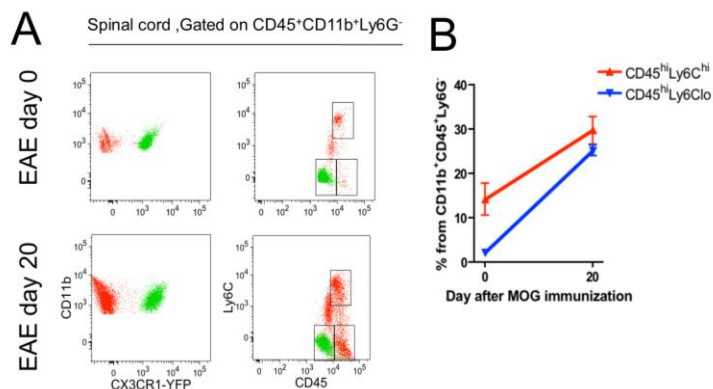


Figure 24. Population dynamics of microglia vs. monocyte-derived cells during EAE. A.

CX3CR1^{CreER}:R26-YFP mice were treated with TAM, 6 weeks later immunized with MOG₃₅₋₅₅ and sacrificed at day 20 after challenge. CD11b⁺YFP⁺ cells are depicted in green, while CD11b⁺YFP⁻ cells are depicted in red. B. Percentages of the different CD11b⁺YFP⁻

infiltrating cells in the spinal cord following MOG₃₅₋₅₅ immunization. N=5-3

In order to monitor microglia phenotypes in EAE, TAM-treated CX3CR1^{CreER}:R26-YFP mice were treated then with MOG₃₅₋₅₅ peptide, and the mice were analyzed at day 17 following immunization, at which time most animals develop severe ascending paralysis. Microglia were gated as the sole YFP⁺ cells (**Figure 25**). Strikingly, the YFP⁺ microglia underwent a broad

systemic phenotypic switch; the cells elevate inflammatory markers, such as CD45, CD11b and CD64, as well as several markers associated with T cell communication and DC fates, such as CD11c, MHCII, Flt3 and the co-stimulatory molecules CD80 and CD86. CD40 was however unaltered, as were CD14.

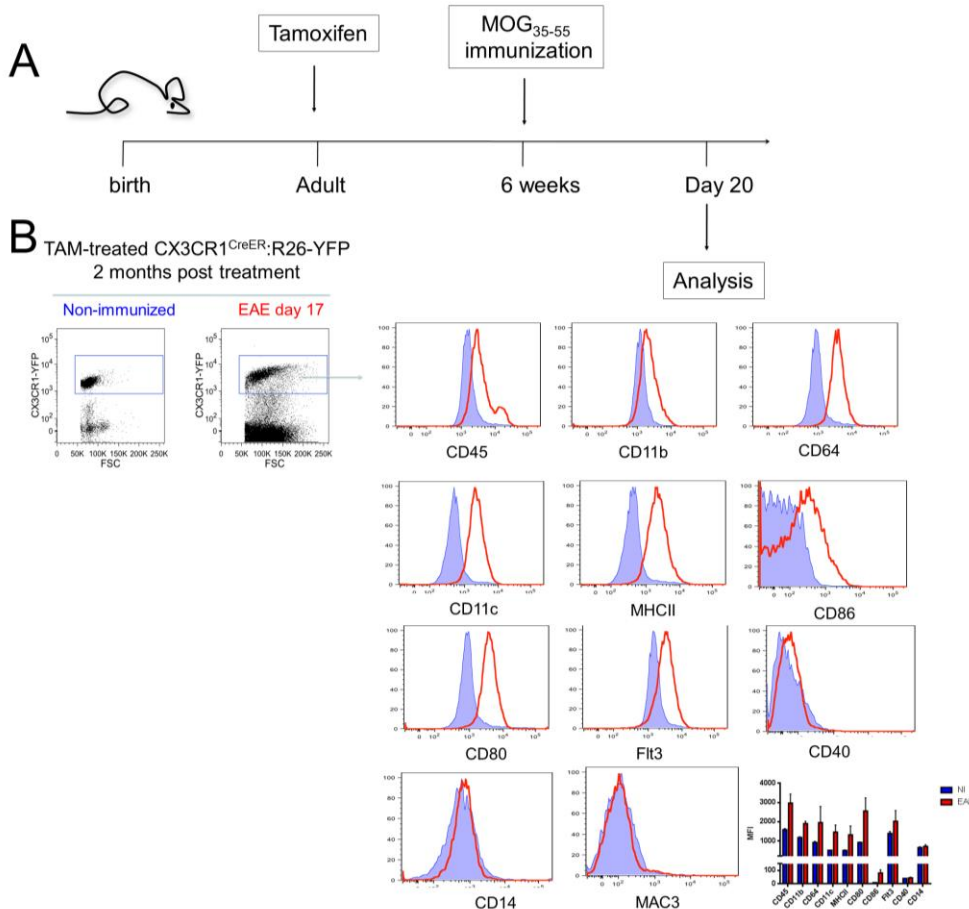


Figure 25. Microglia undergo a significant phenotypic switch. A. scheme of experiment. B. FACS analysis of $CX3CR1^{CreER}:R26-YFP$ mice, treated with TAM, immunized with MOG_{35-55} 6 weeks later, and sacrificed at day 17.

In order to investigate whether microglial MHCII has a direct role in EAE progression, or is a mere activation marker on these cells, we generated mice with a specific microglial MHCII deletion by combining the $CX3CR1^{CreER}$ allele with a $I-A^b$ null allele¹³⁸ and a “floxed” $I-A^b$ allele¹³⁹, yielding $CX3CR1^{CreER}:MHCII^{fl/-}$ mice. TAM treatment of these animals allows restricting the MHCII deletion to microglia, while sparing other cells with the potential of T cell priming, such as DC, B cells and infiltrating macrophages. Mice were TAM-treated and MHCII deletion was monitored, first in peripheral tissues. B cells retained MHCII expression in the TAM-treated $CX3CR1^{CreER}:MHCII^{fl/-}$ mice (**Figure 26A**). Importantly, blood $CD4^+$ and $CD8^+$ T cell numbers in the TAM-treated mice were intact, unlike in $MHCII^{-/-}$ mice, in which $CD4^+$ T cells are severely reduced due to MHCII absence on thymic epithelial cells¹³⁸ (**Figure 26B**). One week following TAM administration splenic DC of $CX3CR1^{CreER}:MHCII^{fl/-}$ mice were mostly

negative for MHCII; however 5 weeks later the mutant cells were replaced by MHCII⁺ DC (Figure 26C). Thus, although initially affected, the DC compartment regains over time its MHCII expression. Microglia of unchallenged mice do not express surface MHCII. To test microglial MHCII expression, we hence subjected TAM-treated CX3CR1^{CreER}: MHCII^{fl/-} mice to EAE. In monocyte-derived CD45^{hi} phagocytes of these animals, shown above to be spared by the CX3CR1^{CreER} system, MHCII levels were found unchanged; however, microglia displayed an efficient MHCII deletion (Figure 26C). Thus after the recovery period following TAM treatment, CX3CR1^{CreER}: MHCII^{fl/-} mice harbor microglia lacking MHCII, but other myeloid cells express normal MHCII levels. Interestingly, not only microglia express MHCII at the peak of EAE, but also the Ly6C⁺ effector monocyte and the Ly6C⁻ population (Figure 26D), which raises the possibility that these populations contribute to antigen presentation.

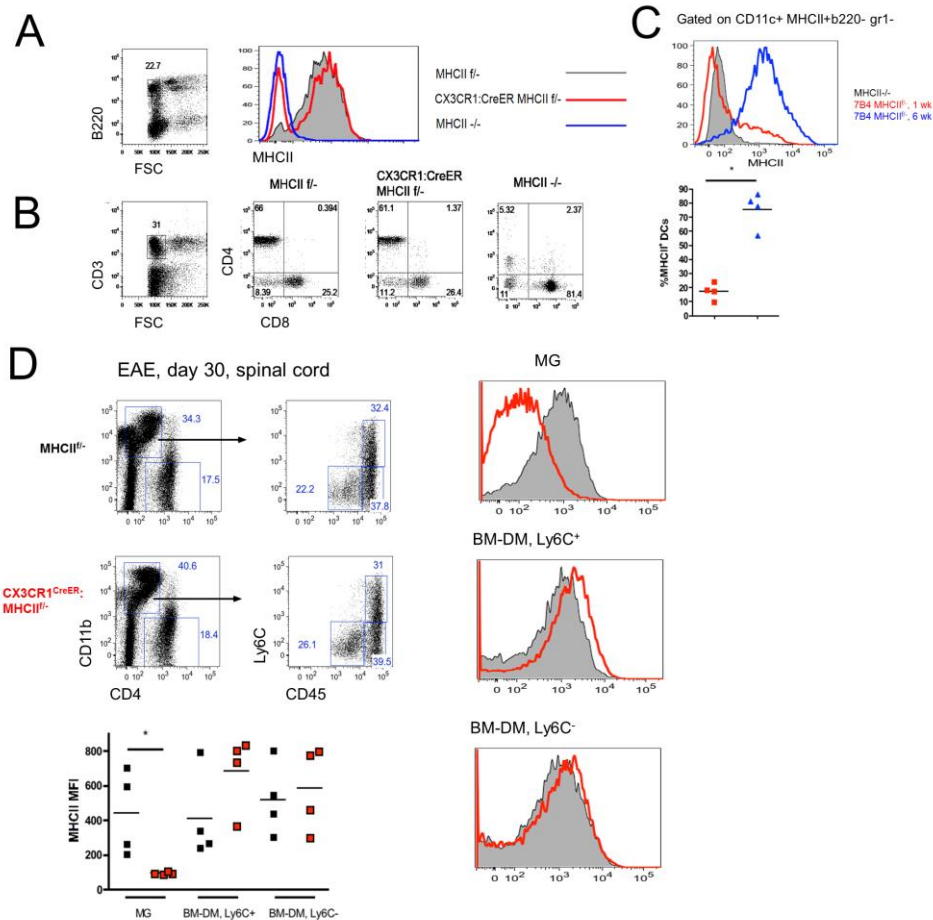


Figure 26. MHCII deletion in CX3CR1^{CreER}: MHCII^{fl/-} mice is transient in peripheral cells, but persistent in microglia. (A) MHCII levels of classical splenic DC and B cells 1 or 6 weeks post TAM administration. (B) B cell MHCII levels and CD4/8⁺ numbers in blood of MHCII^{fl/-}, CX3CR1^{CreER}: MHCII^{fl/-} and MHCII^{-/-} mice. (C) MHCII levels of brain and spinal cord

microglia of immunized $MHCII^{fl/-}$ and $CX3CR1^{CreER}$: $MHCII^{fl/-}$ mice with EAE scoring of 3. $N=4$, $*p<0.05$, Mann-Whitney's u -test.

In order to investigate the involvement of microglial MHCII in EAE, we treated $CX3CR1^{CreER}$: $MHCII^{fl/-}$ mice with 30 mg TAM by gavage and waited a period of 6 weeks, the period of time needed for the full reconstitution of peripheral myeloid cells. We then immunized the mice with MOG₃₅₋₅₅ peptide. Compared to $MHCII^{+/+}$ mice, haplo-sufficient $CX3CR1^{CreER}$: $MHCII^{fl/-}$ and $MHCII^{fl/-}$ mice developed EAE with a slight ~4 day delay. However, $CX3CR1^{CreER}$: $MHCII^{fl/-}$ mice displayed an EAE onset comparable to control littermates, as well as similar severity and disease course (**Figure 27A-C**). No correlation was observed between microglial MHCII levels as measure by MFI and either disease onset or severity (**Figure 27D-E**).

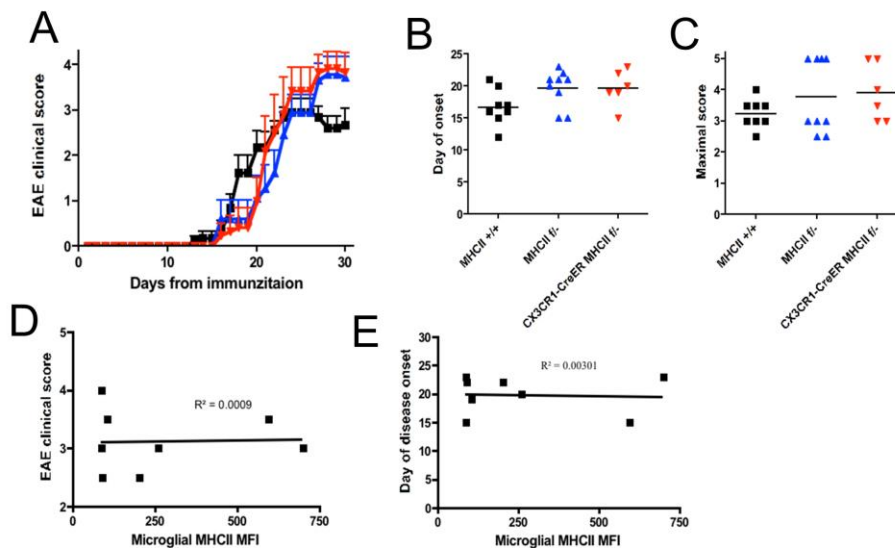


Figure 27. Microglial MHCII deletion does not alter EAE course. (A-C). EAE course (A), individual day of onset (B), and individual maximal score (C) of tamoxifen treated immunized $MHCII^{+/+}$, $MHCII^{fl/-}$ and $CX3CR1^{CreER}$: $MHCII^{fl/-}$ mice. The experiment is a representative of 3 independent experiments. $N=6-9$. (D-E). Correlation between microglial MFI of Fig. 7C (day 30) and clinical EAE scores at the day of analysis (D) or individual day of onset (E).

Spinal cord analysis by FACS revealed no differences in percentages of microglia, infiltrating monocytes/ monocyte-derived macrophages (**Figure 28A-B**), or total $CD4^+$ T cells in the absence of microglial MHCII. Finally, analysis of the infiltrating $CD4^+$ T cell compartment at EAE score 3, at disease peak, following non-specific re-stimulation with PMA/ ionomycin *ex vivo*, revealed similar proportions of Th1 ($CD44^+$ $CD40L^+$ $IFN-\gamma^+$ $IL-17A^-$), Th17 ($CD44^+$ $CD40L^+$ $IFN-\gamma^-$ $IL-17A^+$) and double positive T cells, which are at least part “ex-Th17” cells¹⁶⁷

(CD44⁺ CD40L⁺ IFN- γ ⁺ IL-17A⁺) (**Figure 28C-D**). In addition, similar proportions of Th1/Th17 cells were also evident in MOG specific stimulation performed with MOG₃₅₋₅₅ (**Figure 28E**). Thus, in terms of the disease course, myeloid cell infiltrates and their T cell compartment, we observed no changes in the absence of microglial MHCII during EAE.

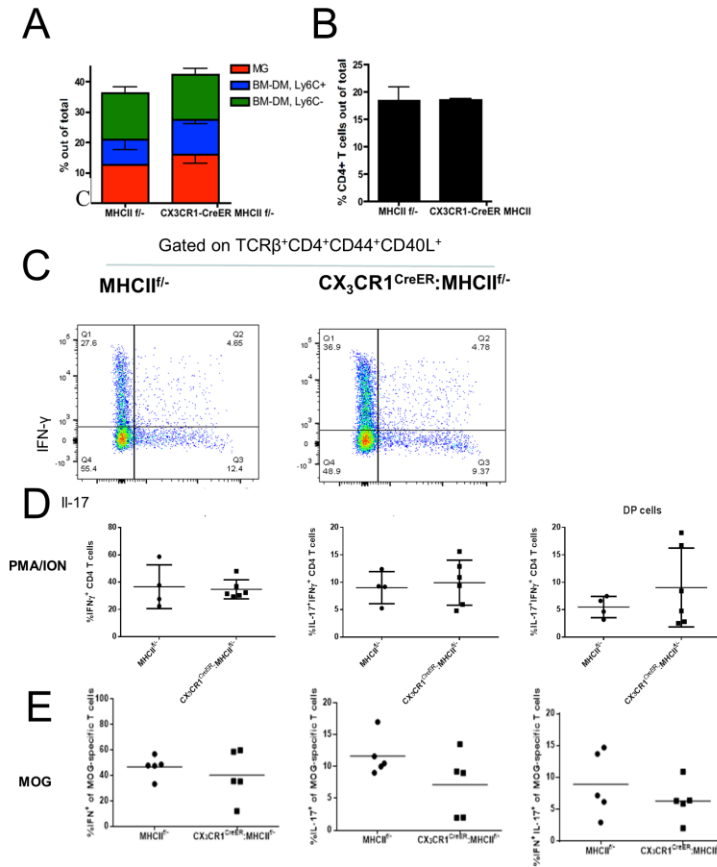


Figure 28. No change in resident or infiltrating cell percentages in absence of microglial MHCII. (A-B). FACS analysis of myeloid cell (A) and CD4⁺ (B) percentages out of total CD45⁺ cells in spinal cord of sick (score 3) MOG₃₅₋₅₅ immunized MHCII^{fl/fl} and CX3CR1^{CreER}; MHCII^{fl/fl} mice. N=6-9. C-D. FACS analysis of CD4⁺ T cells in spinal cord of sick (score 3) immunized MHCII^{fl/fl} and CX3CR1^{CreER}; MHCII^{fl/fl} mice, re-stimulated with PMA / ionomycin for 6 hours and stained intracellular for IFN- γ and IL-17A. n=5. E. FACS. FACS analysis of CD4⁺ T cells in spinal cord of sick (score 3) immunized MHCII^{fl/fl} and CX3CR1^{CreER}; MHCII^{fl/fl} mice, re-stimulated with MOG₃₅₋₅₅ for 6 hours and stained intracellular for IFN- γ and IL-17A. n=5.

4.2. Monocyte-derived, cell intrinsic TNF is pivotal for EAE induction

Monocyte-derived macrophages are known as critical effector cells in EAE^{11,82}. In order to investigate the precise timing of the monocyte infiltration and differentiation into monocyte-derived macrophages, we took advantage of a well-established protocol that allows the depletion of Ly6C^{hi}CCR2⁺ monocytes^{12,25}. Administration of the anti-CCR2 antibody (MC21) at the peak of the disease was reported to attenuate EAE progression, while not altering the disease course, if co-administered with MOG₃₅₋₅₅ peptide⁸². Speculating that also the disease onset, not only its peak, might be affected by infiltrating effector monocytes, we decided to deplete effector monocytes at day 9 and 12. Analysis of blood monocytes of the MC21-treated animals at day 13 showed complete deletion of Ly6C^{hi} monocytes (**Figure 29A**). Interestingly, MC21

administration strongly attenuate the disease course; about half of the MOG immunized mice treated with MC21 did not develop EAE, while the remaining sick mice showed less severe symptoms with no morbidity (**Figure 29B**). Analysis of the spinal cords at day 16 revealed a significant reduction of CD45^{hi}Ly6C^{lo} cells, strongly suggesting that similar to Ly6C^{lo} blood monocytes¹², these parenchymal CD45^{hi}Ly6C^{lo} macrophages derive from Ly6C^{hi} monocytes (**Figure 29C**). In addition, a strong positive correlation could be drawn between the abundance of CD45^{hi}Ly6C^{lo} macrophages in the spinal cord and the clinical EAE scores (**Figure 29D**). Thus, timely monocyte infiltration is crucial for the differentiation into monocyte-derived macrophages and for the outbreak of EAE symptoms. In order to study the physiological importance of myeloid TNF in the development of EAE, we crossed CX3CR1^{Cre} animals with mice harboring ‘floxed’ TNF alleles¹²⁷ generating CX3CR1^{Cre}:TNF^{f/f} mice. To probe for the deletion we challenged the animals with LPS known to result in systemic TNF release associated with septic shock¹²⁷. Sera obtained 4 hours after systemic *i.p.* LPS challenge contained 4 times less TNF in CX3CR1^{Cre}:TNF^{f/f} mice compared to littermate controls (**Figure 30A**). To test a specific macrophage TNF response, microglia were isolated from TNF^{f/f} and CX3CR1^{Cre}:TNF^{f/f} mice and challenged *ex vivo* with 10 µg/ml LPS for 2 hours, followed by incubation with Brefeldin A to block TNF release from the Golgi apparatus (**Figure 30B, C**). Unlike TNF^{f/f} microglia, which responded to the LPS stimulation by robust intracellular expression of TNF, CX3CR1^{Cre}:TNF^{f/f} microglia failed to produce TNF and TNF MFI were even lower than that of unstimulated TNF^{f/f} microglia (**Figure 30B, C**).

Next, in order to assess the general monocyte and macrophage-derived TNF contribution to EAE, we immunized CX3CR1^{Cre}:TNF^{f/f} mice with MOG₃₅₋₅₅ and followed EAE symptoms up to day 70. In accordance with previous studies performed with TNF^{-/-} mice¹²², CX3CR1^{Cre}:TNF^{f/f} mice exhibited a delayed EAE, with an average onset day of 31, unlike TNF^{f/f} mice, which develop symptoms within 14 days. (**Figure 31A, B**). Interestingly, CX3CR1^{Cre}:TNF^{f/f} exhibit higher variability in the average day of onset as regards to littermate controls, which may suggest incomplete penetrance. However, severity of the disease symptoms was comparable between the animals, both with respect to the average maximal score and according to results of the histological analysis for demyelination by luxol fast blue stain (**Figure 31C-D**). Thus, in the absence of myeloid TNF, EAE is delayed but not attenuated in terms of tissue damage. The EAE disease course depends on the CD4⁺ effector T cell compartment, which itself is affected by antigen presentation and T cell priming by peripheral and potentially central DC¹⁶⁸. A delay in

the disease onset may suggest impairment in the T cell compartment due to disrupted antigen presentation. We therefore analyzed T cells from lymph nodes at day 6 after immunization, as well as day 13 (disease onset) and day 24 (chronic stage) of EAE. In all tissues and different EAE times, total CD4⁺ cells, as well as Th₁ and Th₁₇ percentages did not significantly differ between CX3CR1^{Cre}:TNF^{f/f} and TNF^{f/f} mice (**Figure 32A, B**). Also histological assessment by CD3⁺ T cell staining showed similar T cell infiltrates to the spinal

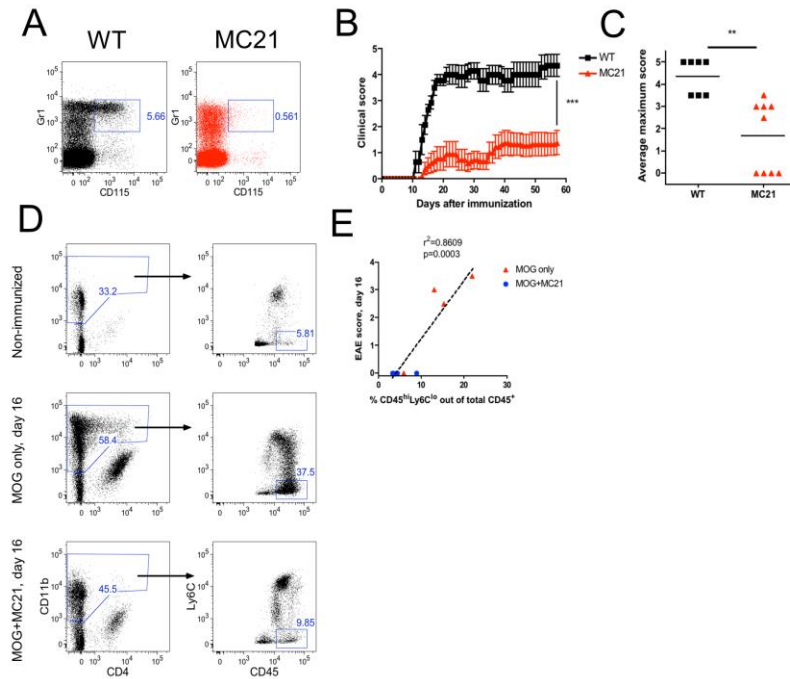


Figure 29. Monocyte depletion before disease onset blocks EAE progression. (A) analysis of blood monocytes 13 days post immunization with (right, red) or without (left, black) MC21 administration at day 9 and 12. B-C. EAE disease course (right) and maximal score (left) in immunized mice vs. immunized MC21-co-treated mice. Data represent three independent experiments. N=9-7, **p<0.01, Student's T test. D. Spinal cord analysis of non-immunized mice (to panel) immunized mice at day 16 post immunization (middle panel) and immunized mice co-treated with MC21 at the same day. E. correlation between total

percentages of CD45^{hi}Ly6C^{lo} phagocytes and EAE scores at day 16. n=3-5 per group

cord (**Figure 32C**). Finally, CD4⁺ T cells isolated from lymph nodes of MOG-immunized CX3CR1^{Cre}:TNF^{f/f} mice were able to be re-activated in a recall assay and, following re-stimulation with MOG, up-regulated CD44, a marker of activated T cells, suggesting that T cell - APC interactions are intact in CX3CR1^{Cre}:TNF^{f/f} mice (**Figure 32D**). Thus, the T cell compartment seems unaffected, suggesting adequate T cell priming and differentiation driven by DC in the mice. The observed attenuated EAE seen in the absence of myeloid TNF may hence be due to direct, cell-intrinsic functions of the microglia or infiltrating cells.

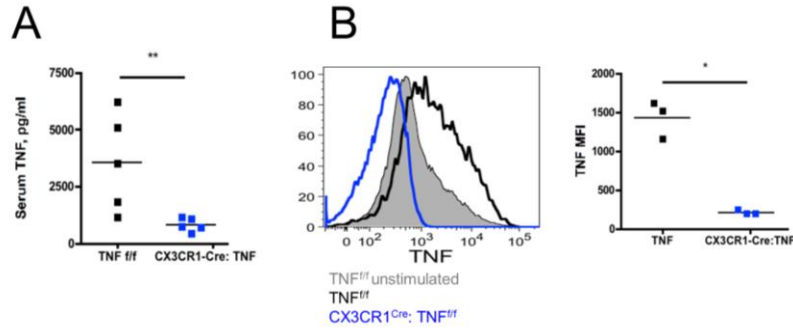


Figure 30. Efficient TNF deletion in $CX3CR1^{Cre};TNF^{f/f}$ mice. A. ELISA of sera collected from $TNF^{f/f}$ or $CX3CR1^{Cre};TNF^{f/f}$ mice 4 hours after treatment with 200 μ g LPS. $N=5$, $**p<0.01$, Mann-Whitney's u -test. B. FACS intracellular stain for TNF expression of $TNF^{f/f}$ or

$CX3CR1^{Cre};TNF^{f/f}$ microglia either unstimulated, or treated ex vivo with 10 μ g/ml LPS. $*p<0.05$, Mann-Whitney's u -test.

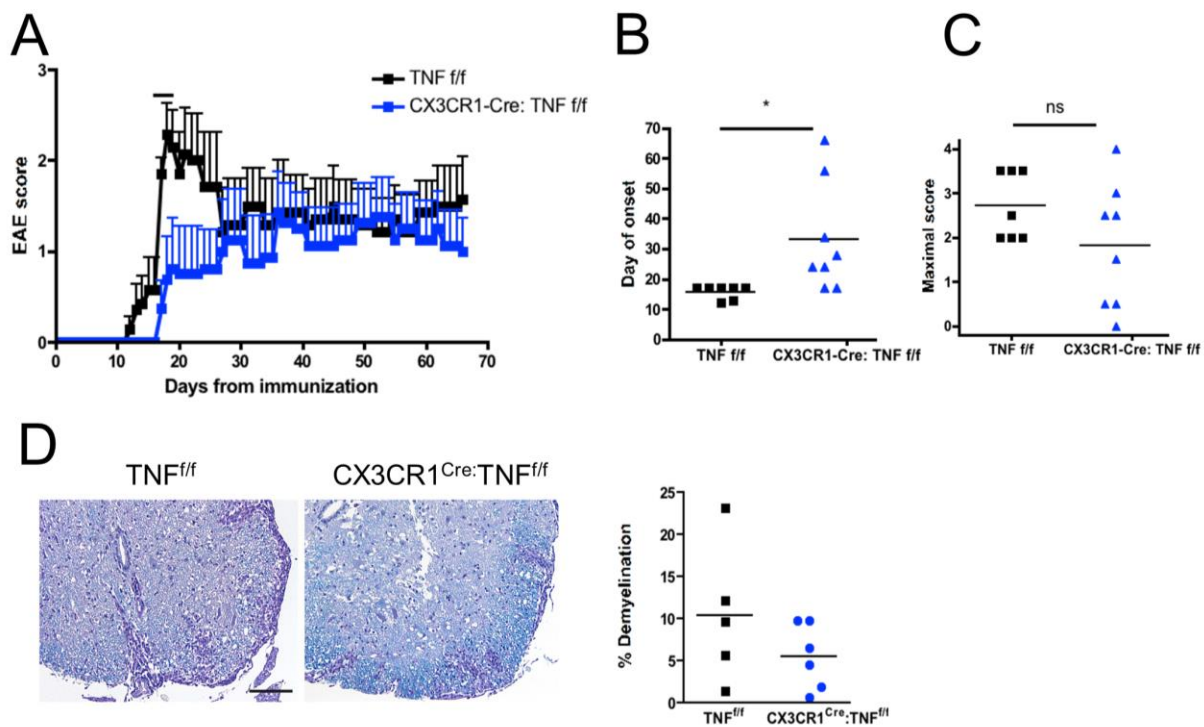


Figure 31. EAE is delayed, but not less severe, in $CX3CR1^{Cre};TNF^{f/f}$ mice. A-C. Disease course (A), day of onset (b) and individual maximal score (c) in $TNF^{f/f}$ and $CX3CR1^{Cre};TNF^{f/f}$ mice immunized with MOG₃₅₋₅₅ peptide. $n=7-8$, $*p<0.05$, $**p<0.01$, student's t -test. Data is representative of 3 independent experiments. D. histological analysis of demyelination by luxol-fast blue stain in spinal cords of $TNF^{f/f}$ and $CX3CR1^{Cre};TNF^{f/f}$ mice at day 24 after immunization. $N=5-6$

Since neither the demyelination *per se* nor the T cell infiltration were found to depend on myeloid TNF, we speculated that kinetics of myeloid infiltration might be impaired in the mutant animals. Blood monocyte counts were similar in $CX3CR1^{Cre};TNF^{f/f}$ and controls (**Figure 33A**);

however, at day 9 post MOG immunization, before disease onset, Ly6C^{hi} effector monocyte numbers in spinal cords were found significantly reduced in the absence of myeloid TNF (**Figure 33B**). Correspondingly, the number of Ly6C^{hi} effector monocytes was also strongly reduced on day 24 of the disease (**Figure 33C**).

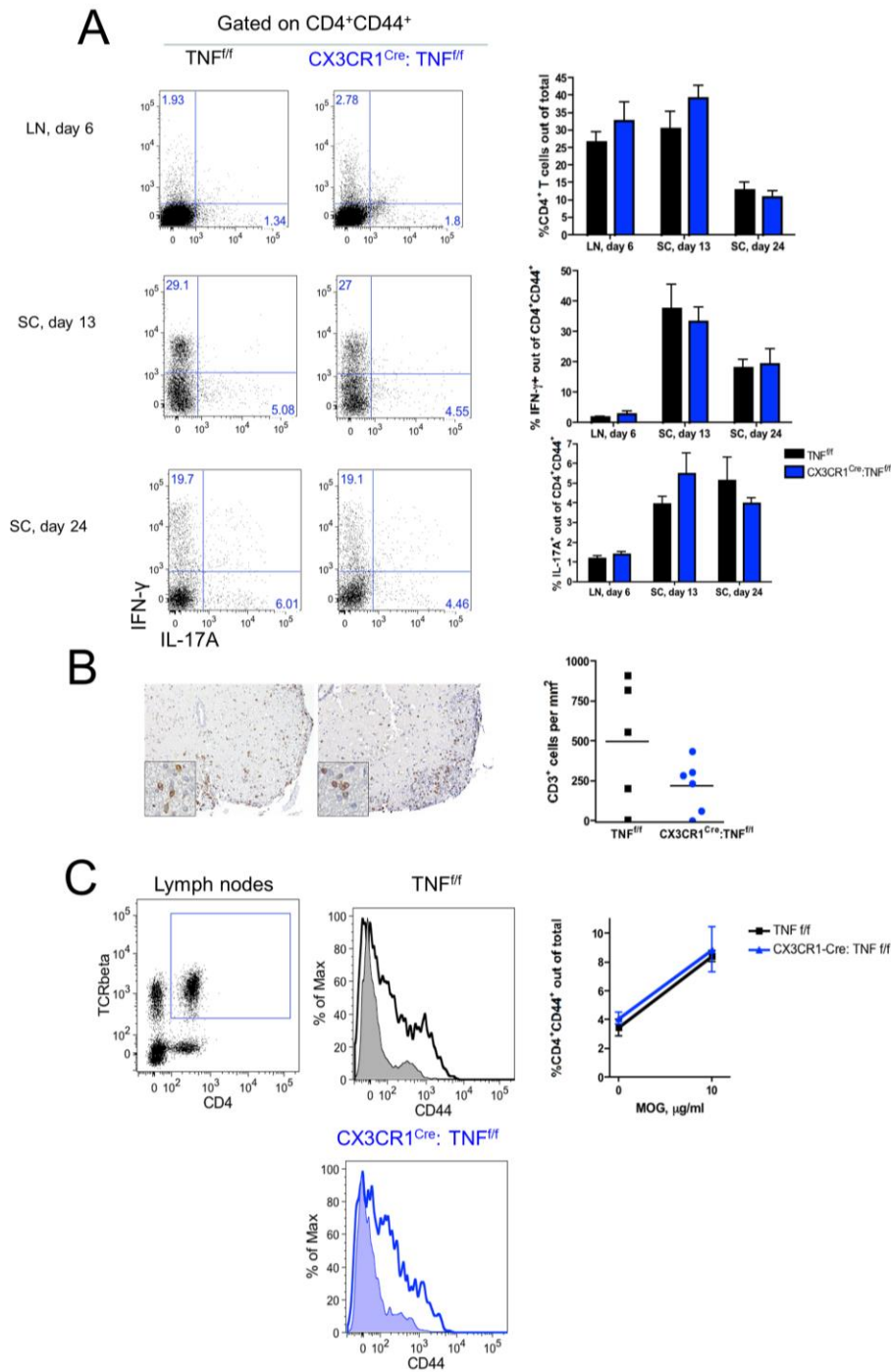


Figure 32. The T cell compartment and recall response is intact in $CX3CR1^{Cre};TNF^{ff}$ mice. A. FACS analysis of Th1 and Th17 cells in lymph nodes at day 6 after immunization, or in spinal cord at day 13 and 24, in TNF^{ff} or $CX3CR1^{Cre};TNF^{ff}$. $n=4-6$. B. CD3 histological stain in spinal cords of TNF^{ff} or $CX3CR1^{Cre};TNF^{ff}$ mice at day 24 after immunization. $N=5-6$. C. FACS analysis of splenocytes, taken at day 6 after MOG₃₅₋₅₅ immunization of TNF^{ff} or $CX3CR1^{Cre};TNF^{ff}$ mice and re-stimulated with MOG₃₅₋₅₅ for 72 hours. Tinted histogram marks unstimulated T cells. $N=3$.

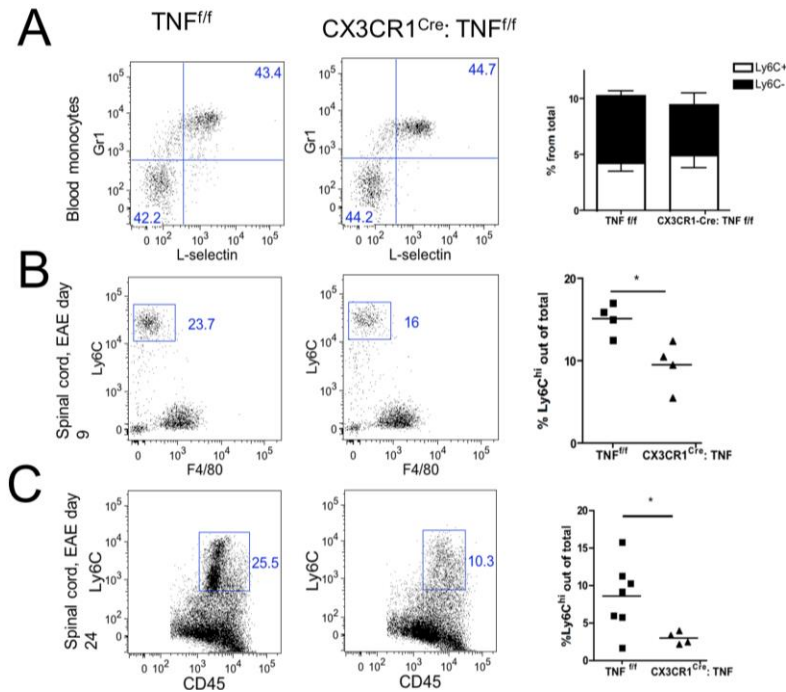


Figure 33. Reduced effector monocyte numbers in spinal cord of $CX3CR1^{Cre};TNF^{fl/fl}$ mice. A. FACS analysis of blood monocytes of $TNF^{fl/fl}$ or $CX3CR1^{Cre};TNF^{fl/fl}$ mice under steady state. $N=9$. B-C. FACS analysis of spinal cord in MOG₃₅₋₅₅ immunized $TNF^{fl/fl}$ or $CX3CR1^{Cre};TNF^{fl/fl}$ mice at day 9 (B, $n=4$) or 24 (C, $n=4-7$) post immunization. $*p < 0.05$, Mann-Whitney's u -test. Intracellular FACS stain for TNF expression of $TNF^{fl/fl}$ or $CX3CR1^{CreER};TNF^{fl/fl}$ microglia, obtained from animals treated with TAM in vivo, unstimulated or treated ex vivo with 10 $\mu\text{g/ml}$ LPS. $*p < 0.05$, Mann-Whitney's u -test.

The $CX3CR1^{Cre}$ system broadly targets tissue macrophages, as well as monocyte-derived cells¹². To investigate the role of microglial TNF we generated $CX3CR1^{CreER};TNF^{fl/fl}$ mice (Figure 34A). To validate restricted and robust microglial TNF deletion, we resorted to two complementary approaches, i.e. genomic PCR for gene deletion and flow cytometry analysis for functional deletion of secreted TNF. For the genomic PCR, we used primers, which can amplify the wild-type TNF gene, the 'floxed' TNF gene and the excised TNF gene, yielding 300 bp, 350 bp and 400 bp products, respectively. We sorted microglia ($CD45^{lo}CD11b^{+}Ly6C^{-}Ly6G^{-}$) from

CX3CR1^{Cre}: TNF^{fl/fl} and CX3CR1^{CreER}: TNF^{fl/fl} mice, which had previously been treated with 30 mg TAM, and extracted DNA from the sorted cells. To confirm microglia-restricted recombination, we also sorted splenic red pulp macrophages (CD11b^{lo}F4/80^{hi}CD11c^{int}MHCII^{int}B220^{int}) (**Figure 34A**). Genomic PCR resulted in amplification of the deleted TNF allele in sorted CX3CR1^{Cre}: TNF^{fl/fl} and CX3CR1^{CreER}: TNF^{fl/fl} microglia, whereas neither untreated, TAM-treated TNF^{fl/fl} microglia nor TAM-treated CX3CR1^{CreER}: TNF^{fl/fl} splenic macrophages showed any amplification of the deleted allele (**Figure 34A**). To analyze protein expression, TNF^{fl/fl} and CX3CR1^{CreER}: TNF^{fl/fl} mice were treated *in vivo* with TAM, and microglia were isolated and challenged with LPS *ex vivo*. Similar to the LPS response of CX3CR1^{Cre}: TNF^{fl/fl} microglia, CX3CR1^{CreER}: TNF^{fl/fl} microglia did not express TNF (**Figure 34B**). We then immunized the mice with MOG to examine their EAE disease course. In contrast to CX3CR1^{Cre}: TNF^{fl/fl} mice, CX3CR1^{CreER}: TNF^{fl/fl} mice displayed an EAE disease course, onset and severity similar to that of littermate controls (**Figure 34C-E**). Moreover, monocyte percentages in the spinal cord of the mice in EAE day 24 were similar to those of littermate controls (**Figure 34F**). Thus, microglial TNF seems obsolete for the initiation of EAE and is not critical for the recruitment of monocytes to the brain.

Our data indicate a requirement of myeloid, but not specifically microglial TNF for unimpaired monocyte infiltration and onset of EAE. Defective monocyte recruitment to the spinal cord could result from a cell-intrinsic problem. Alternatively, it could stem from the impairment of a cell-extrinsic mechanism, such as reduced activation of endothelial cells, which are known to depend on TNF¹⁶⁹ and recruit monocytes via the CCL2/CCR2 axis¹⁷⁰. CD31⁺ CD45⁻ endothelial cells isolated from the spinal cord of CX3CR1^{Cre}: TNF^{fl/fl} mice and controls did not differ in their ICAM1 or VCAM1 expression, suggesting that the reduced monocyte infiltration might not be related to an altered endothelial response (**Figure 35A**). To further investigate the possibility of a cell-intrinsic TNF-mediated mechanism for monocyte survival, we generated competitive mixed BM chimeras by reconstituting lethally-irradiated mice with equal amounts of CX3CR1^{Cre}: TNF^{fl/fl} (CD45.2) and CX3CR1^{gfp}:TNF^{+/+} (CD45.1) BM. Interestingly, we found both the Ly6C^{hi} and Ly6C^{lo} monocyte compartments of these animals to be significantly biased towards the WT TNF (CD45.1) genotype, as compared to the B cells that served as control and even showed a bias towards the CD45.2 donor BM. These results suggest that the absence of TNF in monocytes seems hence to confer a disadvantage on these cells in a cell-intrinsic manner (**Figure 35B**). Analysis of effector monocytes in the spinal cord 9 days after MOG immunization revealed a

complete out competition of the $TNF^{-/-}$ cells by the TNF sufficient effector monocytes; thus, the $TNF^{-/-}$ effector monocytes have a severe disadvantage in either reaching the inflamed tissue or surviving in it (**Figure 35C**).

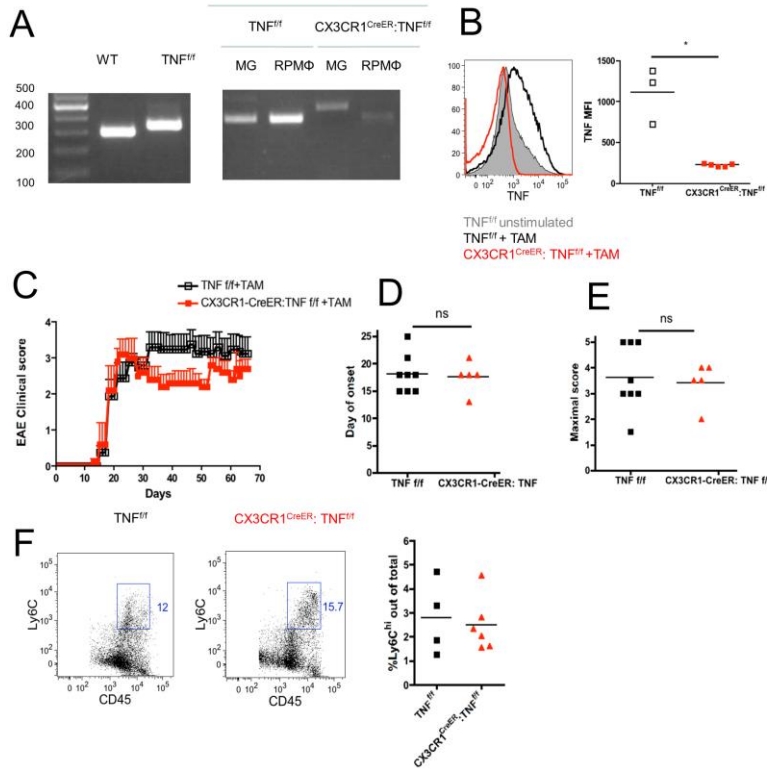


Figure 34. Microglial TNF is dispensable for onset and progression of EAE and does not alter monocyte infiltration. A. Genomic PCR of the deleted $TNF^{fl/fl}$ allele in microglia or red pulp macrophages, sorted from $TNF^{fl/fl}$ and $CX3CR1^{CreER}; TNF^{fl/fl}$ animals treated in vivo with TAM. (B). Intracellular FACS staining for TNF expression of microglia isolated from TAM-treated $TNF^{fl/fl}$ and $CX3CR1^{CreER}; TNF^{fl/fl}$ animals with or without ex vivo treatment with 10 μ g/ml LPS. $N=3-5$, $*p<0.05$, Mann-Whitney's u -test. C-E. Disease course, individual day of onset and individual maximal score of TAM-treated $TNF^{fl/fl}$ and $CX3CR1^{CreER}; TNF^{fl/fl}$ mice

immunized with MOG₃₅₋₅₅. F. FACS analysis of $CD11b^+Ly6C^-$ cell in spinal cord of TAM-treated $TNF^{fl/fl}$ and $CX3CR1^{CreER}; TNF^{fl/fl}$ mice at day 24 after immunization. $N=4-7$

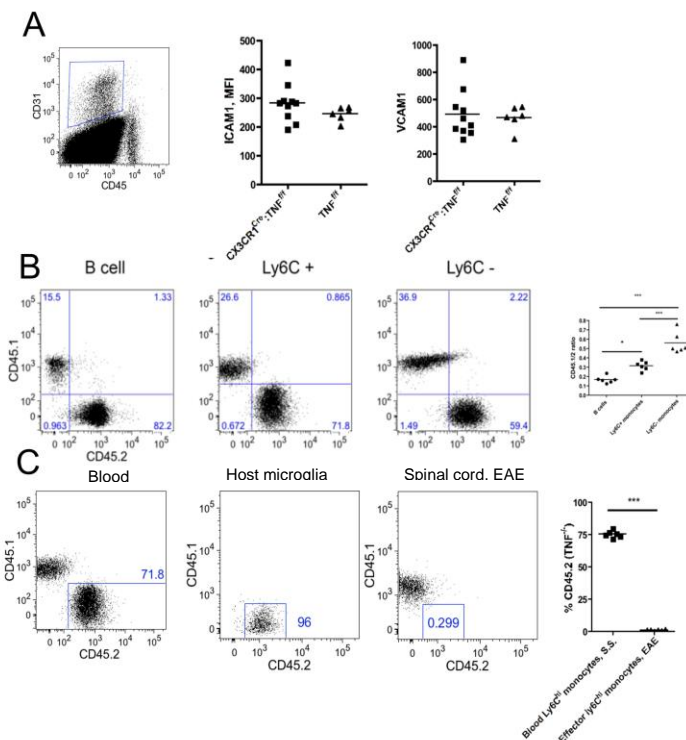


Figure 35. TNF seems to be required for monocyte survival in a cell-intrinsic manner. A. FACS analysis of the endothelial activation markers ICAM1 and VCAM1 on endothelial cells ($CD31+CD45^-$) isolated from spinal cord of $TNF^{fl/fl}$ and $CX3CR1^{CreER}; TNF^{fl/fl}$ mice 9 days after MOG₃₅₋₅₅ immunization. $N=6-10$. (B) FACS analysis of blood chimerism of chimeras, transplanted with $CD45.1 TNF^{fl/fl} CX3CR1^{flp}$ and $CD45.2 CX3CR1^{CreER}; TNF^{fl/fl}$ BM, 4 weeks after the transplantation. $N=6$, $*p<0.05$, $***p<0.001$, two-way Anova followed by Tukey's post-hoc

*test. (C) FACS analysis of CD45.1/2 ratios in CX3CR1^{Cre}: TNF^{fl/fl} mice 9 days after MOG₃₅₋₅₅ immunization. N=5-6, *p<0.05, student's t-test.*

5. Results - Part III: Ontogeny of cardiac macrophages in adulthood

The heart hosts a major population of resident macrophages^{131, 122} and we decided in collaboration with the group of Michael Sieweke (CIML, Marseille) to set out to fate-map the origin of these cardiac macrophages (CM ϕ) using the CX3CR1^{Cre}:YFP and CX3CR1^{CreER}:YFP mice, similar to our recent study that used these tools in the blood monocyte context¹². Recent gene expression studies proposed the existence of a “core signature macrophage”, including expression of the markers CD11b, F4/80, CD64, CD14 and MerTK³². CM ϕ can be traced using these markers (**Figure 36A**). In addition, the cells express CX3CR1 and MHCII, which can be used to further segregate them into four sub-populations according to their level of expression. CX3CR1 promoter activity was validated by CX3CL1-Fc staining (**Figure 36B**). In newborn mice, 95% of the CM ϕ population were CX3CR1⁺ MHCII⁻. However, by 8-weeks, the majority of CM ϕ was CX3CR1⁺ (~80%) and MHCII⁺ (~70%), allowing the delineation of four distinct subpopulations (**Figure 36C**).

Importantly, genetic fate mapping analysis using CX3CR1^{Cre}:YFP mice revealed that all adult CM subpopulations must have developed from a CX3CR1⁺ stage (**Figure 37A**). These results suggested two, not mutually exclusive possibilities for the development of CM ϕ subpopulation: persistence and diversification of embryo-derived CM ϕ as suggested elsewhere¹³² or replacement of embryo-derived CM ϕ by adult monocyte-derived macrophages, as reported for gut macrophages²¹. We further assessed the turnover of CX3CR1⁺ CM ϕ in the adult heart by pulse labeling adult CX3CR1^{CreER}:YFP mice (**Figure 37B**). 1 wk after treatment, the labeling of CM ϕ corresponded to ~60% of microglia labeling, but drastically decreased to ~20% after 4 wk. By comparison, microglia labeling was nearly complete after 1 wk and remained unchanged thereafter⁸⁹.

Whole body irradiation of CD45.2 mice followed by CD45.1 BM engraftment results in the replacement of 90-80% of the CM ϕ (**Figure 38A**). However, a small radio-resistant population (~10-20%) persists regardless of the age of the irradiated mice; this population may represent remaining embryo-derived macrophages. The vast majority of the grafted cells are MHCII⁺ (**Figure 38B**). To further analyze, whether CM ϕ replacement was monocyte-dependent,

we generated mixed chimeras with BM from WT (CD45.1) and CCR2^{-/-} (CD45.2) CX3CR1^{GFP/+} mice (into CD45.1/CD45.2 double-positive WT hosts) (**Figure 38C**). CCR2^{-/-} mice have reduced numbers of Ly6C⁺ monocytes in the blood¹⁷¹ and can therefore be used to analyze the contribution of circulating monocytes and CCR2-dependent progenitors to tissue macrophage

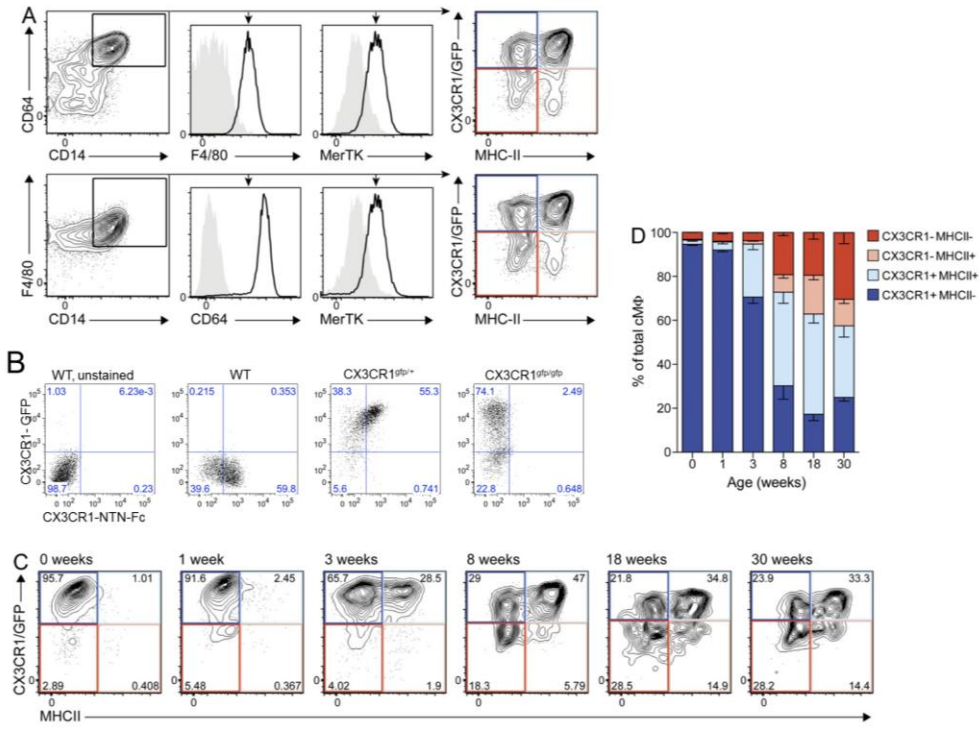


Figure 36. CMφ diversify into 4 subpopulations after birth. (A) FACS profiles of CM populations, pre-gated on living single CD11b⁺ cells with low CD11c and Ly6C expression. (B) FACS analysis of CXCR1^{GFP} CMφ with or without CX3CL1-Fc stain. (C and D) Cytometry analysis (C) and mean percentage (D) of CMφ

subpopulations from CX3CR1^{GFP/+} mice of indicated age. N=3-4

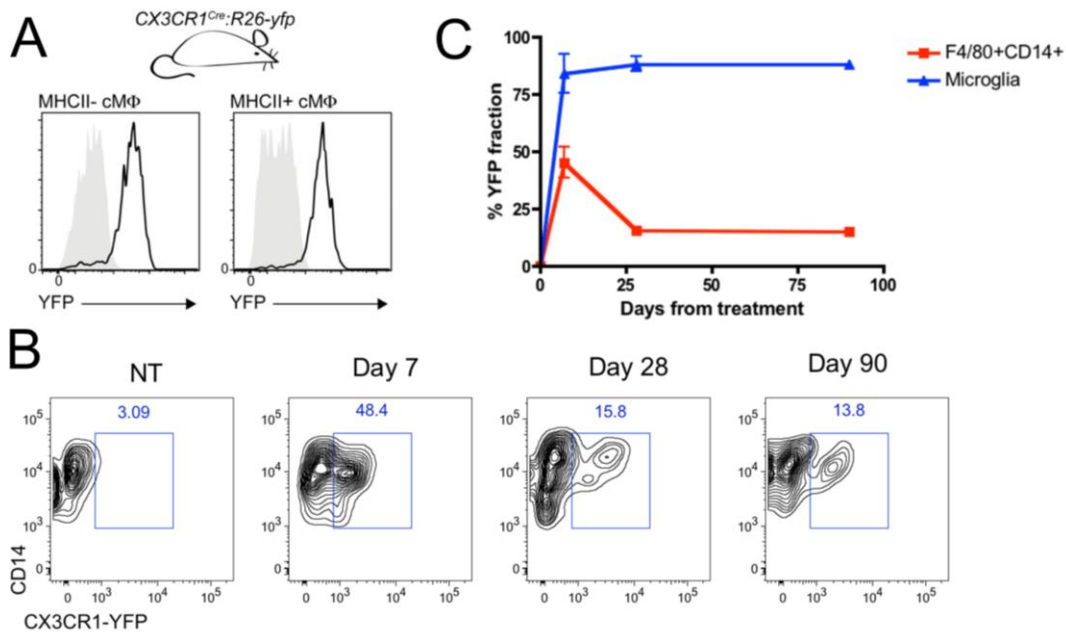


Figure 37. Adult fate-mapping of CM. A. FACS analysis of YFP fluorescence in the MHCII⁺ and MHCII⁻ CM ϕ populations in CX3CR1^{Cre}:YFP mice. B. FACS analysis of CM ϕ populations in TAM-treated CX3CR1^{CreER}:YFP mice, compared to microglia isolated from the same mice. N=3.

populations¹². Blood analysis indeed confirmed that the vast majority of monocytes in these chimeras, but not B cells were of WT origin. Moreover, graft-derived CM ϕ were almost completely derived from WT cells (**Figure 38D**). Collectively, these two experiments established that HSC-derived CCR2-dependent cells, most likely Ly6C⁺ monocytes, have the capacity to differentiate into all CM subsets. Residual host-derived CM included both MHCII⁺ and MHCII⁻ CM ϕ , but showed a lower proportion of MHCII⁺ cells than grafted monocyte-derived CM ϕ ; collectively, our data suggest that monocyte-derived CM ϕ preferably express higher levels of MHCII. To conclude, the initial pool of CM ϕ is of embryonic origin, but with time replaced by MHCII⁺ monocyte-derived *de novo* macrophages.

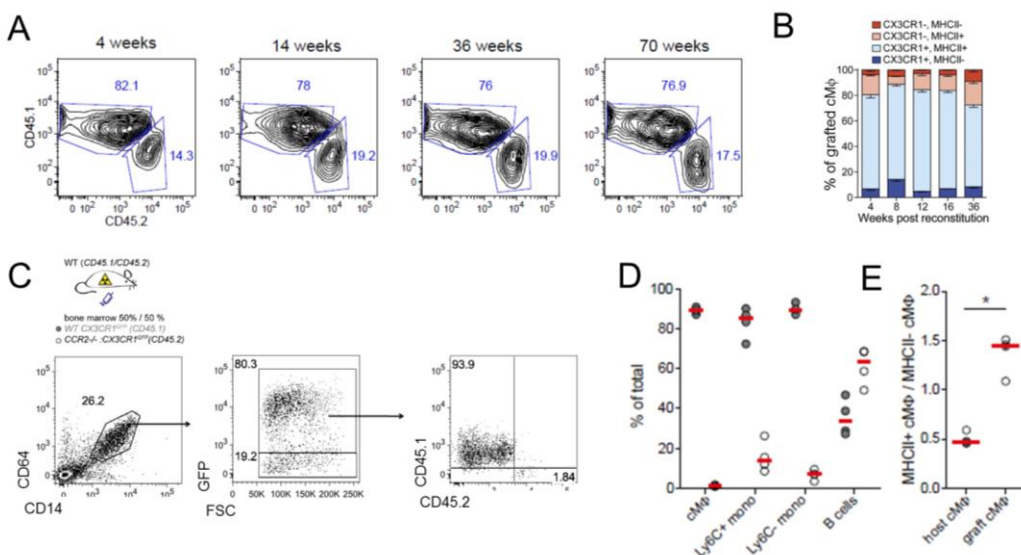


Figure 38. CM ϕ are following irradiation replaced by monocyte-derived macrophages. A. FACS analysis of CM ϕ s of lethally irradiated CD45.2 mice, transplanted with CD45.1 BM. The BM transfers were performed at different ages. B. Mixed BM chimeras were generated by reconstituting lethally irradiated WT mice (CD45.1/CD45.2) with BM from CCR2^{-/-}:CX3CR1^{GFP} (CD45.2) and WT CX3CR1^{GFP} (CD45.1) mice. CM, circulating CD11b⁺CD115⁺ monocytes (Ly6C⁺ and Ly6C⁻) and B220⁺ B cells were analyzed for WT (CD45.1) and CCR2^{-/-} (CD45.2) contribution. Host- and graft-derived CM ϕ were analyzed for the ratio of MHCII⁺/MHCII⁻ CM. Bars show median (n = 4). *, P ≤ 0.05, Mann-Whitney test

6. Discussion

Although the discoverer of macrophages, Ilya Metchnikov had already postulated at the beginning of last century that these cells have dual functions, both in tissue maintenance and the immune defense, macrophage studies have largely focused on the ability of these cells to ingest and destroy pathogens. Only more recently, accumulating evidence has begun to highlight steady-state functions of tissue macrophages. Distinct embryo- and monocyte--derived tissue macrophages have been reported¹⁸, and tissue specific genomic landscapes - both in terms of gene expression and epigenetic signatures have been revealed^{33,172}. All these findings refine our view of the tissue macrophage and contrasts it with cells that arise from monocytes, recruited as a part of the inflammatory response. As is the case for many other in vivo cell compartments, traditionally limited sets of surface markers, such as CD11b and F4/80, have turned out insufficient to match the complexity of the macrophage compartment, since tissue resident and recruited macrophages are often phenotypically indistinguishable. Advanced techniques, such as the use of Cre recombinase in combination with reporter and fate mapping studies, as well as next-generation sequencing and epigenetic screening are currently used to unmask these differences and allow us to understand the very core of macrophage/ monocyte biology.

6.1. Brown adipose tissue macrophages have a homeostatic role in energy balance

Adipose tissue macrophages (ATM) were so far only described in conditions, which disrupt the homeostasis of both the organism and the tissue, such as obesity or cold challenge. In the first part of this thesis, we provide for the first time evidence for a homeostatic role of brown adipose tissue macrophages (BAM). First, we show that, in accordance with recent findings^{32,33}, also ATM display gene expression profiles that are distinct from other tissue resident macrophages. Moreover according to our results, BAM also differ significantly from the macrophages residing the WAT, in terms of ontogeny, in correspondence with the dissimilarities between the tissues. The majority of BAM express the chemokine receptor CX3CR1, have self-renewal capacity, and are not replenished by BM precursors, again in contrast to WAM. So far, within the macrophage compartment, only microglia were known to be both CX3CR1⁺ and harbor self renewal capacity¹⁴⁸. These unique properties make the cells targetable by the CX3CR1^{CreER} system, similar to microglia⁸⁹, and thus we could use the system to efficiently delete specific genes in the cells. Using this approach we revealed an important homeostatic function of these cells. Thus, when

hampered by the loss of the MeCP2, a robust change in the transcriptome of the cells seems ultimately to lead to improper signaling in brown adipocytes, leading to reduced thermogenesis. Similar to other tissue macrophages with emerging homeostatic functions, BAM thus form an integral component of energy homeostasis, due to both their strategically positioning within the brown adipose tissue and their specific gene expression. The MeCP2 deletion in these cells, similar to MeCP2 deletions in specific neuronal subsets with distinct functions⁶⁴, perturbs the homeostatic function of the cells. The exact mechanism by which the BAMs exert their influence on the tissue is still under investigation; we propose that the macrophage MeCP2, by means of repression of transcription, maintains a modulation of either the sympathetic input to the tissue, derived from the sympathetic neurons, or the β_3 adrenergic signaling within the brown adipocytes, themselves. The reduction in *th* mRNA levels in the tissue may suggest a modulation of the sympathetic input, perhaps by means of impaired innervation. In the absence of the repression mediated by MeCP2, these homeostatic functions are impaired and thus the overall β_3 adrenergic signaling is reduced as a consequence (**Figure 39**). At present, since the $CX3CR1^{CreER}$ at the very least targets microglia and possibly other long-lived macrophages (presently uncharacterized), and since the metabolic balance depends greatly on the cross-talk between peripheral adipose tissue and the CNS, we cannot fully exclude the possibility of microglial involvement in the spontaneous obesity phenotype; However, the current data suggests limited CNS involvement.

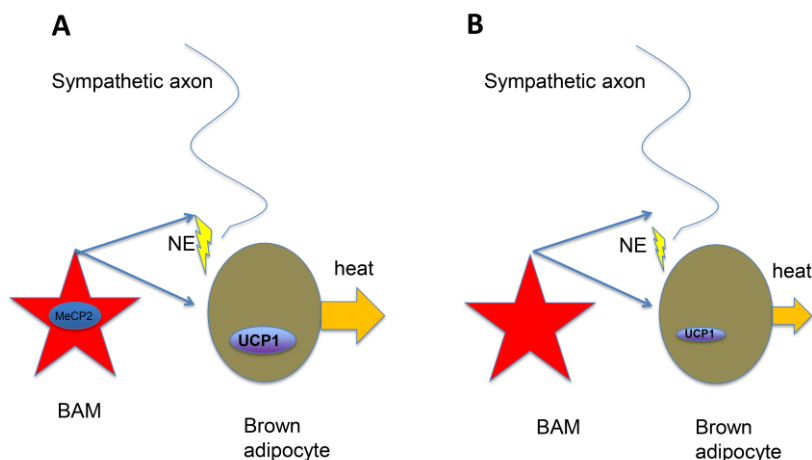


Figure 39. Proposed mechanism for MeCP2-regulated maintenance of BAT homeostasis by BAM. A. MeCP2 regulates proper BAM gene expression, essential for modulation of sympathetic tone, by either acting on the sympathetic neurons or the brown adipocytes. **B.** In the absence of MeCP2-mediated regulation, BAM modulation is impaired, manifested in reduced signaling and energy expenditure.

A seemingly paradoxical observation is the ability of the mice with MeCP2 deletion in BAM to retain their body temperature upon cold challenge in spite of the lower activity of the

tissue in 22 degrees. Even more surprising, the mice exhibit increased 'beiging' of the scWAT, as indicated by increased phosphorylation of HSL and the formation of clusters of UCP1+ cells in the tissue. The later might be explained by hypersensitization of the adrenergic β 3 receptor and that, following acute cold challenge, the sympathetic nervous system supplies an "emergency" noradrenergic tone to brown adipocytes. As a result of the hypersensitization of the receptor, the increased neuron-derived noradrenergic tone induces adequate heat production in the BAT and an even increased beiging in the scWAT. An alternative explanation is a compensatory mechanism of the WAT itself; it has been reported by several groups that in case of impaired lipid metabolism in the WAT, the tissue responds by increased beiging, manifested by increased UCP1 and mitochondrial activity⁴⁷.

Our data suggest a pivotal role of BAM in metabolism regulation of the organism; thus, it would be intriguing to manipulate the net contribution of the macrophages in regards to obesity. Specific MeCP2 mutations are a known cause for Rett's syndrome in humans⁶⁴. However, the impact of MeCP2 mutations in human individuals without Rett's syndrome is poorly described; our data define a role for MeCP2 in BAM and suggest that specific genetic MeCP2 variants in humans might disrupt energy expenditure and BAT homeostasis without causing overt neurodevelopmental impairments.

An interesting aspect not studied in this thesis is the inflammatory function of the cells, if such capacity is substantial to the inflammatory process. The cells were described in this work to participate in a strictly non-inflammatory homeostatic function; given the fact that adipocytes and adipose tissue macrophages share some similarities, namely expression of cytokines and adipokines, response to free fatty acids, phagocytic capabilities and the expression of the transcription factor PPAR-gamma¹⁷³, it is possible to regard them as a hard-wired, stroma-like cells supporting the tissue, rather than inflammatory cells. Interestingly, in lipodystrophic mice, in which the adipose tissue including the BAT is severely hypertrophic, the damage to tissue is correlated with excessive inflammation, accompanied by infiltration of monocyte-derived macrophages¹⁷⁴; however it is impossible to discern the specific role of the resident BAM in this response.

Finally, the exact role of MeCP2 in macrophages, as in many other cells, is elusive and seem to vary from cell to cell. Our data show that in the BAMs, MeCP2 mainly functions as a gene repressor, which is, as opposed to its reported action in neurons^{163,164}, however indifferent to gene length. Recently, MeCP2 was describe to modulate the survival, inflammatory response,

glucocorticoid signaling and hypoxia-induced gene expression⁶⁸. In our study, neither hypothalamic microglia nor BAM seemed to be influenced by MeCP2 deletion in terms of survival or overt inflammation. Since MeCP2 can act in numerous molecular mechanisms which vary between cell types, it may well be that this heterogeneity in mode of action exist between different macrophages, and even within microglia in different brain regions. In addition, the CX3CR1^{Cre}:MeCP2^{f/y} mice do not develop RTT symptoms. Thus the effects we observed represent better the cell-intrinsic involvement of macrophage MeCP2, excluding any artifacts seen in MeCP2-null mice due to the disease. Collectively, we describe a new role for macrophage MeCP2 within the population of BAM; further research is needed to fully substantiate the role of MeCP2 in tissue-resident macrophages.

6.2. Microglia, monocytes, and monocyte-derived macrophages in neuroinflammation: roles of MHCII and TNF

A second issue addressed in the current PhD thesis was the contribution of microglia and monocyte-derived macrophages to autoimmune neuro-inflammation. The mainstream of microglia research thus far focused on the inflammatory response of the cells to inflammatory agents, such as LPS¹⁷⁵, spinal cord injury¹⁷⁶, Alzheimer's disease¹⁷⁷ and EAE⁸⁹. It was recently shown that a deletion of the kinase TAK1, a kinase upstream of NFκB, perturbs the microglial NFκB response in terms of their cytokine (IL-1b) and chemokine expression (CCL2) expression. Notably, a TAK1 deficiency in microglia also partially attenuated EAE development⁸⁹, although the functional contribution of microglia to the disease remains to be defined. By utilizing the CX3CR1^{CreER} system, we ruled out two important immune functions, i.e. microglial antigen presentation via MHCII and microglial expression of the key pro-inflammatory cytokine TNFα. However, in the course of our studies, we revealed an unorthodox yet important intrinsic role for TNF in the effector monocytes infiltrating the spinal cord.

Here, we showed *in vivo* for the first time that microglial antigen presentation is not required for proper EAE induction, in terms of pathology and the CD4⁺ T cell compartment. Our data do not suggest that microglia cannot present antigen to T cells, but rather show that such presentation is not crucial to the adequate priming of encephalitogenic T cells, meaning that other APC in the CNS can compensate for the loss of microglia contribution in terms of antigen presentation.

Importantly, we used the chronic model of MOG₃₅₋₅₅ induced EAE. The compartment of pathogenic CD4⁺ T cells is intact in the absence of microglial MHCII, in spite of the overall elevation of MHCII surface expression in microglia. MHCII expression in itself is not sufficient for active antigen presentation, and also requires the co-stimulatory molecules CD80, CD86 and CD40. Our data show expression of the first two but not CD40. Naive T cell engagement of MHCII in the absence of proper co-stimulation leads to T cell apoptosis or anergy⁹⁷. Thus, although we excluded the requirement for microglial MHCII in priming CD4⁺ T cells, it is still possible that microglia can interact with these cells resulting in anergy.

In this thesis we utilized the MOG₃₅₋₅₅ model of EAE in C57B/6 mice, where remyelination and recovery from the disease are limited. In the MS pathology in humans, most patients however present a relapse-remitting pathology, in which recurrent attacks of demyelination leading to paralysis are followed by recovery¹⁷⁸. Such relapse-remitting EAE models exist in mice, such as the PLP₁₃₉₋₁₅₁ induced model¹⁷⁹. Our data show no involvement of microglial MHCII in the induction phase of the disease, however we did not exclude to possible involvement of microglial MHCII in the recovery phase. The PLP model is restricted to SJL mice¹⁸⁰ and its use would hence require extensive back-crossing of the CX3CR1^{CreER} system. In addition, Monocytes derived -macrophages that enter the brain parenchyma also express MHCII and costimulatory molecules¹⁸¹, and thus might contribute to antigen presentation. However the currently available experimental toolbox cannot target specifically the monocyte-derived macrophages in EAE, without targeting the microglia and DC as well. In addition, for technical reasons, i.e. the leakiness of the ‘floxed’ *i-ab* allele, CX3CR1^{Cre}:MHCII^{f/-} mice that we generated were not informative and we hence could not assess the antigen presentation capacity of monocyte-derived macrophages in EAE. This should be done in the future, since these cells likely contribute to the stimulation of T cell compartment. Interestingly, another CNS-resident, but more rare, macrophages, such as perivascular/meningeal phagocytes, can present auto-antigens to adoptively transferred pathogenic T cells¹⁸²; these cells have different origin and different gene profile than microglia¹⁸³; again, experimental systems that allows to specifically target these cells are not available.

Functions of MHCII that do not relate to antigen presentation remain poorly understood. MHCII was shown to synergize with TLR2 and TLR4¹⁸⁴, and modulate general TLR response via the phosphatase Btk¹¹⁴. The MHCII invariant chain, Ii or CD74, is known to regulate motility

and chemotaxis of both DC and macrophages^{185,186}. MHCII ligation can also induce apoptosis in mature DC¹⁸⁷. Interestingly, the antibiotic compound minocycline, administered as an anti-inflammatory drug in many CNS pathologies, negatively regulate microglial MHCII expression¹⁸⁸; whether this reduction in MHCII directly attenuates the activation of the cells or is a consequence of the attenuation has not been determined. Given the relatively scarce literature on the unique properties of MHCII, the notion of MHCII involvement in active phagocytosis is stimulating. Microglial phagocytic activity is instrumental for supporting remyelination following cuprizone challenge¹⁰⁸, and CX₃CR1-deficient microglia have impaired phagocytosis and contribute less to remyelination¹⁰⁹.

In future experiments, we will utilize the cuprizone model for sterile demyelination to test if MHCII is involved in phagocytosis, a very basic function for microglia¹⁸⁹. Recently, magnetic resonance imaging (MRI) has been used extensively to measure cuprizone-induced demyelination longitudinal and at high resolution^{190,191}; the obvious advantage of the system is the ability to monitor both demyelination and remyelination stages within the same animal. We will use the MRI in order to establish the excess demyelination in CX₃CR1^{CreER}:MHCII^{fl/y} mice. In addition we will look into phagocytosis assays, such as the uptake of FITC-conjugated zymosan by peritoneal macrophages¹⁹² and Cy3-conjugated myelin by microglia¹⁹³ from MHCII^{-/-} mice.

In a second set of experiment, we discovered a novel role for TNF in effector monocytes in EAE. In the absence of TNF, monocyte infiltration into the CNS was reduced in cell-intrinsic manner, resulting in delayed EAE (**Figure 40**). Monocytes have emerged as a crucial cell in mediating EAE development¹¹. We show that monocytes devoid of TNF α expression caused delay of the disease, and the transient depletion of monocytes at a very specific time window remarkably blocked disease progression. Importantly, all our study focus on the disease onset, since we have no relapsing remitting EAE model that would allow us to investigate the microglia role in EAE re-occurrence. The deletion of myeloid TNF α does not seem to alter the tissue damage, but to reduced monocyte numbers in the tissue; thus, myeloid TNF α is not required for the demyelination itself, which is probably mediated by other inflammatory agents. Whereas microglial TNF is not required for the induction of EAE, monocyte-derived TNF acts upon the monocytes themselves in a cell-autonomous, autocrine fashion.

TNF is known primarily as a pro-inflammatory cytokine and a mediator of apoptosis. However, some reports have shown that TNF can, in specific setting, function as a survival

factor. In human neutrophils, TNF can induce survival in NFkB dependent manner¹⁹⁴. In human DC, autocrine TNF protects against apoptosis by activation of the anti-apoptotic protein BAK and others¹⁹⁵, and TNF co-stimulation protects monocyte-derived DCs from poly (i:c) induced apoptosis¹⁹⁶. Recently, it was shown that the orphan nuclear receptor NR4A1 / Nur77 is differentially expressed in BM and blood monocyte subsets, and is important for the cell-intrinsic survival of Ly6C^{lo} monocytes¹⁷⁰. Nur77 expression is triggered by TNF in various cells, including macrophages^{197,198} and remains in the nucleus as a survival factor after TNF stimulation¹⁹⁹.

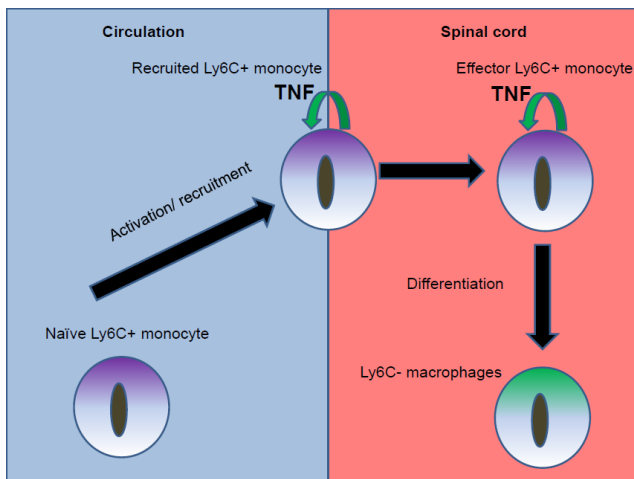


Figure 40. Proposed model for monocyte-derived TNF in EAE. Upon signals from the inflamed tissue, monocytes are being recruited from the blood, and express TNF at the process, which is important for their survival. Once they enter the spinal cord as effector cells, they can further differentiate into Ly6C⁻ macrophages which actively participate in the inflammatory/demyelination process.

A key question is, by which mechanism autocrine TNF exerts its functions in monocytes. TNFR1 or TNFR2 can each mediate this function. Thus, we will generate mixed BM chimeras from TNFR1 or TNFR2 chimeras. In this manner, since the observed TNF-dependent phenotype is autocrine, we expect to recreate the phenotype with a deficiency in one of the receptors, or both. Once we address the identity of the receptor we can further investigate the exact molecular mechanism behind the observed reduction in effector monocyte numbers.

An even more important question is whether this intrinsic TNF survival mechanism exists in human monocytes. TNF antagonist so far proved to be inefficient, or even detrimental in EAE. However, our data suggest that neutralization of monocytic TNF, either by a specific antagonist or by blockade of the corresponding receptor, could be tested clinically for its potential to ameliorate MS in humans. In addition, the TNF survival mechanism may also contribute to other conditions; for instance, reconstitution of TNF^{-/-} monocytes in DSS-induced colitis after IpDC depletion caused milder colitis compares to reconstitution with WT monocytes²⁰; whether in that

condition the reduced pathology is due to less secretion of the cytokine, or the survival of the graft, is unclear at present.

6.3. Cardiac macrophages undergo progressive replacement by monocyte-derived cells in adulthood

Finally, we have shown that the CM ϕ compartment is undergoing dynamic changes with age. Embryo-derived heart macrophages present in newborn mice are all CX3CR1⁺MHCII⁻. After birth, the CM ϕ compartment diversifies into four subpopulations defined by MHCII and CX3CR1 expression. Our results show that this diversification is due both to differentiation of persisting embryo-derived CX3CR1⁺MHCII⁻ CM ϕ and infiltrating monocyte-derived macrophages, which both can contribute to all four cM Φ subpopulations. However, monocytes preferentially give rise to MHCII⁺ CM ϕ , whereas embryo-derived or radio-resistant CM ϕ had a higher proportion of MHCII⁻ cells, explaining the relative increase of MHCII⁺ CM ϕ and the reduction of the CX3CR1⁺MHCII⁻ CM ϕ subpopulation with age (**Figure 41**). The dynamic change of the CM ϕ subpopulation distribution therefore appears to reflect the gradual replacement of embryo-derived CM ϕ by monocyte-derived macrophages. Thus, the heart stands out as a unique tissue; unlike the CNS, infiltration of BM, monocyte-derived macrophages occurs under normal, homeostatic conditions, regardless of tissue inflammation.

Our studies on the CM ϕ , raise a number of basic questions: Do monocyte-derived cells differ in terms of gene expression from the embryo-derived cells? Are monocyte-derived cells derived from BM transplants functionally distinct from host monocyte-derived and embryo derived cells? Novel techniques such as the RNA-seq, in combination with *in-utero* fate mapping will be needed to address these questions. The different ontogeny of the various macrophages might hint towards different functionalities.

The functionality of the different embryo- or monocyte-derived cells is still unclear and further studies are needed to elucidate specific general and immunological contributions of these cells. Since the rodent heart has a high regeneration capacity at the first week after birth²⁰⁰, i.e. the time window during which most CM ϕ are CX3CR1⁺MHCII⁻, one can speculate that this population might be beneficial for the regeneration process; in such a scenario, monocyte-derived

CX3CR1⁺MHCII⁺ may be more important for immuno-surveillance of the tissue. However, to be substantiated, this model will require solid experimental evidence. Also, the significance of MHCII expression in CM ϕ , similar to that of activated microglia, is unclear; whether or not these cells are in a more active state than MHCII⁻ cells, and whether these cells can actively present antigens to T cells in the organ, requires further investigation.

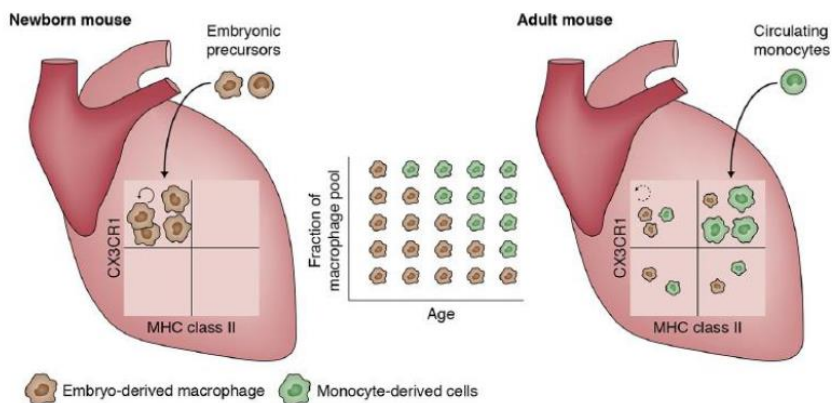


Figure 41. Summary of the turnover of CM ϕ . Embryo-derived MHCII⁺ macrophages are gradually being replaced by monocyte-derived macrophages, which express higher levels of MHCII, adopted from reference ²⁰¹.

Another key question is the requirement of the heart for such monocytic contribution, which is unique to this organ. Gut macrophages are continuously replenished from monocytes, presumably due to the low inflammatory tone of the tissue, which hosts the microbiota in its lumen; thus, the tissue itself might arguably require cells, which are slightly more 'prone' to inflammation. One might speculate that due to the importance of the heart in the circulation, the organ becomes vulnerable with adulthood to infections and thus requires monocytic cells, which are more 'alert'. Another possibility is that the embryo-derived macrophages slowly die with age, possibly due to 'wear and tear', and have more limited self-renewal capacity than microglia, and thus require replacement by the monocyte-derived cells.

6.4. Concluding remarks

In this thesis, a novel CX3CR1 promoter based gene manipulation approach enabled us to study various tissue resident, embryo-derived macrophages, such as microglia, embryo-derived cardiac macrophages, brown adipose tissue macrophages, as well as circulating monocytes, effector monocytes infiltrating the tissue, and monocyte-derived macrophages.

Using the CX3CR1 Cre systems we were able to show for the first time a prominent role for

brown adipose tissue macrophages in the maintenance and homeostasis of metabolism and energy expenditure. In our study, deletion of the transcriptional regulator MeCP2 hampered the functionality of the cells resulting in obesity. The data call both for a more extensive research of the interrelations between adipose tissue macrophages, adipocytes, and obesity, and also shed a new light on MeCP2 function in the organism. Thus, our data suggest that the brown adipose macrophages, of which so far a very scarce literature exists, should gain more focus in the research of metabolism and obesity, due to their apparent crucial role in regulation of energy expenditure.

While a relatively solid body of evidence describes microglia function under inflammatory conditions, much less is known about their role in steady state. Indeed, emerging evidence suggests an activity-dependent involvement of microglia in synapse refinement in the resting adult brain²⁰². Moreover, microglia have been shown to actively phagocytosis apoptotic neurons during early adult neurogenesis^{8,203}, induce apoptosis of developmental Purkinje cells in the cerebellum²⁰⁴ and modulate synaptic pruning²⁰⁵. Collectively, these findings point at a profound role for microglia in the steady state. In light of the difficulty to define microglial contributions to the neuro-inflammation of EAE, one might speculate that microglia are more important as modulators of brain architecture and activity, similar to the maintenance functions of other tissue-resident macrophages. Thus, while it may still be possible that microglia play a significant role in the EAE initiation by other mechanism, our findings suggest that microglia are of minor importance for the EAE initiation. This however does not explain the results obtained with the TAK1 deficiency⁸⁹. Moreover the role of microglia in relapsing remitting settings should be explored.

By utilizing the CX3CR1^{cre} system, which is a considerable improvement over the earlier LysM^{cre} system in terms of efficiency and exclusiveness of targeting^{89,206}, we could show for the first time a cell-intrinsic mechanism for the survival of effector monocytes, which is dependent of the autocrine signaling of TNF. In its absence, effector monocyte numbers in the spinal cord are reduced, leading to a delayed, yet not attenuated, EAE pathology. The effect is attributed solely to the monocytes, since the CD4⁺ T cell compartment is intact, and the microglia-derived TNF is not required for the pathology of the disease, as shown by using the more restricted CX3CR1^{CreER} system. Thus, TNF emerges as an important molecule for monocyte function not as a pro-inflammatory agent, but rather as a signal for the integrity of the monocyte compartment. Once more, monocytes should gain more focus in the research of EAE and MS, as they appear to be crucial myeloid cells in this pathology, and their ablation prevents in animal models most of the

pathological outcomes.

Finally, the $CX3CR1^{Cre}$ and $CX3CR1^{CreER}$ systems were used to study the ontogeny of a novel macrophage subset, the $CM\phi$. In collaboration with the Sieweke group, we were able to use these systems to show that upon establishment of the embryo-derived heart macrophage pool, due to slow turn-over monocyte-derived macrophages emerge. Similar to the brown adipose macrophages, cardiac macrophages, received until very recently few attention; our data show that these cells are unique throughout the mononuclear phagocyte system at least in terms of cell ontogeny, and thus may have also special functionalities within the organ.

To conclude, in this thesis we show that the $CX3CR1^{Cre}$ based systems are powerful new tools to study the mononuclear phagocyte system in ways never done before, excluding some of the limitations and artifacts of previous methods. The systems offer vast opportunities and possibilities in the research of mononuclear phagocytes, and expand the limitations of the research; the systems can be used to shed light on overlooked or completely new macrophage subtypes, as well as deleting specific genes in known subtype with much finer resolution.

References

- 1 Geissmann, F. *et al.* Development of Monocytes, Macrophages, and Dendritic Cells. *Science* **327**, 656-661, doi:10.1126/science.1178331 (2010).
- 2 Davies, L. C., Jenkins, S. J., Allen, J. E. & Taylor, P. R. Tissue-resident macrophages. *Nat Immunol* **14**, 986-995, doi:10.1038/ni.2705 (2013).
- 3 Kohyama, M. *et al.* Role for Spi-C in the development of red pulp macrophages and splenic iron homeostasis. *Nature* **457**, 318-321, doi:http://www.nature.com/nature/journal/v457/n7227/supinfo/nature07472_S1.html (2009).
- 4 Theurl, M. *et al.* Kupffer cells modulate iron homeostasis in mice via regulation of hepcidin expression. *J Mol Med* **86**, 825-835, doi:10.1007/s00109-008-0346-y (2008).
- 5 Kollet, O. *et al.* Osteoclasts degrade endosteal components and promote mobilization of hematopoietic progenitor cells. *Nat Med* **12**, 657-664, doi:10.1038/nm1417 (2006).
- 6 Parkhurst, Christopher N. *et al.* Microglia Promote Learning-Dependent Synapse Formation through Brain-Derived Neurotrophic Factor. *Cell* **155**, 1596-1609, doi:<http://dx.doi.org/10.1016/j.cell.2013.11.030> (2013).
- 7 Schafer, Dorothy P. *et al.* Microglia Sculpt Postnatal Neural Circuits in an Activity and Complement-Dependent Manner. *Neuron* **74**, 691-705, doi:<http://dx.doi.org/10.1016/j.neuron.2012.03.026> (2012).
- 8 Sierra, A. *et al.* Microglia Shape Adult Hippocampal Neurogenesis through Apoptosis-Coupled Phagocytosis. *Cell stem cell* **7**, 483-495 (2010).
- 9 Guilliams, M. *et al.* Dendritic cells, monocytes and macrophages: a unified nomenclature based on ontogeny. *Nat Rev Immunol* **14**, 571-578, doi:10.1038/nri3712 (2014).
- 10 Ginhoux, F. & Jung, S. Monocytes and macrophages: developmental pathways and tissue homeostasis. *Nat Rev Immunol* **14**, 392-404, doi:10.1038/nri3671 (2014).

- 11 Ajami, B., Bennett, J. L., Krieger, C., McNagny, K. M. & Rossi, F. M. V. Infiltrating monocytes trigger EAE progression, but do not contribute to the resident microglia pool. *Nat Neurosci* **14**, 1142-1149 (2011).
- 12 Yona, S. *et al.* Fate Mapping Reveals Origins and Dynamics of Monocytes and Tissue Macrophages under Homeostasis. *Immunity* **38**, 79-91, doi:10.1016/j.immuni.2012.12.001 (2013).
- 13 Chorro, L. *et al.* Langerhans cell (LC) proliferation mediates neonatal development, homeostasis, and inflammation-associated expansion of the epidermal LC network. *J Exp Med* **206**, 3089-3100, doi:10.1084/jem.20091586 (2009).
- 14 Ginhoux, F. *et al.* Fate Mapping Analysis Reveals That Adult Microglia Derive from Primitive Macrophages. *Science* **330**, 841-845, doi:10.1126/science.1194637 (2010).
- 15 Hashimoto, D. *et al.* Tissue-resident macrophages self-maintain locally throughout adult life with minimal contribution from circulating monocytes. *Immunity* **38**, 792-804, doi:10.1016/j.immuni.2013.04.004 (2013).
- 16 Hoeffel, G. *et al.* Adult Langerhans cells derive predominantly from embryonic fetal liver monocytes with a minor contribution of yolk sac-derived macrophages. *J Exp Med* **209**, 1167-1181, doi:10.1084/jem.20120340 (2012).
- 17 Schulz, C. *et al.* A lineage of myeloid cells independent of Myb and hematopoietic stem cells. *Science* **336**, 86-90, doi:10.1126/science.1219179 (2012).
- 18 Varol, C., Mildner, A. & Jung, S. Macrophages: development and tissue specialization. *Annual review of immunology* **33**, 643-675, doi:10.1146/annurev-immunol-032414-112220 (2015).
- 19 Gomez Perdiguero, E. *et al.* Tissue-resident macrophages originate from yolk-sac-derived erythro-myeloid progenitors. *Nature* **518**, 547-551, doi:10.1038/nature13989 (2015).
- 20 Varol, C. *et al.* Intestinal lamina propria dendritic cell subsets have different origin and functions. *Immunity* **31**, 502-512, doi:10.1016/j.immuni.2009.06.025 (2009).
- 21 Bain, C. C. *et al.* Constant replenishment from circulating monocytes maintains the macrophage pool in the intestine of adult mice. *Nat Immunol* **15**, 929-937, doi:10.1038/ni.2967 (2014).
- 22 Carlin, L. M. *et al.* Nr4a1-dependent Ly6C(low) monocytes monitor endothelial cells and orchestrate their disposal. *Cell* **153**, 362-375, doi:10.1016/j.cell.2013.03.010 (2013).

- 23 Cros, J. *et al.* Human CD14^{dim} monocytes patrol and sense nucleic acids and viruses via TLR7 and TLR8 receptors. *Immunity* **33**, 375-386, doi:10.1016/j.immuni.2010.08.012 (2010).
- 24 Geissmann, F., Jung, S. & Littman, D. R. Blood monocytes consist of two principal subsets with distinct migratory properties. *Immunity* **19**, 71-82 (2003).
- 25 Zigmond, E. *et al.* Ly6C^{hi} monocytes in the inflamed colon give rise to proinflammatory effector cells and migratory antigen-presenting cells. *Immunity* **37**, 1076-1090, doi:10.1016/j.immuni.2012.08.026 (2012).
- 26 Fogg, D. K. *et al.* A clonogenic bone marrow progenitor specific for macrophages and dendritic cells. *Science* **311**, 83-87, doi:10.1126/science.1117729 (2006).
- 27 Hettinger, J. *et al.* Origin of monocytes and macrophages in a committed progenitor. *Nat Immunol* **14**, 821-830, doi:10.1038/ni.2638 (2013).
- 28 Varol, C. *et al.* Monocytes give rise to mucosal, but not splenic, conventional dendritic cells. *J Exp Med* **204**, 171-180, doi:10.1084/jem.20061011 (2007).
- 29 Mildner, A., Yona, S. & Jung, S. A close encounter of the third kind: monocyte-derived cells. *Advances in immunology* **120**, 69-103, doi:10.1016/B978-0-12-417028-5.00003-X (2013).
- 30 Yamasaki, R. *et al.* Differential roles of microglia and monocytes in the inflamed central nervous system. *J Exp Med* **211**, 1533-1549, doi:10.1084/jem.20132477 (2014).
- 31 Zigmond, E. *et al.* Infiltrating monocyte-derived macrophages and resident kupffer cells display different ontogeny and functions in acute liver injury. *J Immunol* **193**, 344-353, doi:10.4049/jimmunol.1400574 (2014).
- 32 Gautier, E. L. *et al.* Gene-expression profiles and transcriptional regulatory pathways that underlie the identity and diversity of mouse tissue macrophages. *Nat Immunol* **13**, 1118-1128, doi:10.1038/ni.2419 (2012).
- 33 Lavin, Y. *et al.* Tissue-resident macrophage enhancer landscapes are shaped by the local microenvironment. *Cell* **159**, 1312-1326, doi:10.1016/j.cell.2014.11.018 (2014).
- 34 Odegaard, J. I. & Chawla, A. The immune system as a sensor of the metabolic state. *Immunity* **38**, 644-654, doi:10.1016/j.immuni.2013.04.001 (2013).
- 35 McNelis, J. C. & Olefsky, J. M. Macrophages, immunity, and metabolic disease. *Immunity* **41**, 36-48, doi:10.1016/j.immuni.2014.05.010 (2014).

- 36 Lumeng, C. N., Bodzin, J. L. & Saltiel, A. R. Obesity induces a phenotypic switch in adipose tissue macrophage polarization. *J Clin Invest* **117**, 175-184, doi:10.1172/JCI29881 (2007).
- 37 Weisberg, S. P. *et al.* CCR2 modulates inflammatory and metabolic effects of high-fat feeding. *J Clin Invest* **116**, 115-124, doi:10.1172/JCI24335 (2006).
- 38 Nagareddy, P. R. *et al.* Adipose tissue macrophages promote myelopoiesis and monocytosis in obesity. *Cell metabolism* **19**, 821-835, doi:10.1016/j.cmet.2014.03.029 (2014).
- 39 Amano, S. U. *et al.* Local proliferation of macrophages contributes to obesity-associated adipose tissue inflammation. *Cell metabolism* **19**, 162-171, doi:10.1016/j.cmet.2013.11.017 (2014).
- 40 Chawla, A., Nguyen, K. D. & Goh, Y. P. Macrophage-mediated inflammation in metabolic disease. *Nat Rev Immunol* **11**, 738-749, doi:10.1038/nri3071 (2011).
- 41 Deng, T. *et al.* Class II major histocompatibility complex plays an essential role in obesity-induced adipose inflammation. *Cell metabolism* **17**, 411-422, doi:10.1016/j.cmet.2013.02.009 (2013).
- 42 Kosteli, A. *et al.* Weight loss and lipolysis promote a dynamic immune response in murine adipose tissue. *J Clin Invest* **120**, 3466-3479, doi:10.1172/JCI42845 (2010).
- 43 Lee, Y. H., Petkova, A. P., Konkar, A. A. & Granneman, J. G. Cellular origins of cold-induced brown adipocytes in adult mice. *FASEB journal : official publication of the Federation of American Societies for Experimental Biology* **29**, 286-299, doi:10.1096/fj.14-263038 (2015).
- 44 Nguyen, K. D. *et al.* Alternatively activated macrophages produce catecholamines to sustain adaptive thermogenesis. *Nature* **480**, 104-108, doi:10.1038/nature10653 (2011).
- 45 Qiu, Y. *et al.* Eosinophils and type 2 cytokine signaling in macrophages orchestrate development of functional beige fat. *Cell* **157**, 1292-1308, doi:10.1016/j.cell.2014.03.066 (2014).
- 46 Brestoff, J. R. *et al.* Group 2 innate lymphoid cells promote beiging of white adipose tissue and limit obesity. *Nature* **519**, 242-246, doi:10.1038/nature14115 (2015).
- 47 Richard, D. & Picard, F. Brown fat biology and thermogenesis. *Front Biosci (Landmark Ed)* **16**, 1233-1260 (2011).

- 48 Cannon, B. & Nedergaard, J. Brown adipose tissue: function and physiological significance. *Physiological reviews* **84**, 277-359, doi:10.1152/physrev.00015.2003 (2004).
- 49 Seale, P., Kajimura, S. & Spiegelman, B. M. Transcriptional control of brown adipocyte development and physiological function--of mice and men. *Genes Dev* **23**, 788-797, doi:10.1101/gad.1779209 (2009).
- 50 Seale, P. *et al.* Transcriptional control of brown fat determination by PRDM16. *Cell metabolism* **6**, 38-54, doi:10.1016/j.cmet.2007.06.001 (2007).
- 51 Harms, M. & Seale, P. Brown and beige fat: development, function and therapeutic potential. *Nat Med* **19**, 1252-1263, doi:10.1038/nm.3361 (2013).
- 52 Ryu, V., Garretson, J. T., Liu, Y., Vaughan, C. H. & Bartness, T. J. Brown adipose tissue has sympathetic-sensory feedback circuits. *J Neurosci* **35**, 2181-2190, doi:10.1523/JNEUROSCI.3306-14.2015 (2015).
- 53 Virtanen, K. A. *et al.* Functional brown adipose tissue in healthy adults. *The New England journal of medicine* **360**, 1518-1525, doi:10.1056/NEJMoa0808949 (2009).
- 54 van Marken Lichtenbelt, W. D. *et al.* Cold-activated brown adipose tissue in healthy men. *The New England journal of medicine* **360**, 1500-1508, doi:10.1056/NEJMoa0808718 (2009).
- 55 Feldmann, H. M., Golozoubova, V., Cannon, B. & Nedergaard, J. UCP1 ablation induces obesity and abolishes diet-induced thermogenesis in mice exempt from thermal stress by living at thermoneutrality. *Cell metabolism* **9**, 203-209, doi:10.1016/j.cmet.2008.12.014 (2009).
- 56 Ouellet, V. *et al.* Brown adipose tissue oxidative metabolism contributes to energy expenditure during acute cold exposure in humans. *J Clin Invest* **122**, 545-552, doi:10.1172/JCI60433 (2012).
- 57 Chahrouh, M. & Zoghbi, H. Y. The story of Rett syndrome: from clinic to neurobiology. *Neuron* **56**, 422-437, doi:S0896-6273(07)00756-8 [pii] 10.1016/j.neuron.2007.10.001 (2007).
- 58 Chen, R. Z., Akbarian, S., Tudor, M. & Jaenisch, R. Deficiency of methyl-CpG binding protein-2 in CNS neurons results in a Rett-like phenotype in mice. *Nat Genet* **27**, 327-331 (2001).
- 59 Guy, J., Gan, J., Selfridge, J., Cobb, S. & Bird, A. Reversal of neurological defects in a mouse model of Rett syndrome. *Science* **315**, 1143-1147, doi:1138389 [pii]

10.1126/science.1138389 (2007).

- 60 Guy, J., Hendrich, B., Holmes, M., Martin, J. E. & Bird, A. A mouse *Mecp2*-null mutation causes neurological symptoms that mimic Rett syndrome. *Nat Genet* **27**, 322-326 (2001).
- 61 Shahbazian, M. D. *et al.* Mice with Truncated MeCP2 Recapitulate Many Rett Syndrome Features and Display Hyperacetylation of Histone H3. *Neuron* **35**, 243-254 (2002).
- 62 Collins, A. L. *et al.* Mild overexpression of MeCP2 causes a progressive neurological disorder in mice. *Human Molecular Genetics* **13**, 2679-2689, doi:10.1093/hmg/ddh282 (2004).
- 63 Smyk, M. *et al.* Different-sized duplications of Xq28, including MECP2, in three males with mental retardation, absent or delayed speech, and recurrent infections. *Am J Med Genet B Neuropsychiatr Genet* **147B**, 799-806, doi:10.1002/ajmg.b.30683 (2008).
- 64 Lyst, M. J. & Bird, A. Rett syndrome: a complex disorder with simple roots. *Nat Rev Genet*, doi:10.1038/nrg3897 (2015).
- 65 Bienvenu, T. & Chelly, J. Molecular genetics of Rett syndrome: when DNA methylation goes unrecognized. *Nat Rev Genet* **7**, 583-583 (2006).
- 66 Chahrouh, M. *et al.* MeCP2, a key contributor to neurological disease, activates and represses transcription. *Science* **320**, 1224-1229, doi:10.1126/science.1153252 (2008).
- 67 Cheng, T. L. & Qiu, Z. MeCP2: multifaceted roles in gene regulation and neural development. *Neuroscience bulletin* **30**, 601-609, doi:10.1007/s12264-014-1452-6 (2014).
- 68 Cronk, J. C. *et al.* Methyl-CpG Binding Protein 2 Regulates Microglia and Macrophage Gene Expression in Response to Inflammatory Stimuli. *Immunity* **42**, 679-691, doi:10.1016/j.immuni.2015.03.013 (2015).
- 69 Derecki, N. C. *et al.* Wild-type microglia arrest pathology in a mouse model of Rett syndrome. *Nature* **484**, 105-109, doi:10.1038/nature10907 (2012).
- 70 Kleefstra, T. *et al.* De novo MECP2 frameshift mutation in a boy with moderate mental retardation, obesity and gynaecomastia. *Clin Genet* **61**, 359-362 (2002).
- 71 Fyffe, S. L. *et al.* Deletion of *Mecp2* in *Sim1*-expressing neurons reveals a critical role for MeCP2 in feeding behavior, aggression, and the response to stress. *Neuron* **59**, 947-958, doi:10.1016/j.neuron.2008.07.030 (2008).
- 72 Wang, X., Lacza, Z., Sun, Y. E. & Han, W. Leptin resistance and obesity in mice with deletion of methyl-CpG-binding protein 2 (MeCP2) in hypothalamic pro-

- opiomelanocortin (POMC) neurons. *Diabetologia* **57**, 236-245, doi:10.1007/s00125-013-3072-0 (2014).
- 73 Viemari, J. C. *et al.* Mecp2 deficiency disrupts norepinephrine and respiratory systems in mice. *J Neurosci* **25**, 11521-11530, doi:10.1523/JNEUROSCI.4373-05.2005 (2005).
- 74 Lang, M. *et al.* Rescue of behavioral and EEG deficits in male and female Mecp2-deficient mice by delayed Mecp2 gene reactivation. *Hum Mol Genet* **23**, 303-318, doi:10.1093/hmg/ddt421 (2014).
- 75 Wither, R. G. *et al.* Daily rhythmic behaviors and thermoregulatory patterns are disrupted in adult female MeCP2-deficient mice. *PloS one* **7**, e35396, doi:10.1371/journal.pone.0035396 (2012).
- 76 Prinz, M., Tay, T. L., Wolf, Y. & Jung, S. Microglia: unique and common features with other tissue macrophages. *Acta neuropathologica* **128**, 319-331, doi:10.1007/s00401-014-1267-1 (2014).
- 77 Kierdorf, K. *et al.* Microglia emerge from erythromyeloid precursors via Pu.1- and Irf8-dependent pathways. *Nat Neurosci* **16**, 273-280, doi:10.1038/nn.3318 (2013).
- 78 Tremblay, M. E. *et al.* The role of microglia in the healthy brain. *J Neurosci* **31**, 16064-16069, doi:10.1523/JNEUROSCI.4158-11.2011 (2011).
- 79 Glass, C. K., Saijo, K., Winner, B., Marchetto, M. C. & Gage, F. H. Mechanisms underlying inflammation in neurodegeneration. *Cell* **140**, 918-934, doi:10.1016/j.cell.2010.02.016 (2010).
- 80 Lucin, K. M. & Wyss-Coray, T. Immune Activation in Brain Aging and Neurodegeneration: Too Much or Too Little? *Neuron* **64**, 110-122 (2009).
- 81 Ransohoff, R. M. & Cardona, A. E. The myeloid cells of the central nervous system parenchyma. *Nature* **468**, 253-262 (2010).
- 82 Mildner, A. *et al.* CCR2+Ly-6Chi monocytes are crucial for the effector phase of autoimmunity in the central nervous system. *Brain* **132**, 2487-2500, doi:10.1093/brain/awp144 (2009).
- 83 McDonald, W. I. Relapse, remission, and progression in multiple sclerosis. *The New England journal of medicine* **343**, 1486-1487, doi:10.1056/NEJM200011163432010 (2000).
- 84 Steinman, L. Multiple sclerosis: a coordinated immunological attack against myelin in the central nervous system. *Cell* **85**, 299-302, doi:M.D L" [pii] (1996).

- 85 de Rosbo, N. K. *et al.* The myelin-associated oligodendrocytic basic protein region MOBP15-36 encompasses the immunodominant major encephalitogenic epitope(s) for SJL/J mice and predicted epitope(s) for multiple sclerosis-associated HLA-DRB1*1501. *J Immunol* **173**, 1426-1435 (2004).
- 86 Prinz, M. *et al.* Innate immunity mediated by TLR9 modulates pathogenicity in an animal model of multiple sclerosis. *J Clin Invest* **116**, 456-464, doi:10.1172/JCI26078 (2006).
- 87 Goverman, J. Autoimmune T cell responses in the central nervous system. *Nat Rev Immunol* **9**, 393-407 (2009).
- 88 Heppner, F. L. *et al.* Experimental autoimmune encephalomyelitis repressed by microglial paralysis. *Nat Med* **11**, 146-152, doi:nm1177 [pii]
10.1038/nm1177 (2005).
- 89 Goldmann, T. *et al.* A new type of microglia gene targeting shows TAK1 to be pivotal in CNS autoimmune inflammation. *Nat Neurosci* **16**, 1618-1626, doi:10.1038/nn.3531 (2013).
- 90 Greter, M. *et al.* Dendritic cells permit immune invasion of the CNS in an animal model of multiple sclerosis. *Nat Med* **11**, 328-334, doi:nm1197 [pii]
10.1038/nm1197 (2005).
- 91 Ponomarev, E. D., Shriver, L. P., Maresz, K. & Dittel, B. N. Microglial cell activation and proliferation precedes the onset of CNS autoimmunity. *J Neurosci Res* **81**, 374-389, doi:10.1002/jnr.20488 (2005).
- 92 McMahon, E. J., Bailey, S. L., Castenada, C. V., Waldner, H. & Miller, S. D. Epitope spreading initiates in the CNS in two mouse models of multiple sclerosis. *Nat Med* **11**, 335-339, doi:nm1202 [pii]
10.1038/nm1202 (2005).
- 93 Anandasabapathy, N. *et al.* Flt3L controls the development of radiosensitive dendritic cells in the meninges and choroid plexus of the steady-state mouse brain. *J Exp Med* **208**, 1695-1705, doi:jem.20102657 [pii]
10.1084/jem.20102657 (2011).

- 94 Wu, G. F. *et al.* Limited sufficiency of antigen presentation by dendritic cells in models of central nervous system autoimmunity. *J Autoimmun* **36**, 56-64, doi:S0896-8411(10)00138-1 [pii]
10.1016/j.jaut.2010.10.006 (2011).
- 95 Yogeve, N. *et al.* Dendritic cells ameliorate autoimmunity in the CNS by controlling the homeostasis of PD-1 receptor(+) regulatory T cells. *Immunity* **37**, 264-275, doi:10.1016/j.immuni.2012.05.025 (2012).
- 96 Mempel, T. R., Henrickson, S. E. & Von Andrian, U. H. T-cell priming by dendritic cells in lymph nodes occurs in three distinct phases. *Nature* **427**, 154-159, doi:10.1038/nature02238 (2004).
- 97 Almolda, B., Gonzalez, B. & Castellano, B. Antigen presentation in EAE: role of microglia, macrophages and dendritic cells. *Front Biosci* **16**, 1157-1171, doi:3781 [pii] (2011).
- 98 Prinz, M. & Mildner, A. Microglia in the CNS: Immigrants from another world. *Glia* **59**, 177-187, doi:10.1002/glia.21104 (2011).
- 99 Ponomarev, E. D., Veremeyko, T., Barteneva, N., Krichevsky, A. M. & Weiner, H. L. MicroRNA-124 promotes microglia quiescence and suppresses EAE by deactivating macrophages via the C/EBP-[alpha]-PU.1 pathway. *Nat Med* **advance online publication**, doi:<http://www.nature.com/nm/journal/vaop/ncurrent/abs/nm.2266.html#supplementary-information> (2010).
- 100 Codarri, L. *et al.* ROR[gamma]t drives production of the cytokine GM-CSF in helper T cells, which is essential for the effector phase of autoimmune neuroinflammation. *Nat Immunol* **12**, 560-567, doi:<http://www.nature.com/ni/journal/v12/n6/abs/ni.2027.html#supplementary-information> (2011).
- 101 Sosa, R. A., Murphey, C., Ji, N., Cardona, A. E. & Forsthuber, T. G. The kinetics of myelin antigen uptake by myeloid cells in the central nervous system during experimental autoimmune encephalomyelitis. *J Immunol* **191**, 5848-5857, doi:10.4049/jimmunol.1300771 (2013).

- 102 Gudi, V., Gingele, S., Skripuletz, T. & Stangel, M. Glial response during cuprizone-induced de- and remyelination in the CNS: lessons learned. *Front Cell Neurosci* **8**, 73, doi:10.3389/fncel.2014.00073 (2014).
- 103 Ebner, F. *et al.* Microglial activation milieu controls regulatory T cell responses. *J Immunol* **191**, 5594-5602, doi:10.4049/jimmunol.1203331 (2013).
- 104 Lodygin, D. *et al.* A combination of fluorescent NFAT and H2B sensors uncovers dynamics of T cell activation in real time during CNS autoimmunity. *Nat Med* **19**, 784-790, doi:10.1038/nm.3182 (2013).
- 105 Town, T., Nikolic, V. & Tan, J. The microglial "activation" continuum: from innate to adaptive responses. *J Neuroinflammation* **2**, 24, doi:10.1186/1742-2094-2-24 (2005).
- 106 Remington, L. T., Babcock, A. A., Zehntner, S. P. & Owens, T. Microglial recruitment, activation, and proliferation in response to primary demyelination. *Am J Pathol* **170**, 1713-1724, doi:S0002-9440(10)61383-1 [pii] 10.2353/ajpath.2007.060783 (2007).
- 107 Voss, E. V. *et al.* Characterisation of microglia during de- and remyelination: can they create a repair promoting environment? *Neurobiology of disease* **45**, 519-528, doi:10.1016/j.nbd.2011.09.008 (2012).
- 108 Olah, M. *et al.* Identification of a microglia phenotype supportive of remyelination. *Glia* **60**, 306-321, doi:10.1002/glia.21266 (2012).
- 109 Lampron, A. *et al.* Inefficient clearance of myelin debris by microglia impairs remyelinating processes. *J Exp Med*, doi:10.1084/jem.20141656 (2015).
- 110 Poliani, P. L. *et al.* TREM2 sustains microglial expansion during aging and response to demyelination. *J Clin Invest*, doi:10.1172/JCI77983 (2015).
- 111 Hiremath, M. M., Chen, V. S., Suzuki, K., Ting, J. P. & Matsushima, G. K. MHC class II exacerbates demyelination in vivo independently of T cells. *J Neuroimmunol* **203**, 23-32, doi:S0165-5728(08)00231-2 [pii] 10.1016/j.jneuroim.2008.06.034 (2008).
- 112 Arnett, H. A., Wang, Y., Matsushima, G. K., Suzuki, K. & Ting, J. P. Functional genomic analysis of remyelination reveals importance of inflammation in oligodendrocyte regeneration. *J Neurosci* **23**, 9824-9832 (2003).

113 Moran, L. B. & Graeber, M. B. The facial nerve axotomy model. *Brain Res Brain Res Rev* **44**, 154-178, doi:10.1016/j.brainresrev.2003.11.004

S0165017303002595 [pii] (2004).

114 Liu, X. *et al.* Intracellular MHC class II molecules promote TLR-triggered innate immune responses by maintaining activation of the kinase Btk. *Nat Immunol* **12**, 416-424, doi:ni.2015 [pii]

10.1038/ni.2015 (2011).

115 Murphy, Á. C., Lalor, S. J., Lynch, M. A. & Mills, K. H. G. Infiltration of Th1 and Th17 cells and activation of microglia in the CNS during the course of experimental autoimmune encephalomyelitis. *Brain, Behavior, and Immunity* **24**, 641-651 (2010).

116 Bitsch, A. *et al.* Tumour necrosis factor alpha mRNA expression in early multiple sclerosis lesions: correlation with demyelinating activity and oligodendrocyte pathology. *Glia* **29**, 366-375 (2000).

117 Hofman, F. M., Hinton, D. R., Johnson, K. & Merrill, J. E. Tumor necrosis factor identified in multiple sclerosis brain. *J Exp Med* **170**, 607-612 (1989).

118 Aggarwal, B. B. Signalling pathways of the TNF superfamily: a double-edged sword. *Nat Rev Immunol* **3**, 745-756 (2003).

119 Horiuchi, K. *et al.* Cutting Edge: TNF- α -Converting Enzyme (TACE/ADAM17) Inactivation in Mouse Myeloid Cells Prevents Lethality from Endotoxin Shock. *The Journal of Immunology* **179**, 2686-2689 (2007).

120 Caminero, A., Comabella, M. & Montalban, X. Tumor necrosis factor alpha (TNF- α), anti-TNF- α and demyelination revisited: An ongoing story. *Journal of neuroimmunology* **234**, 1-6 (2011).

121 Solomon, A. J., Spain, R. I., Kruer, M. C. & Bourdette, D. Inflammatory neurological disease in patients treated with tumor necrosis factor alpha inhibitors. *Multiple Sclerosis Journal*, doi:10.1177/1352458511412996 (2011).

122 Kassiotis, G. & Kollias, G. Uncoupling the proinflammatory from the immunosuppressive properties of tumor necrosis factor (TNF) at the p55 TNF receptor level: implications for pathogenesis and therapy of autoimmune demyelination. *J Exp Med* **193**, 427-434 (2001).

123 Korner, H. *et al.* Critical points of tumor necrosis factor action in central nervous system autoimmune inflammation defined by gene targeting. *J Exp Med* **186**, 1585-1590 (1997).

- 124 Barker, V., Middleton, G., Davey, F. & Davies, A. M. TNF α contributes to the death of NGF-dependent neurons during development. *Nature neuroscience* **4**, 1194-1198, doi:10.1038/nn755 (2001).
- 125 Arnett, H. A. *et al.* TNF α promotes proliferation of oligodendrocyte progenitors and remyelination. *Nature neuroscience* **4**, 1116-1122, doi:10.1038/nn738 (2001).
- 126 Tsakiri, N., Papadopoulos, D., Denis, M. C., Mitsikostas, D. D. & Kollias, G. TNFR2 on non-haematopoietic cells is required for Foxp3⁺ Treg-cell function and disease suppression in EAE. *Eur J Immunol* **42**, 403-412, doi:10.1002/eji.201141659 (2012).
- 127 Grivennikov, S. I. *et al.* Distinct and Nonredundant In Vivo Functions of TNF Produced by T Cells and Macrophages/Neutrophils: Protective and Deleterious Effects. *Immunity* **22**, 93-104 (2005).
- 128 Kruglov, A. A., Lampropoulou, V., Fillatreau, S. & Nedospasov, S. A. Pathogenic and protective functions of TNF in neuroinflammation are defined by its expression in T lymphocytes and myeloid cells. *J Immunol* **187**, 5660-5670, doi:10.4049/jimmunol.1100663 (2011).
- 129 Nahrendorf, M. *et al.* The healing myocardium sequentially mobilizes two monocyte subsets with divergent and complementary functions. *J Exp Med* **204**, 3037-3047, doi:10.1084/jem.20070885 (2007).
- 130 Swirski, F. K. *et al.* Identification of splenic reservoir monocytes and their deployment to inflammatory sites. *Science* **325**, 612-616, doi:10.1126/science.1175202 (2009).
- 131 Pinto, A. R. *et al.* An abundant tissue macrophage population in the adult murine heart with a distinct alternatively-activated macrophage profile. *PloS one* **7**, e36814, doi:10.1371/journal.pone.0036814 (2012).
- 132 Epelman, S. *et al.* Embryonic and adult-derived resident cardiac macrophages are maintained through distinct mechanisms at steady state and during inflammation. *Immunity* **40**, 91-104, doi:10.1016/j.immuni.2013.11.019 (2014).
- 133 Molawi, K. *et al.* Progressive replacement of embryo-derived cardiac macrophages with age. *J Exp Med* **211**, 2151-2158, doi:10.1084/jem.20140639 (2014).
- 134 Jung, S. *et al.* Analysis of fractalkine receptor CX(3)CR1 function by targeted deletion and green fluorescent protein reporter gene insertion. *Mol Cell Biol* **20**, 4106-4114 (2000).

- 135 Srinivas, S. *et al.* Cre reporter strains produced by targeted insertion of EYFP and ECFP into the ROSA26 locus. *BMC Dev Biol* **1**, 4 (2001).
- 136 Wlodarczyk, A., Lobner, M., Cedile, O. & Owens, T. Comparison of microglia and infiltrating CD11c(+) cells as antigen presenting cells for T cell proliferation and cytokine response. *J Neuroinflammation* **11**, 57, doi:10.1186/1742-2094-11-57 (2014).
- 137 Madisen, L. *et al.* A robust and high-throughput Cre reporting and characterization system for the whole mouse brain. *Nat Neurosci* **13**, 133-140, doi:10.1038/nn.2467 (2010).
- 138 Madsen, L. *et al.* Mice lacking all conventional MHC class II genes. *Proceedings of the National Academy of Sciences* **96**, 10338-10343, doi:10.1073/pnas.96.18.10338 (1999).
- 139 Hashimoto, K., Joshi, S. K. & Koni, P. A. A conditional null allele of the major histocompatibility IA-beta chain gene. *Genesis* **32**, 152-153 (2002).
- 140 Boring, L. *et al.* Impaired monocyte migration and reduced type 1 (Th1) cytokine responses in C-C chemokine receptor 2 knockout mice. *J Clin Invest* **100**, 2552-2561, doi:10.1172/JCI119798 (1997).
- 141 Maus, U. A. *et al.* CCR2-positive monocytes recruited to inflamed lungs downregulate local CCL2 chemokine levels. *American journal of physiology. Lung cellular and molecular physiology* **288**, L350-358, doi:10.1152/ajplung.00061.2004 (2005).
- 142 Shaked, I. *et al.* MicroRNA-132 potentiates cholinergic anti-inflammatory signaling by targeting acetylcholinesterase. *Immunity* **31**, 965-973, doi:10.1016/j.immuni.2009.09.019 (2009).
- 143 Stromnes, I. M. & Goverman, J. M. Passive induction of experimental allergic encephalomyelitis. *Nat Protoc* **1**, 1952-1960, doi:10.1038/nprot.2006.284 (2006).
- 144 Jaitin, D. A. *et al.* Massively parallel single-cell RNA-seq for marker-free decomposition of tissues into cell types. *Science* **343**, 776-779, doi:10.1126/science.1247651 (2014).
- 145 Huang da, W., Sherman, B. T. & Lempicki, R. A. Systematic and integrative analysis of large gene lists using DAVID bioinformatics resources. *Nat Protoc* **4**, 44-57, doi:10.1038/nprot.2008.211 (2009).
- 146 Feil, S., Valtcheva, N. & Feil, R. Inducible Cre mice. *Methods Mol Biol* **530**, 343-363, doi:10.1007/978-1-59745-471-1_18 (2009).

- 147 Aycheh, T. *et al.* IL-23-mediated mononuclear phagocyte crosstalk protects mice from *Citrobacter rodentium*-induced colon immunopathology. *Nature communications* **6**, 6525, doi:10.1038/ncomms7525 (2015).
- 148 Wolf, Y., Yona, S., Kim, K.-W. & Jung, S. Microglia, seen from the CX3CR1 angle. *Frontiers in Cellular Neuroscience* **7**, doi:10.3389/fncel.2013.00026 (2013).
- 149 Zhu, H. *et al.* Ubiquitous expression of mRFP1 in transgenic mice. *Genesis* **42**, 86-90, doi:10.1002/gene.20129 (2005).
- 150 Bar-On, L. *et al.* CX3CR1+ CD8 α + dendritic cells are a steady-state population related to plasmacytoid dendritic cells. *Proceedings of the National Academy of Sciences* **107**, 14745-14750, doi:10.1073/pnas.1001562107 (2010).
- 151 Shahbazian, M. *et al.* Mice with truncated MeCP2 recapitulate many Rett syndrome features and display hyperacetylation of histone H3. *Neuron* **35**, 243-254 (2002).
- 152 Greenman, Y. *et al.* Postnatal ablation of POMC neurons induces an obese phenotype characterized by decreased food intake and enhanced anxiety-like behavior. *Mol Endocrinol* **27**, 1091-1102, doi:10.1210/me.2012-1344 (2013).
- 153 Christoffolete, M. A. *et al.* Mice with Targeted Disruption of the Dio2 Gene Have Cold-Induced Overexpression of the Uncoupling Protein 1 Gene but Fail to Increase Brown Adipose Tissue Lipogenesis and Adaptive Thermogenesis. *Diabetes* **53**, 577-584, doi:10.2337/diabetes.53.3.577 (2004).
- 154 Liang, H. & Ward, W. F. *PGC-1 α : a key regulator of energy metabolism*. Vol. 30 (2006).
- 155 Horvath, T. L. The hardship of obesity: a soft-wired hypothalamus. *Nat Neurosci* **8**, 561-565, doi:10.1038/nn1453 (2005).
- 156 Balthasar, N. *et al.* Divergence of melanocortin pathways in the control of food intake and energy expenditure. *Cell* **123**, 493-505, doi:10.1016/j.cell.2005.08.035 (2005).
- 157 Huszar, D. *et al.* Targeted disruption of the melanocortin-4 receptor results in obesity in mice. *Cell* **88**, 131-141 (1997).
- 158 Chen, A. S. *et al.* Inactivation of the mouse melanocortin-3 receptor results in increased fat mass and reduced lean body mass. *Nat Genet* **26**, 97-102, doi:10.1038/79254 (2000).
- 159 Krashes, M. J., Shah, B. P., Koda, S. & Lowell, B. B. Rapid versus delayed stimulation of feeding by the endogenously released AgRP neuron mediators GABA, NPY, and AgRP. *Cell metabolism* **18**, 588-595, doi:10.1016/j.cmet.2013.09.009 (2013).

- 160 Krashes, M. J. *et al.* An excitatory paraventricular nucleus to AgRP neuron circuit that drives hunger. *Nature* **507**, 238-242, doi:10.1038/nature12956 (2014).
- 161 Pinteaux, E. *et al.* Leptin induces interleukin-1beta release from rat microglial cells through a caspase 1 independent mechanism. *Journal of neurochemistry* **102**, 826-833, doi:10.1111/j.1471-4159.2007.04559.x (2007).
- 162 Tang, C. H. *et al.* Leptin-induced IL-6 production is mediated by leptin receptor, insulin receptor substrate-1, phosphatidylinositol 3-kinase, Akt, NF-kappaB, and p300 pathway in microglia. *J Immunol* **179**, 1292-1302 (2007).
- 163 Gabel, H. W. *et al.* Disruption of DNA-methylation-dependent long gene repression in Rett syndrome. *Nature*, doi:10.1038/nature14319 (2015).
- 164 Sugino, K. *et al.* Cell-type-specific repression by methyl-CpG-binding protein 2 is biased toward long genes. *J Neurosci* **34**, 12877-12883, doi:10.1523/JNEUROSCI.2674-14.2014 (2014).
- 165 Ben-Shachar, S., Chahrour, M., Thaller, C., Shaw, C. A. & Zoghbi, H. Y. Mouse models of MeCP2 disorders share gene expression changes in the cerebellum and hypothalamus. *Hum Mol Genet* **18**, 2431-2442, doi:10.1093/hmg/ddp181 (2009).
- 166 Tudor, M., Akbarian, S., Chen, R. Z. & Jaenisch, R. Transcriptional profiling of a mouse model for Rett syndrome reveals subtle transcriptional changes in the brain. *Proceedings of the National Academy of Sciences of the United States of America* **99**, 15536-15541, doi:10.1073/pnas.242566899 (2002).
- 167 Hirota, K. *et al.* Fate mapping of IL-17-producing T cells in inflammatory responses. *Nat Immunol* **12**, 255-263, doi:10.1038/ni.1993 (2011).
- 168 Codarri, L., Greter, M. & Becher, B. Communication between pathogenic T cells and myeloid cells in neuroinflammatory disease. *Trends in immunology* **34**, 114-119, doi:10.1016/j.it.2012.09.007 (2013).
- 169 Madge, L. A. & Pober, J. S. TNF signaling in vascular endothelial cells. *Experimental and molecular pathology* **70**, 317-325, doi:10.1006/exmp.2001.2368 (2001).
- 170 Paul, D. *et al.* Cell-selective knockout and 3D confocal image analysis reveals separate roles for astrocyte-and endothelial-derived CCL2 in neuroinflammation. *J Neuroinflammation* **11**, 10, doi:10.1186/1742-2094-11-10 (2014).

- 171 Serbina, N. V. & Pamer, E. G. Monocyte emigration from bone marrow during bacterial infection requires signals mediated by chemokine receptor CCR2. *Nat Immunol* **7**, 311-317, doi:10.1038/ni1309 (2006).
- 172 Gosselin, D. *et al.* Environment drives selection and function of enhancers controlling tissue-specific macrophage identities. *Cell* **159**, 1327-1340, doi:10.1016/j.cell.2014.11.023 (2014).
- 173 Gustafson, B., Hammarstedt, A., Andersson, C. X. & Smith, U. Inflamed adipose tissue: a culprit underlying the metabolic syndrome and atherosclerosis. *Arteriosclerosis, thrombosis, and vascular biology* **27**, 2276-2283, doi:10.1161/ATVBAHA.107.147835 (2007).
- 174 Herrero, L., Shapiro, H., Nayer, A., Lee, J. & Shoelson, S. E. Inflammation and adipose tissue macrophages in lipodystrophic mice. *Proceedings of the National Academy of Sciences of the United States of America* **107**, 240-245, doi:10.1073/pnas.0905310107 (2010).
- 175 Cardona, A. E. *et al.* Control of microglial neurotoxicity by the fractalkine receptor. *Nat Neurosci* **9**, 917-924, doi:10.1038/nn1715 (2006).
- 176 Shechter, R. *et al.* Infiltrating blood-derived macrophages are vital cells playing an anti-inflammatory role in recovery from spinal cord injury in mice. *PLoS medicine* **6**, e1000113, doi:10.1371/journal.pmed.1000113 (2009).
- 177 Grathwohl, S. A. *et al.* Formation and maintenance of Alzheimer's disease beta-amyloid plaques in the absence of microglia. *Nat Neurosci* **12**, 1361-1363, doi:10.1038/nn.2432 (2009).
- 178 Compston, A. & Coles, A. Multiple sclerosis. *Lancet* **372**, 1502-1517, doi:10.1016/S0140-6736(08)61620-7 (2008).
- 179 Miller, S. D. & Karpus, W. J. Experimental autoimmune encephalomyelitis in the mouse. *Current protocols in immunology / edited by John E. Coligan ... [et al.]* **Chapter 15**, Unit 15 11, doi:10.1002/0471142735.im1501s77 (2007).
- 180 Hart, B. A., Gran, B. & Weissert, R. EAE: imperfect but useful models of multiple sclerosis. *Trends in molecular medicine* **17**, 119-125, doi:10.1016/j.molmed.2010.11.006 (2011).

- 181 Jiang, Z., Jiang, J. X. & Zhang, G. X. Macrophages: a double-edged sword in experimental autoimmune encephalomyelitis. *Immunology letters* **160**, 17-22, doi:10.1016/j.imlet.2014.03.006 (2014).
- 182 Bartholomaeus, I. *et al.* Effector T cell interactions with meningeal vascular structures in nascent autoimmune CNS lesions. *Nature* **462**, 94-98, doi:10.1038/nature08478 (2009).
- 183 Zeisel, A. *et al.* Brain structure. Cell types in the mouse cortex and hippocampus revealed by single-cell RNA-seq. *Science* **347**, 1138-1142, doi:10.1126/science.aaa1934 (2015).
- 184 Frei, R. *et al.* MHC class II molecules enhance Toll-like receptor mediated innate immune responses. *PloS one* **5**, e8808, doi:10.1371/journal.pone.0008808 (2010).
- 185 Fan, H. *et al.* Macrophage migration inhibitory factor and CD74 regulate macrophage chemotactic responses via MAPK and Rho GTPase. *J Immunol* **186**, 4915-4924, doi:10.4049/jimmunol.1003713 (2011).
- 186 Faure-Andre, G. *et al.* Regulation of dendritic cell migration by CD74, the MHC class II-associated invariant chain. *Science* **322**, 1705-1710, doi:10.1126/science.1159894 (2008).
- 187 Leverkus, M. *et al.* MHC class II-mediated apoptosis in dendritic cells: a role for membrane-associated and mitochondrial signaling pathways. *International immunology* **15**, 993-1006 (2003).
- 188 Nikodemova, M., Watters, J. J., Jackson, S. J., Yang, S. K. & Duncan, I. D. Minocycline down-regulates MHC II expression in microglia and macrophages through inhibition of IRF-1 and protein kinase C (PKC)alpha/betaII. *The Journal of biological chemistry* **282**, 15208-15216, doi:10.1074/jbc.M611907200 (2007).
- 189 Perry, V. H. & Teeling, J. Microglia and macrophages of the central nervous system: the contribution of microglia priming and systemic inflammation to chronic neurodegeneration. *Seminars in immunopathology* **35**, 601-612, doi:10.1007/s00281-013-0382-8 (2013).
- 190 Schregel, K. *et al.* Demyelination reduces brain parenchymal stiffness quantified in vivo by magnetic resonance elastography. *Proceedings of the National Academy of Sciences of the United States of America* **109**, 6650-6655, doi:10.1073/pnas.1200151109 (2012).
- 191 Thiessen, J. D. *et al.* Quantitative MRI and ultrastructural examination of the cuprizone mouse model of demyelination. *NMR in biomedicine* **26**, 1562-1581, doi:10.1002/nbm.2992 (2013).

- 192 Nuutila, J. & Lilius, E. M. Flow cytometric quantitative determination of ingestion by phagocytes needs the distinguishing of overlapping populations of binding and ingesting cells. *Cytometry. Part A : the journal of the International Society for Analytical Cytology* **65**, 93-102, doi:10.1002/cyto.a.20139 (2005).
- 193 Liu, Y. *et al.* Suppression of microglial inflammatory activity by myelin phagocytosis: role of p47-PHOX-mediated generation of reactive oxygen species. *J Neurosci* **26**, 12904-12913, doi:10.1523/JNEUROSCI.2531-06.2006 (2006).
- 194 Cowburn, A. S., Deighton, J., Walmsley, S. R. & Chilvers, E. R. The survival effect of TNF-alpha in human neutrophils is mediated via NF-kappa B-dependent IL-8 release. *Eur J Immunol* **34**, 1733-1743, doi:10.1002/eji.200425091 (2004).
- 195 Lehner, M. *et al.* Autocrine TNF is critical for the survival of human dendritic cells by regulating BAK, BCL-2, and FLIPL. *J Immunol* **188**, 4810-4818, doi:10.4049/jimmunol.1101610 (2012).
- 196 Thorne, A. *et al.* Tumor necrosis factor-alpha promotes survival and phenotypic maturation of poly(I:C)-treated dendritic cells but impairs their Th1 and Th17 polarizing capability. *Cytotherapy* **17**, 633-646, doi:10.1016/j.jcyt.2014.11.006 (2015).
- 197 Pei, L., Castrillo, A., Chen, M., Hoffmann, A. & Tontonoz, P. Induction of NR4A Orphan Nuclear Receptor Expression in Macrophages in Response to Inflammatory Stimuli. *Journal of Biological Chemistry* **280**, 29256-29262, doi:10.1074/jbc.M502606200 (2005).
- 198 Pei, L., Castrillo, A. & Tontonoz, P. Regulation of Macrophage Inflammatory Gene Expression by the Orphan Nuclear Receptor Nur77. *Molecular Endocrinology* **20**, 786-794, doi:doi:10.1210/me.2005-0331 (2006).
- 199 Suzuki, S. *et al.* Nur77 as a survival factor in tumor necrosis factor signaling. *Proceedings of the National Academy of Sciences of the United States of America* **100**, 8276-8280, doi:10.1073/pnas.0932598100 (2003).
- 200 Laflamme, M. A. & Murry, C. E. Heart regeneration. *Nature* **473**, 326-335, doi:10.1038/nature10147 (2011).
- 201 Lambrecht, B. & Guillems, M. Monocytes find a new place to dwell in the niche of heartbreak hotel. *J Exp Med* **211**, 2136, doi:10.1084/jem.21111insight1 (2014).
- 202 Tremblay, M. E., Lowery, R. L. & Majewska, A. K. Microglial interactions with synapses are modulated by visual experience. *PLoS Biol* **8**, e1000527, doi:10.1371/journal.pbio.1000527 (2010).

- 203 Peri, F. & Nüsslein-Volhard, C. Live Imaging of Neuronal Degradation by Microglia Reveals a Role for v0-ATPase a1 in Phagosomal Fusion In Vivo. *Cell* **133**, 916-927 (2008).
- 204 Marin-Teva, J. L. *et al.* Microglia promote the death of developing Purkinje cells. *Neuron* **41**, 535-547, doi:S0896627304000698 [pii] (2004).
- 205 Paolicelli, R. C. *et al.* Synaptic Pruning by Microglia Is Necessary for Normal Brain Development. *Science* **333**, 1456-1458, doi:10.1126/science.1202529 (2011).
- 206 Clausen, B. E., Burkhardt, C., Reith, W., Renkawitz, R. & Forster, I. Conditional gene targeting in macrophages and granulocytes using LysMcre mice. *Transgenic research* **8**, 265-277 (1999).

Appendix- Progressive replacement of embryo-derived cardiac macrophages with age, by Molawi, Wolf *et al*

Published September 22, 2014

JEM

Brief Definitive Report

Progressive replacement of embryo-derived cardiac macrophages with age

Kaaweh Molawi,^{1,2,3,4} Yochai Wolf,⁵ Prashanth K. Kandalla,^{1,2,3} Jeremy Favret,^{1,2,3} Nora Hagemeyer,⁶ Kathrin Frenzel,⁶ Alexander R. Pinto,⁸ Kay Klapproth,⁹ Sandrine Henri,^{1,2,3} Bernard Malissen,^{1,2,3} Hans-Reimer Rodewald,⁹ Nadia A. Rosenthal,^{8,10} Marc Bajenoff,^{1,2,3} Marco Prinz,^{6,7} Steffen Jung,⁵ and Michael H. Sieweke^{1,2,3,4}

¹Centre d'Immunologie de Marseille-Luminy (CIML), Aix-Marseille Université, UM2, 13288 Marseille, France

²Institut National de la Santé et de la Recherche Médicale (INSERM), U1104, 13288 Marseille, France

³Centre National de la Recherche Scientifique (CNRS), UMR7280, 13288 Marseille, France

⁴Max-Delbrück-Centrum für Molekulare Medizin (MDC), Robert-Rössle-Strasse 10, 13125 Berlin, Germany

⁵Department of Immunology, The Weizmann Institute of Science, 7610001 Rehovot, Israel

⁶Institute of Neuropathology and ⁷BIOSS Centre for Biological Signaling Studies, University of Freiburg, 79106 Freiburg, Germany

⁸Australian Regenerative Medicine Institute (ARMI), Monash University, Clayton 3800, Victoria, Australia

⁹Division of Cellular Immunology, German Cancer Research Center (DKFZ), D-69120 Heidelberg, Germany

¹⁰National Heart and Lung Institute, Imperial College London, London SW7 2AZ, England, UK

Cardiac macrophages (cMΦ) are critical for early postnatal heart regeneration and fibrotic repair in the adult heart, but their origins and cellular dynamics during postnatal development have not been well characterized. Tissue macrophages can be derived from embryonic progenitors or from monocytes during inflammation. We report that within the first weeks after birth, the embryo-derived population of resident CX3CR1⁺ cMΦ diversifies into MHCII⁺ and MHCII⁻ cells. Genetic fate mapping demonstrated that cMΦ derived from CX3CR1⁺ embryonic progenitors persisted into adulthood but the initially high contribution to resident cMΦ declined after birth. Consistent with this, the early significant proliferation rate of resident cMΦ decreased with age upon diversification into subpopulations. Bone marrow (BM) reconstitution experiments showed monocyte-dependent quantitative replacement of all cMΦ populations. Furthermore, parabiotic mice and BM chimeras of nonirradiated recipient mice revealed a slow but significant donor contribution to cMΦ. Together, our observations indicate that in the heart, embryo-derived cMΦ show declining self-renewal with age and are progressively substituted by monocyte-derived macrophages, even in the absence of inflammation.

The Journal of Experimental Medicine

Downloaded from jem.rupress.org on April 27, 2015

CORRESPONDENCE

Michael H. Sieweke:
sieweke@ciml.univ-mrs.fr

Abbreviations used: cMΦ, cardiac macrophages; HSC, hematopoietic stem cell; YS, yolk sac.

Cardiovascular disease represents a leading cause of death in the developed world, and many pathologies result from insufficient repair of cardiac injury. Mammalian wound healing mechanisms in the adult heart involve scar formation, but for a short time window after birth the neonatal heart maintains full regeneration capacity of cardiac tissue (Porrello *et al.*, 2011), a process which requires macrophages (Aurora *et al.*, 2014). Studies of cardiac repair after myocardial infarction in the adult have highlighted the critical role of infiltrating monocytes and monocyte-derived macrophages for the healing

process (Nahrendorf *et al.*, 2007; Swirski *et al.*, 2009). The focus of these studies has been on monocyte-derived cells, consistent with the traditional view that macrophages are part of the mononuclear phagocyte system and monocyte-derived (van Furth and Cohn, 1968; Geissmann *et al.*, 2010). Recent evidence, however, suggests that monocyte contribution to macrophages only represents an emergency pathway, as many tissue macrophage populations get seeded in the developing embryo and can self-maintain without major monocyte contribution

K. Molawi and Y. Wolf contributed equally to this paper.
Steffen Jung and M.H. Sieweke contributed equally to this paper.

© 2014 Molawi *et al.* This article is distributed under the terms of an Attribution-NonCommercial-Share Alike-No Mirror Sites license for the first six months after the publication date (see <http://www.rupress.org/terms>). After six months it is available under a Creative Commons License (Attribution-NonCommercial-Share Alike 3.0 Unported license, as described at <http://creativecommons.org/licenses/by-nc-sa/3.0/>).

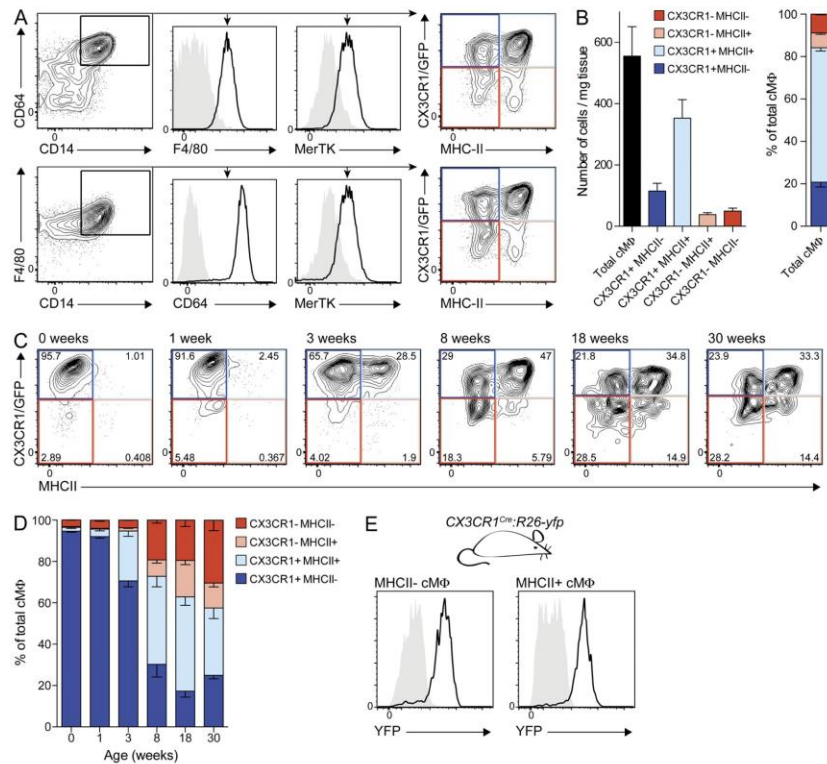


Figure 1. cMΦ develop into 4 subpopulations after birth. (A and B) Cytometry analysis of cMΦ from adult *CX3CR1^{GFP/+}* mice. (A) FACS profiles of cMΦ populations, pregated on living single CD11b⁺ cells with low CD11c and Ly6C expression. (B) Mean of total and subpopulations of cMΦ in absolute numbers (left) or as percentage of total (right) as determined by bead-normalized flow cytometry. Error bars represent SEM ($n = 4$). (C and D) Cytometry analysis (C) and mean percentage (D) of cMΦ subpopulations from *CX3CR1^{GFP/+}* mice of indicated age. Error bars represent SEM ($n = 3-4$). (E) MHCII⁻ and MHCII⁺ cMΦ from adult *CX3CR1^{Cre};R26-yfp* mice (black line) were analyzed for YFP expression and compared with Cre⁻ littermate controls (gray area; $n = 3-4$). Data in all panels are representative of at least two independent experiments.

(Chorro et al., 2009; Ginhoux et al., 2010; Hoeffel et al., 2012; Schulz et al., 2012; Hashimoto et al., 2013; Yona et al., 2013). Macrophages can massively expand in the tissue by local proliferation in response to challenge (Jenkins et al., 2011; Hashimoto et al., 2013; Sieweke and Allen, 2013) and can extensively self-renew without loss of differentiated function in culture upon inactivation of MafB and cMaf transcription factors (Aziz et al., 2009). This has led to the proposition that tissue macrophages may have a long-term self-renewal capacity akin to that of stem cells (Sieweke and Allen, 2013).

Examples of tissue macrophages that are independent from monocytes are microglia in the brain and epidermal Langerhans cells (Ajami et al., 2007; Chorro et al., 2009; Ginhoux et al., 2010; Hoeffel et al., 2012). In contrast, intestinal or dermal macrophages have a high turnover rate and are constantly replaced from Ly6C⁺ blood monocytes (Zigmond

et al., 2012; Tamoutounour et al., 2013). Thus, origin and turnover of tissue macrophages are highly tissue specific and need to be assessed individually for different organ systems (Sieweke and Allen, 2013).

Resident macrophages can be found in all tissues, where they fulfill a variety of tissue-specific functions contributing to homeostasis, development, and regeneration (Davies et al., 2013), making them prominent candidates for therapeutic intervention. This holds in particular for the heart, where tissue-resident cardiac macrophages (cMΦ) have been described as CX3CR1⁺ cells that can be found throughout the myocardium (Pinto et al., 2012). A recent study identified several cMΦ populations, including short-lived monocyte-derived cells that resemble monocyte-derived DCs as well as tissue-resident cMΦ, which were suggested to be primarily of embryonic origin and to self-maintain under homeostatic conditions (Epelman et al., 2014).

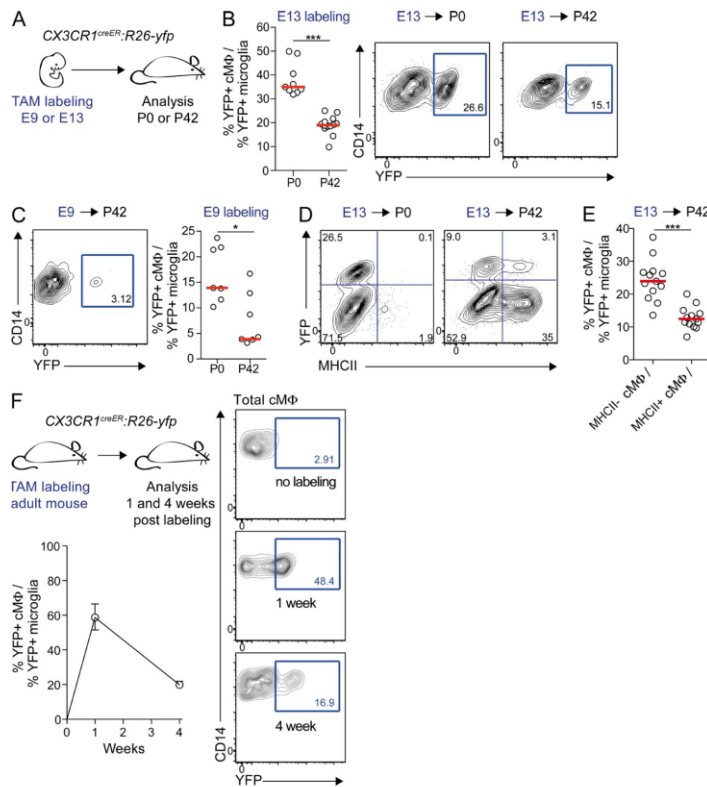


Figure 2. Decreased contribution of embryo-derived macrophages to cMΦ with age.

(A) *CX3CR1^{CreER};R26-yfp* embryos were treated with TAM on E9 or E13 and analyzed on the day of delivery (P0) or 6 wk after delivery (P42). (B) Percentage of microglia-normalized YFP⁺ cMΦ and representative cytometry plots pregated on total cMΦ at P0 and P42 after E13 labeling. Bars show median ($n = 9-13$). ***, $P \leq 0.005$, Mann-Whitney test. Data were pooled from two independent experiments. (C) Representative cytometry plot showing YFP⁺ within total cMΦ at P42 and percentage of microglia-normalized YFP⁺ cMΦ at P0 and P42 after E9 labeling. Bars show median ($n = 7$). *, $P \leq 0.05$. Data were pooled from three independent experiments. (D) Representative cytometry plots showing YFP⁺ cells within MHCII⁻ and MHCII⁺ cMΦ at P0 and P42 after E13 labeling ($n = 9-13$). (E) Quantification of YFP⁺ cells within MHCII⁻ and MHCII⁺ cMΦ at P42 after E13 labeling. Bars show the median ($n = 9-13$). ***, $P \leq 0.005$, Mann-Whitney test. Data were pooled from two independent experiments. (F) Adult TAM-treated *CX3CR1^{CreER};R26-yfp* mice were analyzed for YFP⁺ cMΦ and microglia at 1 and 4 wk after treatment. Percentage of microglia-normalized YFP⁺ cMΦ is shown as median with extreme samples as error bars ($n = 3$). Representative cytometry plots show YFP⁺ within total cMΦ. Unless otherwise indicated data in all panels are representative of two independent experiments.

Here, we examined the origin and turnover of tissue-resident cMΦ during postnatal development. Using genetic lineage tracing, parabiotic mice, and unconditioned BM chimeras, we demonstrate that embryo-derived cMΦ are gradually replaced by monocyte-derived macrophages with age and in the absence of inflammation or injury. This replacement is mirrored by dynamic changes in the resident cMΦ population composition and decreasing cMΦ self-renewal over time.

RESULTS AND DISCUSSION

We focused on the resident cMΦ population and applied a rigorous flow cytometry gating strategy to exclude potential infiltrating leukocytes (Fig. S1, A–C). Tissue-resident macrophages were identified as positive for the core macrophage signature markers CD14, CD64, and MerTK (Gautier et al., 2012; Tamoutounour et al., 2013) and the classical macrophage marker F4/80 (Fig. 1 A). The chemokine receptor CX3CR1 is widely expressed in the mononuclear phagocyte system (Jung et al., 2000) and cMΦ have been reported to be CX3CR1-positive (Pinto et al., 2012). Therefore, we refined our analysis of the global cMΦ population by testing CX3CR1 expression in *CX3CR1^{GFP/+}* knock-in mice (Jung et al., 2000). Additionally, we included MHCII in our analysis, which can be differentially expressed on tissue macrophages

(Tamoutounour et al., 2013). We found that in 8-wk-old mice, the majority of cMΦ was CX3CR1⁺ (~80%) and MHCII⁺ (~70%), allowing the delineation of four distinct cMΦ subpopulations (Fig. 1, A and B). Additional populations of CD11c⁺MHCII⁺ or Ly6C⁺ cells, referred to as cMΦ by others (Epelman et al., 2014), were excluded from our analysis (Fig. S1 B), as data from other tissues suggest that these are monocytes and monocyte-derived dendritic cells (Tamoutounour et al., 2013). Consistent with this, these cells have been shown to be short-lived and monocyte-derived (Epelman et al., 2014).

To investigate the development of the four cMΦ populations, we analyzed CX3CR1 and MHCII expression in cMΦ from newborn to 30-wk-old mice (Fig. 1, C and D). We observed that almost all embryo-derived cMΦ present at birth were CX3CR1⁺MHCII⁻. This homogenous cMΦ compartment diversified with age into four subpopulations with a progressive increase of MHCII⁺ cMΦ and a decrease of CX3CR1⁺ cMΦ. Importantly, genetic fate mapping analysis using *CX3CR1^{Cre}* mice crossed to *R26-yfp* reporter mice (*CX3CR1^{Cre};R26-yfp*; Yona et al., 2013) revealed that all adult cMΦ subpopulations must have developed from a CX3CR1⁺ stage (Fig. 1 E). These results suggested two not mutually exclusive possibilities for cMΦ subpopulation development: persistence

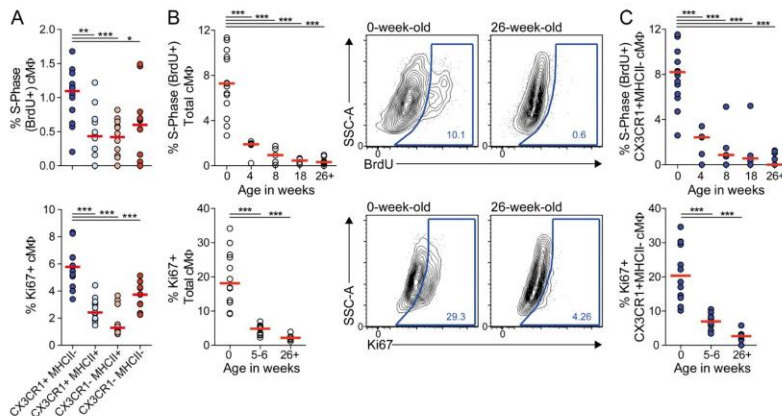


Figure 3. Decreased proliferation rate of embryo-derived cMΦ with age. (A) cMΦ subpopulations of adult $CX3CR1^{fl/fl}$ mice were analyzed for BrdU incorporation and expression of Ki67 by flow cytometry four hours after BrdU injection (i.p.). Bars show median ($n = 12-13$). *, $P \leq 0.05$; **, $P \leq 0.01$; ***, $P \leq 0.005$; Wilcoxon test. (B and C) Total (B) or $CX3CR1^+$ MHCII $^-$ (C) cMΦ of $CX3CR1^{fl/fl}$ mice of indicated age were analyzed for BrdU incorporation and Ki67 expression by flow cytometry 4 h after BrdU injection (i.p.). Bars show median ($n = 4-15$). ***, $P \leq 0.005$, Mann-Whitney test. Data in all panels were pooled from 2-3 independent experiments.

and diversification of embryo-derived cMΦ as suggested elsewhere (Epelman et al., 2014), or replacement of embryo-derived cMΦ by adult monocyte-derived macrophages.

To address these alternatives, we first analyzed the persistence of embryo-derived cMΦ by genetic lineage tracing using $CX3CR1$ -driven tamoxifen (TAM)-inducible Cre recombinase (CreERT2) and $R26-yfp$ reporter mice ($CX3CR1^{CreERT2}; R26-yfp$; Fig. 2 A; Yona et al., 2013). Tamoxifen-induced pulse labeling at E9 permits us to identify cells derived from yolk sac (YS) $CX3CR1^+$ macrophages before the onset of definitive hematopoiesis. Labeling at E13 cannot distinguish YS- and hematopoietic stem cell (HSC)-derived macrophages, but should increase cMΦ labeling because the heart is colonized by $CX3CR1^+$ macrophages at this time (Epelman et al., 2014). cMΦ labeling was normalized to YFP $^+$ microglia, which are YS-derived, remain $CX3CR1^+$ throughout development, self-maintain without contribution of HSC-derived cells (Ginhoux et al., 2010; Kierdorf et al., 2013), and therefore represent an internal control for maximal $CX3CR1$ labeling efficiency. E13 labeling revealed that relative cMΦ labeling declined from $\sim 35\%$ in newborn mice to $\sim 18\%$ in 6-wk-old mice (Fig. 2 B), indicating a loss of embryo-derived cMΦ with age. E9 labeling showed that embryo-derived cMΦ were at least partially of YS origin and similarly declined from $\sim 14\%$ in neonates to $\sim 4\%$ in 6-wk-old mice (Fig. 2 C). Interestingly, all embryo-derived YFP $^+$ cMΦ were MHCII $^-$ at birth but had partially differentiated into MHCII $^+$ cMΦ after 6 wk (Fig. 2 D). Although this demonstrated that both populations can develop from cells of embryonic origin, the relative contribution of embryo-derived YFP $^+$ cMΦ to MHCII $^+$ cMΦ was significantly lower than to MHCII $^-$ cMΦ, (Fig. 2 E).

We further assessed the turnover of $CX3CR1^+$ cMΦ in the adult heart by pulse labeling adult $CX3CR1^{CreERT2}; R26-yfp$ (Fig. 2 F). 1 wk after treatment, labeling in cMΦ corresponded to $\sim 60\%$ of microglia labeling but drastically decreased to $\sim 20\%$ after 4 wk. By comparison, microglia labeling was nearly complete after 1 wk and remained unchanged thereafter (Goldmann et al., 2013). Collectively, our lineage tracing experiments argue that a significant proportion of macrophages established in early embryonic development is still present at birth but is gradually lost with age.

The relatively fast turnover of labeled tissue-resident cMΦ suggested that local self-renewal was insufficient to maintain the resident cMΦ pool. We therefore analyzed the proliferative activity of cMΦ subpopulations in adult mice by BrdU incorporation after a 4-h pulse labeling period and by Ki67 staining (Fig. 3 A). The overall number of proliferating macrophages in adult hearts was low, particularly in MHCII $^+$ populations, but the proliferative rate of $CX3CR1^+$ MHCII $^-$ cMΦ significantly exceeded that of all other subpopulations. Interestingly, this population was also the only cMΦ subset present at birth but declined with age at the expense of the other cMΦ populations (Fig. 1, C and D). We therefore analyzed the evolution of cMΦ proliferation with age. Both BrdU incorporation and Ki67 staining showed a high proliferative rate in newborn $CX3CR1^+$ MHCII $^-$ cMΦ, which gradually decreased by 8-10-fold both in total cMΦ (Fig. 3 B) and in the $CX3CR1^+$ MHCII $^-$ cMΦ population (Fig. 3 C). Together, these data suggest that both a successive loss of the cell population with the highest proliferative rate ($CX3CR1^+$ MHCII $^-$ cMΦ) and a strong decrease of the proliferation rate collectively result in progressively decreasing self-renewal of the tissue-resident cMΦ pool.

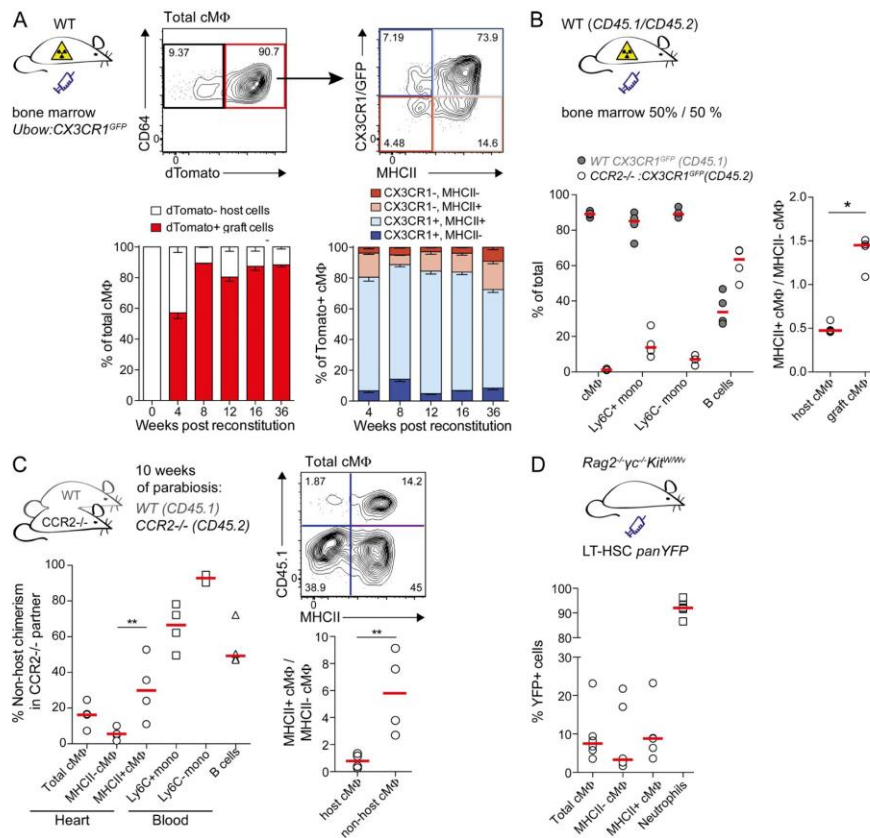


Figure 4. Monocytes contribute to four cMΦ subpopulations in adult mice. (A) WT mice were lethally irradiated and reconstituted with BM from *Ubow: CX3CR1^{GFP/+}* mice. cMΦ were analyzed for contribution of dTomato⁺ cells at indicated time points after reconstitution and graft-derived cells were analyzed for CX3CR1 and MHCII expression. Data are presented as mean percentage \pm SEM ($n = 3-7$) and derived from two independent experiments. (B) Mixed BM chimeras were generated by reconstituting lethally irradiated WT mice (*CD45.1/CD45.2*) with BM from *CCR2^{-/-}: CX3CR1^{GFP/+} (CD45.2)* and *WT CX3CR1^{GFP/+} (CD45.1)* mice. cMΦ, circulating CD11b⁺CD115⁺ monocytes (Ly6C⁺ and Ly6C⁻) and B220⁺ B cells were analyzed for WT (*CD45.1*) and *CCR2^{-/-} (CD45.2)* contribution. Host- and graft-derived cMΦ were analyzed for the ratio of MHCII⁺/MHCII⁻ cMΦ. Bars show median ($n = 4$). *, $P \leq 0.05$, Mann-Whitney test. (C) Parabiosis was established between adult *CCR2^{-/-} (CD45.2)* and *WT (CD45.1)* mice. After 10 wk, *CCR2^{-/-}* mice were analyzed for contribution of CD45.1⁺ non-host cells to cMΦ (total, MHCII⁺, and MHCII⁻), circulating monocytes (Ly6C⁺ and Ly6C⁻), and B cells. For CD45.1⁻ host and CD45.1⁺ non-host cMΦ, the ratio of MHCII⁺/MHCII⁻ cMΦ was calculated and compared. Bars show median ($n = 4$). **, $P \leq 0.01$, Mann-Whitney test. (D) BM chimeras were generated by transfer of LT-HSC isolated from *panYFP* mice into nonirradiated *Rag2^{-/-}γ^{-/-}Kit^{W/W}* mice. cMΦ (total, MHCII⁺, and MHCII⁻) and neutrophils (Gr1^{hi} and SSC^{hi}) were analyzed for contribution of grafted YFP⁺ cells 8 wk after transplantation. Bars show median ($n = 6$). **, $P \leq 0.01$, Mann-Whitney test. Data in all panels are representative of two independent experiments.

We next addressed the question of how the age-dependent loss of embryo-derived macrophages is compensated. To test the ability of monocytes to contribute to cMΦ populations, we generated BM chimeras using WT hosts and BM from transgenic mice expressing dTomato from a ubiquitously expressed human Ubiquitin-C promoter (Ubow mice; Ghigo et al., 2013) and GFP from the CX3CR1 locus that makes it possible to monitor grafted cells in all four cMΦ populations. Graft-derived dTomato⁺ cMΦ contributed to all four cMΦ populations from 4 wk after transplantation and almost completely replaced host cMΦ populations within 8 wk (Fig. 4 A).

However, a small radio-resistant population ($\sim 10\%$) persisted for 36 wk without monocyte contribution. To further analyze whether cMΦ replacement was monocyte-dependent, we generated mixed chimeras with BM from WT (*CD45.1*) and *CCR2^{-/-} (CD45.2)* *CX3CR1^{GFP/+}* mice in *CD45.1/CD45.2* double-positive WT hosts (Fig. 4 B). *CCR2^{-/-}* mice have reduced numbers of Ly6C⁺ monocytes in the blood (Serbina and Pamer, 2006) and can therefore be used to analyze the contribution of circulating monocytes and *CCR2*-dependent progenitors to tissue macrophage populations (Yona et al., 2013; Tamoutounour et al., 2013). Blood analysis indeed

confirmed that the vast majority of monocytes but not B cells were of WT origin. Graft-derived cMΦ were almost completely derived from WT cells (Fig. 4 B). Collectively these two experiments established that HSC-derived CCR2-dependent cells, most likely Ly6C⁺ monocytes, have the capacity to differentiate into all cMΦ subsets. Residual host-derived cMΦ included both MHCII⁺ and MHCII⁻ cMΦ but showed a lower proportion of MHCII⁺ cells than grafted monocyte-derived cMΦ (Fig. 4 B).

To examine monocyte contribution to cMΦ populations under homeostatic conditions, we generated parabiotic couples of WT (CD45.1) and CCR2^{-/-} (CD45.2) mice and analyzed non-host contributions after 10 wk of parabiosis in CCR2^{-/-} partners (Fig. 4 C). Circulating B cells were equally distributed between the partner mice. In the CCR2-deficient host Ly6C⁺ monocytes had reached ~70% non-host chimerism. About 16% of total cMΦ in CCR2-deficient mice were of non-host origin. Given a 70% chimerism in Ly6C⁺ monocytes, the likely cells of origin, and the possibility that depending on lifetime and exchange rate cMΦ may not be fully equilibrated after 10 wk, these observations indicated a significant monocyte contribution to tissue-resident cMΦ. Again, non-host contribution to MHCII⁺ cMΦ (~30%) was significantly higher compared with MHCII⁻ cMΦ (~5%) as highlighted by MHCII⁺/MHCII⁻ cMΦ ratios for non-host and host-derived cells (Fig. 4 C).

As a complimentary experimental approach that does not depend on myeloablative conditioning, we used *Rag2*^{-/-}*γ_c*^{-/-}*Kit*^{W/W^v} mice, which are universal HSC recipients that accept grafts without prior irradiation (Waskow et al., 2009), and generated BM chimeras by transplantation of HSC from *panYFP* mice (Luche et al., 2013). More than 90% of neutrophils were YFP⁺ after 8 wk, demonstrating efficient reconstitution (Fig. 4 D). Analysis of cMΦ revealed ~7% YFP⁺ cells in the total population. Again, donor cells showed a higher contribution to MHCII⁺ (~8% YFP⁺) than to MHCII⁻ cMΦ (~4% YFP⁺) (Fig. 4 D). In the same mice, no donor contribution to microglia cells was observed (K. Klapproth and H.R. Rodewald, personal communication). Together, these experiments clearly demonstrated a slow but significant replacement of tissue-resident cMΦ by infiltrating monocyte-derived macrophages, which preferentially contributed to MHCII⁺ cMΦ.

In the present study, we have analyzed homeostasis, origin, and turnover of resident macrophages in the heart during postnatal development. We have shown that the cMΦ compartment is undergoing dynamic changes with age. Embryo-derived macrophages present in newborn mice are all CX3CR1⁺ MHCII⁻ and at least partially YS-derived. After birth, the cMΦ compartment diversifies into four subpopulations defined by MHCII and CX3CR1 expression. Our results show that this diversification is due both to differentiation of persisting embryo-derived CX3CR1⁺ MHCII⁻ cMΦ and infiltrating monocyte-derived macrophages, which both can contribute to all four cMΦ subpopulations. However, monocytes preferentially give rise to MHCII⁺ cMΦ, whereas embryo-derived or radio-resistant cMΦ had a higher proportion of

MHCII⁻ cells, explaining the relative increase of MHCII⁺ cMΦ and the reduction of the CX3CR1⁺ MHCII⁻ cMΦ subpopulation with age. The dynamic change of the cMΦ subpopulation distribution therefore appears to reflect the gradual replacement of embryo-derived cMΦ by monocyte-derived macrophages. The increasing contribution of monocyte-derived macrophages to the cMΦ pool with age may be explained by the decreasing self-renewal of embryo-derived cMΦ. Although CX3CR1⁺ MHCII⁻ cMΦ that contain the majority of embryo-derived macrophages have a higher proliferative rate than the other subpopulations, overall cMΦ self-renewal is decreasing with age and is insufficient to sustain the cMΦ pool without input from infiltrating monocytes. It will be interesting to determine whether the loss of self-renewal capacity in cMΦ is permanent or might be reactivated. The observed mechanism of cMΦ homeostasis differs from other macrophage populations such as microglia, Langerhans cells, or alveolar macrophages, which in the absence of tissue damage or inflammation appear to self-maintain in tissues without replacement from circulating cells. It is also distinct from the high turnover rate of dermal tissue macrophages or intestinal lamina propria macrophages that are constantly replenished from circulating monocytes (Zigmond et al., 2012; Tamoutounour et al., 2013). In contrast to what was proposed elsewhere (Epelman et al., 2014), our results also show that inflammation or injury are not necessarily required for replacement of embryo-derived cardiac tissue macrophages by monocytes. It will be interesting to determine whether dynamic age-dependent changes in resident tissue macrophage populations also occur in other tissues and whether they may be important for the differences in repair mechanisms and regenerative capacity observed between young and old individuals.

MATERIALS AND METHODS

Mice. CD45.1 and CD45.2 C57BL/6 mice were obtained from Charles River. All transgenic mice used in this study have a C57BL/6 background (>7 backcrosses). *CX3CR1*^{CFP/+} mice (Jung et al., 2000), *CCR2*^{-/-}, *Rosa-26-*yfp**, *CX3CR1*^{Cre} (JAX Stock No. 25524 B6.C-Cx3cr1<tm1.1(cre)Jung>/J), and *CX3CR1*^{CreER} mice (JAX Stock No. 20940 B6J.129-Cx3cr1<tm1.1(cre/ERT2)Jung>/J; Yona et al., 2013), *Ulow* mice (Ghigo et al., 2013), *Rag2*^{-/-}*γ_c*^{-/-}*Kit*^{W/W^v} mice (Waskow et al., 2009), and *panYFP* mice (Luche et al., 2013) were described elsewhere. Experiments were performed on 6–10-wk-old mice, if not stated otherwise. Experiments involving *CX3CR1*^{Cre} and *CX3CR1*^{CreER} mice included littermate controls. For other experiments C57BL/6 mice served as controls. All mouse experiments were performed under specific pathogen-free conditions. Animals were handled according to protocols approved by the Weizmann Institute Animal Care Committee (Israel), the Federal Ministry for Nature, Environment and Consumers' Protection of the state of Baden-Württemberg (Germany) or the animal ethics committee of Marseille (France) and were performed in accordance to the respective international, national, and institutional regulations.

Parabiosis. 9-wk-old C57BL/6 CD45.1 mice were sutured together with 9-wk-old B6 *CCR2*^{-/-} CD45.2 and subsequently kept under Bactrim for 10 wk before analysis.

BM chimeras. 7–10-wk-old host animals were lethally irradiated and were reconstituted with donor BM by i.v. injection of minimum 10⁶ BM cells. Donor BM was isolated from femur and tibia of donor mice, filtered through a 70-μm mesh and resuspended in PBS for i.v. injection. *Rag2*^{-/-}*γ_c*^{-/-}*Kit*^{W/W^v}

mice were reconstituted with long-term (LT)-HSC from *panYFP* BM without prior conditioning as previously described (Waskow et al., 2009). LT-HSCs were defined as lineage-negative (B220⁻, CD3e⁻, CD4⁻, CD8a⁻, CD11b⁻, CD19⁻, Gr1⁻, Ter119⁻, NK1.1⁻), Kit⁺, Sca1⁺, CD48⁻, and CD150⁺.

Tamoxifen treatment. Tamoxifen (TAM; Sigma-Aldrich) was dissolved in 100% ethanol to get a 1 g/ml solution and was 10-fold diluted in corn oil (Sigma-Aldrich) to get the 100 mg/ml final solution for oral or i.p. administration. To induce Cre-mediated gene recombination in 5- to 7-wk-old *CX3CR1^{intRE}* mice, 5 mg TAM was administered orally for 5 consecutive days (25 mg total). For Cre induction in the embryo, 200 μ l of 20 mg/ml TAM and 10 mg/ml Progesterone dissolved in corn oil was injected i.p. into pregnant females at 9 or 13 days post coitum (dpc).

BrdU pulsing. BrdU was purchased from Sigma-Aldrich. Mice were injected with 0.1 mg BrdU/g body weight. Newborn mice were injected subcutaneously, older mice intraperitoneally. cM Φ isolated from BrdU injected mice were analyzed 4 h after injection for BrdU incorporation using the BrdU Flow kit (BD).

Flow cytometry. Cells were acquired on FACSCanto, LSRII, and LSRFortessa systems (BD) and analyzed with FlowJo software (Tree Star). The following antibodies were used for staining cells: anti-CD11b (clone M1/70; eBioscience), anti-CD11c (clone N418; eBioscience), anti-CD14 (clone Sa2-8; eBioscience), anti-F4/80 (clone BM8; eBioscience), anti-MHCII (clone M5/114.15.2; eBioscience), anti-CD45.1 (clone A20; eBioscience), anti-CD45.2 (clone 104; eBioscience), anti-B220 (clone RA3-6B2; eBioscience), anti-CD115 (clone AFS98; eBioscience), anti-CD117 (clone 2B8; eBioscience), anti-Sca1 (clone D7; eBioscience), anti-CD48 (clone JM48-1; eBioscience), anti-Gr1 (clone RB6-8C5; BioLegend), anti-CD64 (clone X54-5/7.1; BioLegend), anti-Ly6G (clone 1A8; BioLegend), anti-CD150 (clone TC15-12F12.2; BioLegend), anti-Ly6C (clone AL21; BD), anti-Ki67 (clone B56; BD), anti-CD4 (clone H129.19; BD), anti-CD8 (clone 53-6.7; BD), anti-CD19 (clone ID3; BD), Ter119 (clone Ter119; BD), NK1.1 (clone PK136; BD), anti-F4/80, anti-MerTK (clone BAF591; R&D Systems), anti-BrdU (clone MoBU-1; Life Technologies). Before staining, cells were preincubated with Fc receptor blocking antibody (clone 2.4 G2; BD). LIVE/DEAD Fixable Aqua Dead Cell Stain kit (Life Technologies) was used to stain dead cells. Absolute cell numbers were determined by using Flow-Count Fluorospere (Beckman Coulter) according to the manufacturer's instructions.

Preparation of tissue samples. Peripheral blood leukocytes were isolated by density separation using Lympholite-M solution (Cedarlane) according to manufacturer's instructions. For preparing single cell suspension from heart and brain, the mice were perfused with PBS before collecting the tissue. For cM Φ , the heart was macerated and incubated with 1 mg/ml collagenase-2 (Worthington Biochemical Corporation) and 0.15 mg/ml DNase1 (Sigma-Aldrich) at 37°C for 30 min during constant agitation. Resulting cell suspension was filtered through a 70- μ m mesh and erythrocytes were removed by ACK lysis. For microglia isolation a gradient of 70, 37, 30% Percoll was used. The brain tissue was homogenized and incubated with HBSS solution containing 2% BSA (Sigma-Aldrich), 1 mg/ml collagenase D (Roche), and 0.15 mg/ml DNase1, filtered through a 70- μ m mesh, and resuspended in 70% Percoll, before density centrifugation (800 g for 30 min at 20°C with low acceleration and no brake).

Online supplemental material. Fig. S1 depicts the full gating strategy and population characterization of cM Φ . Online supplemental material is available at <http://www.jem.org/cgi/content/full/jem.20140639/DC1>.

We thank Dr. Sandrine Sarrazin for critical reading of the manuscript and help with statistical analysis, L. Razafindramanana for animal handling, and M. Barad, A. Zouine, and S. Bigot for cytometry support.

K. Molawi was supported by an HFSP long-term fellowship. The work was supported by grants to M.H. Sieweke from Aviesan ITMO IHP exploratory Project A12194AS and CNRS PICS program No. 5730. M.H. Sieweke is a Fondation pour la Recherche Médicale (DEQ. 20071210559 and DEQ. 20110421320) and INSERM-Helmholtz group leader. The work was further supported by the Israel Science Foundation (ISF), the Deutsche Forschungsgemeinschaft (DFG) Research Unit (FOR) 1336 (S. Jung and M. Prinz), and DFG-SFB 938-project L (H.-R. Rodewald and K. Klapproth).

The authors declare no competing financial interests.

Submitted: 6 April 2014

Accepted: 19 August 2014

REFERENCES

- Ajami, B., J.L. Bennett, C. Krieger, W. Tetzlaff, and F.M.V. Rossi. 2007. Local self-renewal can sustain CNS microglia maintenance and function throughout adult life. *Nat. Neurosci.* 10:1538–1543. <http://dx.doi.org/10.1038/nn2014>
- Aurora, A.B., E.R. Porrello, W. Tan, A.I. Mahmoud, J.A. Hill, R. Bassel-Duby, H.A. Sadek, and E.N. Olson. 2014. Macrophages are required for neonatal heart regeneration. *J. Clin. Invest.* 124:1382–1392. <http://dx.doi.org/10.1172/JCI72181>
- Aziz, A., E. Soucie, S. Sarrazin, and M.H. Sieweke. 2009. MafB/c-Maf deficiency enables self-renewal of differentiated functional macrophages. *Science*. 326:867–871. <http://dx.doi.org/10.1126/science.1176056>
- Chorro, L., A. Sarde, M. Li, K.J. Woollard, P. Chambon, B. Malissen, A. Kissenpfennig, J.-B. Barbaroux, R. Groves, and F. Geissmann. 2009. Langerhans cell (LC) proliferation mediates neonatal development, homeostasis, and inflammation-associated expansion of the epidermal LC network. *J. Exp. Med.* 206:3089–3100. <http://dx.doi.org/10.1084/jem.20091586>
- Davies, L.C., S.J. Jenkins, J.E. Allen, and P.R. Taylor. 2013. Tissue-resident macrophages. *Nat. Immunol.* 14:986–995. <http://dx.doi.org/10.1038/ni.2705>
- Epelman, S., K.J. Lavine, A.E. Beaudin, D.K. Sojka, J.A. Carrero, B. Calderon, T. Brija, E.L. Gautier, S. Ivanov, A.T. Satpathy, et al. 2014. Embryonic and adult-derived resident cardiac macrophages are maintained through distinct mechanisms at steady state and during inflammation. *Immunity*. 40:91–104. <http://dx.doi.org/10.1016/j.immuni.2013.11.019>
- Gautier, E.L., T. Shay, J. Miller, M. Greter, C. Jakubzick, S. Ivanov, J. Helft, A. Chow, K.G. Elpek, S. Gordonov, et al. Immunological Genome Consortium. 2012. Gene-expression profiles and transcriptional regulatory pathways that underlie the identity and diversity of mouse tissue macrophages. *Nat. Immunol.* 13:1118–1128. <http://dx.doi.org/10.1038/ni.2419>
- Geissmann, F., M.G. Manz, S. Jung, M.H. Sieweke, M. Merad, and K. Ley. 2010. Development of monocytes, macrophages, and dendritic cells. *Science*. 327:656–661. <http://dx.doi.org/10.1126/science.1178331>
- Ghigo, C., I. Mondor, A. Jorquera, J. Nowak, S. Wienert, S.P. Zahner, B.E. Clausen, H. Luche, B. Malissen, F. Klauschen, and M. Bajénoff. 2013. Multicolor fate mapping of Langerhans cell homeostasis. *J. Exp. Med.* 210:1657–1664. <http://dx.doi.org/10.1084/jem.20130403>
- Ginhoux, F., M. Greter, M. Leboeuf, S. Nandi, P. See, S. Gokhan, M.F. Mehler, S.J. Conway, L.G. Ng, E.R. Stanley, et al. 2010. Fate mapping analysis reveals that adult microglia derive from primitive macrophages. *Science*. 330:841–845. <http://dx.doi.org/10.1126/science.1194637>
- Goldmann, T., P. Wieghofer, P.F. Müller, Y. Wolf, D. Varol, S. Yona, S.M. Brendecke, K. Kierdorf, O. Staszewski, M. Datta, et al. 2013. A new type of microglia gene targeting shows TAK1 to be pivotal in CNS autoimmune inflammation. *Nat. Neurosci.* 16:1618–1626. <http://dx.doi.org/10.1038/nn.3531>
- Hashimoto, D., A. Chow, C. Noizat, P. Teo, M.B. Beasley, M. Leboeuf, C.D. Becker, P. See, J. Price, D. Lucas, et al. 2013. Tissue-resident macrophages self-maintain locally throughout adult life with minimal contribution from circulating monocytes. *Immunity*. 38:792–804. <http://dx.doi.org/10.1016/j.immuni.2013.04.004>
- Hoefl, G., Y. Wang, M. Greter, P. See, P. Teo, B. Malleret, M. Leboeuf, D. Low, G. Oller, F. Almeida, et al. 2012. Adult Langerhans cells derive predominantly from embryonic fetal liver monocytes with a minor contribution

- of yolk sac-derived macrophages. *J. Exp. Med.* 209:1167–1181. <http://dx.doi.org/10.1084/jem.20120340>
- Jenkins, S.J., D. Ruckerl, P.C. Cook, L.H. Jones, E.D. Finkelman, N. van Rooijen, A.S. MacDonald, and J.E. Allen. 2011. Local macrophage proliferation, rather than recruitment from the blood, is a signature of TH2 inflammation. *Science*. 332:1284–1288. <http://dx.doi.org/10.1126/science.1204351>
- Jung, S., J. Aliberti, P. Graemmel, M.J. Sunshine, G.W. Kreutzberg, A. Sher, and D.R. Littman. 2000. Analysis of fractalkine receptor CX₃CR1 function by targeted deletion and green fluorescent protein reporter gene insertion. *Mol. Cell. Biol.* 20:4106–4114. <http://dx.doi.org/10.1128/MCB.20.11.4106-4114.2000>
- Kierdorf, K., D. Emy, T. Goldmann, V. Sander, C. Schulz, E.G. Perdiguer, P. Wieghofer, A. Heinrich, P. Riemke, C. Hölscher, et al. 2013. Microglia emerge from erythromyeloid precursors via Pu.1- and Irf8-dependent pathways. *Nat. Neurosci.* 16:273–280. <http://dx.doi.org/10.1038/nn.3318>
- Luhe, H., T. Nageswara Rao, S. Kumar, A. Tasdogan, F. Beckel, C. Blum, V.C. Martins, H.-R. Rodewald, and H.J. Fehling. 2013. In vivo fate mapping identifies pre-TCR α expression as an intra- and extrathymic, but not prethymic, marker of T lymphopoiesis. *J. Exp. Med.* 210:699–714. <http://dx.doi.org/10.1084/jem.20122609>
- Nahrendorf, M., F.K. Swirski, E. Aikawa, L. Stangenberg, T. Wurdinger, J.L. Figueiredo, P. Libby, R. Weissleder, and M.J. Pittet. 2007. The healing myocardium sequentially mobilizes two monocyte subsets with divergent and complementary functions. *J. Exp. Med.* 204:3037–3047. <http://dx.doi.org/10.1084/jem.20070885>
- Pinto, A.R., R. Paolicelli, E. Salimova, J. Gospocic, E. Slonimsky, D. Bilbao-Cortes, J.W. Godwin, and N.A. Rosenthal. 2012. An abundant tissue macrophage population in the adult murine heart with a distinct alternatively-activated macrophage profile. *PLoS ONE*. 7:e36814. <http://dx.doi.org/10.1371/journal.pone.0036814>
- Porrello, E.R., A.I. Mahmoud, E. Simpson, J.A. Hill, J.A. Richardson, E.N. Olson, and H.A. Sadek. 2011. Transient regenerative potential of the neonatal mouse heart. *Science*. 331:1078–1080. <http://dx.doi.org/10.1126/science.1200708>
- Schulz, C., E. Gomez Perdiguer, L. Chorro, H. Szabo-Rogers, N. Cagnard, K. Kierdorf, M. Prinz, B. Wu, S.E.W. Jacobsen, J.W. Pollard, et al. 2012. A lineage of myeloid cells independent of Myb and hematopoietic stem cells. *Science*. 336:86–90. <http://dx.doi.org/10.1126/science.1219179>
- Serbina, N.V., and E.G. Pamer. 2006. Monocyte emigration from bone marrow during bacterial infection requires signals mediated by chemokine receptor CCR2. *Nat. Immunol.* 7:311–317. <http://dx.doi.org/10.1038/ni1309>
- Sieweke, M.H., and J.E. Allen. 2013. Beyond stem cells: self-renewal of differentiated macrophages. *Science*. 342:1242974. <http://dx.doi.org/10.1126/science.1242974>
- Swirski, F.K., M. Nahrendorf, M. Etzrodt, M. Wildgruber, V. Cortez-Retamozo, P. Panizzi, J.L. Figueiredo, R.H. Kohler, A. Chudnovskiy, P. Waterman, et al. 2009. Identification of splenic reservoir monocytes and their deployment to inflammatory sites. *Science*. 325:612–616. <http://dx.doi.org/10.1126/science.1175202>
- Tamoutounour, S., M. Guillemins, F. Montanana Sanchis, H. Liu, D. Terhorst, C. Malosse, E. Pollet, L. Ardouin, H. Luhe, C. Sanchez, et al. 2013. Origins and functional specialization of macrophages and of conventional and monocyte-derived dendritic cells in mouse skin. *Immunity*. 39:925–938. <http://dx.doi.org/10.1016/j.immuni.2013.10.004>
- van Furth, R., and Z.A. Cohn. 1968. The origin and kinetics of mononuclear phagocytes. *J. Exp. Med.* 128:415–435. <http://dx.doi.org/10.1084/jem.128.3.415>
- Waskow, C., V. Madan, S. Bartels, C. Costa, R. Blasig, and H.R. Rodewald. 2009. Hematopoietic stem cell transplantation without irradiation. *Nat. Methods*. 6:267–269. <http://dx.doi.org/10.1038/nmeth.1309>
- Yona, S., K.-W. Kim, Y. Wolf, A. Mildner, D. Varol, M. Breker, D. Strauss-Ayali, S. Viukov, M. Guillemins, A. Misharin, et al. 2013. Fate mapping reveals origins and dynamics of monocytes and tissue macrophages under homeostasis. *Immunity*. 38:79–91. <http://dx.doi.org/10.1016/j.immuni.2012.12.001>
- Zigmond, E., C. Varol, J. Farache, E. Elmaliyah, A.T. Satpathy, G. Friedlander, M. Mack, N. Shpigel, I.G. Boneca, K.M. Murphy, et al. 2012. Ly6C hi monocytes in the inflamed colon give rise to proinflammatory effector cells and migratory antigen-presenting cells. *Immunity*. 37:1076–1090. <http://dx.doi.org/10.1016/j.immuni.2012.08.026>

Statement of the author

The author states that the results presented in this PhD thesis are his own independent work. The western blots of immunohistochemistry in section 3.2. were performed with Dr. Sigalit Boura-Halfon, as who joined the author at an advanced stage of the MecP2 project. The metabolic cage analysis in section 3.2 was performed with Dr. Yael Kuperman, Department of Veterinary Resources, Weizmann Institute. The bioinformatic analysis in section 3.2 was performed with the help of Eyal David. Parts of section 3.3 were performed in collaboration with a master student in the Jung laboratory, Anat Shemer, and are continued by Anat. The histology presented in section 3.4 was performed by Dr. Tobias Goldmann in the laboratory of Prof. Marco Prinz, University of Freiburg, Germany. Section 3.5., i.e the study of the heart macrophages was part of a collaboration with Dr. Kaaweh Molawi and Prof. Michael Sieweke, Centre d'Immunologie de Marseille-Luminy (CIML), France. The work presented in the thesis was performed by the author.

Statement of the supervisor

This is to confirm that the studies presented in this thesis were performed by Yochai Wolf, with help from collaborators, as indicated. Yochai's contribution to the Yona et al study (Immunity 2013), that earned him a first- co-authorship was the analysis of the blood monocyte compartment. In the Goldmann et al. study, Yochai Wolf contributed the in depth characterization of the experimental system, i.e the Cre and CreER mice. In the study on the heart macrophages, Yochai made with his collaborator at the Weizmann Institute the first triggering observation, and then substantially added to the completion of the study with the experimentation that is presented in this thesis. Expert help was recruited were needed and is indicated, but throughout the studies Yochai was the driving force. We are currently in the process of preparing a manuscript summarizing the results related to the MecP2 and TNF deficiencies in macrophages.

Acknowledgements

This work was done with the help of many contributors, of which I dearly want to thank:

First of all, to Steffen, my mentor in every sense of the word, for his everlasting passion and never-ending quest for the purest form of knowledge and curiosity, and for his door in his office which was always open for me in the past 5 years;

To my collaborators in the lab- Simon, Ki-Wook, Alex, Anat and Sigalit; I have learned so much from each and every one of you, and I am both delighted and proud of having working together;

To the Jung lab and its present and past members-, Tege, Udi, Diana, Alon, Biana, Mor, Goran, Cate, Neta, Zhana, Jung-Soek, Yifat, Yaara, Anita, Amir, Gitit, Tamir, Noa and Rita, for making this lab into both a think tank and an amusement park, it's been quite a ride;

To our collaborators abroad- Jonathan Kipnis in Virginia,USA, Marco Prinz and Tobias Goldmann in Freiburg,Germany , Kaaweh Molawi and Michael Sieweke in Marcie, France, for their fruitful collaborative work and their support;

To my Parents, Niza and Yehuda, who always were and always will be an endless source of support and love, and who always helped me make my dreams come true;

To my brothers, Nadav and Bat-Chen, for their listening ears and their smiles, happiness and their cheerful laughter;

To my grandmother Haviva, for her huge heart which I think is the biggest in the world, you are the rock of Gibraltar for me;

To my wife, Avigal, who makes me a complete person and struggled with me almost equally in the making of this thesis, and is the ultimate partner for this journey of a life;

Lastly, to my son Tom, who taught me and continues to teach me everything I hadn't known about love and the world.

This work is dedicated to the loving memory of my late grandparents, Itzhak Adelberg 1925-1991, Moshe Wolf 1928-1993 and Mania Wolf 1926-2004.